We thank the reviewers for their reviews and recommendation to publish. We have considered every point and corrected the paper to include their points. The referees comments are in blue, responds from the authors are in black and revised text are in red.

Referee 1

(1) Atmospheric nitrate (gaseous HNO_3 + particulate nitrate) is assumed to be dominated by gaseous HNO_3 (which is supported by previous studies). In this work, the physical exchange of gaseous HNO_3 in the snow interstitial air (SIA) and the snow grains is described explicitly by different models. However, the mass exchange of HNO_3 between the SIA and air above snow (where the atmospheric nitrate is measured) is missing. Mass exchange between the SIA and air above snow is largely controlled by processes such as turbulent transport and wind pumping. How these processes would affect the bulk nitrate in the skin layer of snow needs to be clearly addressed.

It is assumed that the boundary layer was well mixed such that the surface HNO_3 concentration is same as the observation made at approximately 1 m above the surface. A table of characteristic times of different processes has now been added to the manuscript. The focus of this paper is to describe the interaction between the skin layer of the snowpack (top 4 mm) and the overlying atmosphere. The characteristic time of molecular diffusion for vertical mass transport between the SIA at 4 mm and the air above is only of the order of a second, therefore, is assumed to be in equilibrium.

The characteristic time of various processes are listed in Table. 1

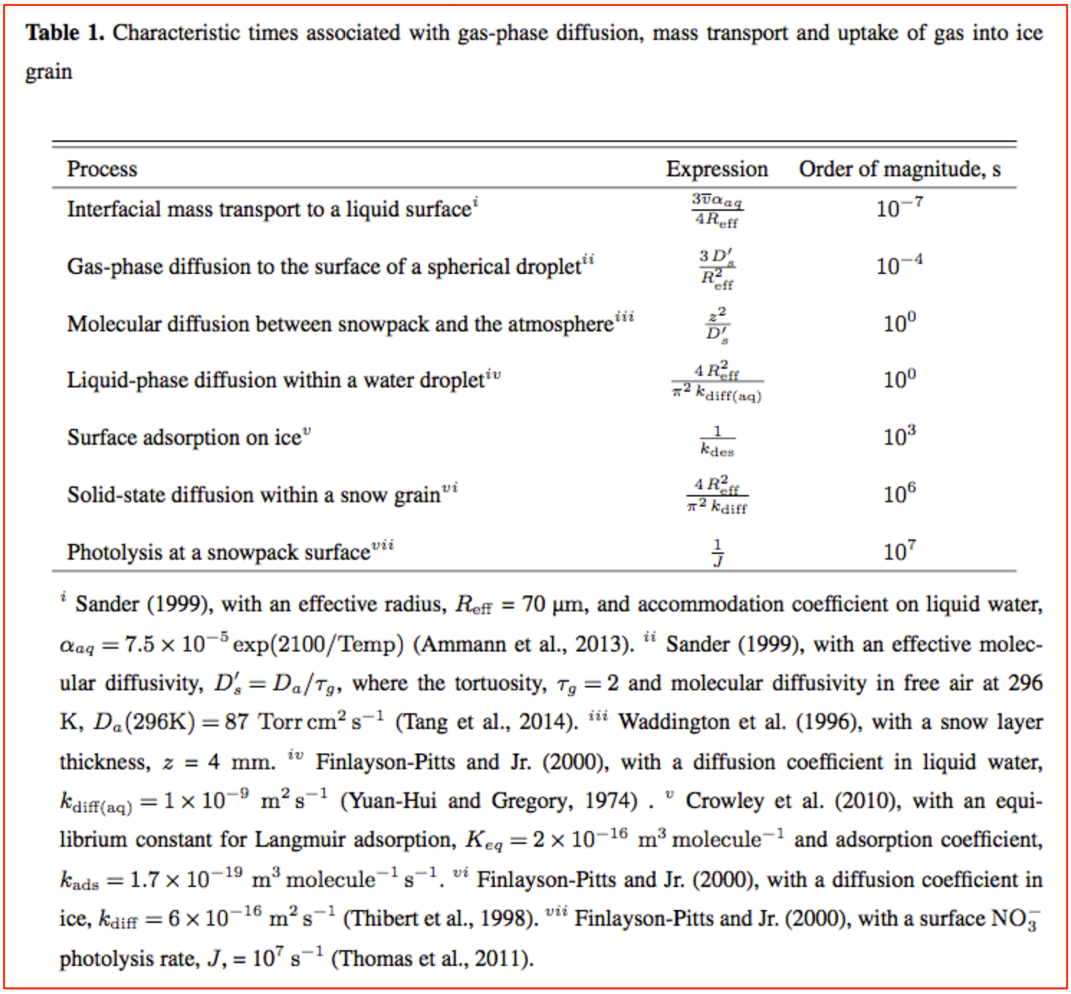

Table 1. Characteristic times associated with gas-phase diffusion, mass transport and uptake of gas into ice grain

Process	Expression	Order of magnitude, s
Interfacial mass transport to a liquid surface^{i}	$\frac{3\overline{v}\alpha_{aq}}{4R_{\mathrm{eff}}}$	10^{-7}
Gas-phase diffusion to the surface of a spherical droplet^{ii}	$\frac{3\,D'_s}{R^2_{\mathrm{eff}}}$	10^{-4}
Molecular diffusion between snowpack and the atmosphere^{iii}	$\frac{z^2}{D'_s}$	10^{0}
Liquid-phase diffusion within a water droplet^{iv}	$\frac{4\,R^2_{\mathrm{eff}}}{\pi^2\,k_{\mathrm{diff(aq)}}}$	10^{0}
Surface adsorption on ice^{v}	$\frac{1}{k_{\mathrm{des}}}$	10^{3}
Solid-state diffusion within a snow grain^{vi}	$\frac{4\,R^2_{\mathrm{eff}}}{\pi^2\,k_{\mathrm{diff}}}$	10^{6}
Photolysis at a snowpack surface^{vii}	$\frac{1}{J}$	10^{7}

^{i} Sander (1999), with an effective radius, R_{eff} = 70 µm, and accommodation coefficient on liquid water, $\alpha_{aq} = 7.5 \times 10^{-5} \exp(2100/\mathrm{Temp})$ (Ammann et al., 2013). ^{ii} Sander (1999), with an effective molecular diffusivity, $D'_s = D_a/\tau_g$, where the tortuosity, $\tau_g = 2$ and molecular diffusivity in free air at 296 K, $D_a(296\mathrm{K}) = 87\ \mathrm{Torr\,cm^2\,s^{-1}}$ (Tang et al., 2014). ^{iii} Waddington et al. (1996), with a snow layer thickness, z = 4 mm. ^{iv} Finlayson-Pitts and Jr. (2000), with a diffusion coefficient in liquid water, $k_{\mathrm{diff(aq)}} = 1 \times 10^{-9}\ \mathrm{m^2\,s^{-1}}$ (Yuan-Hui and Gregory, 1974) . ^{v} Crowley et al. (2010), with an equilibrium constant for Langmuir adsorption, $K_{eq} = 2 \times 10^{-16}\ \mathrm{m^3\,molecule^{-1}}$ and adsorption coefficient, $k_{\mathrm{ads}} = 1.7 \times 10^{-19}\ \mathrm{m^3\,molecule^{-1}\,s^{-1}}$. ^{vi} Finlayson-Pitts and Jr. (2000), with a diffusion coefficient in ice, $k_{\mathrm{diff}} = 6 \times 10^{-16}\ \mathrm{m^2\,s^{-1}}$ (Thibert et al., 1998). ^{vii} Finlayson-Pitts and Jr. (2000), with a surface NO_3^- photolysis rate, J, = $10^7\ \mathrm{s^{-1}}$ (Thomas et al., 2011).

Such information and assumptions are now included in in Sect. 4.1 (Page 12, line 359-363)

"The atmospheric boundary layer is assumed to be well mixed so that the atmospheric nitrate at the snowpack surface would be the same at 1 m. The characteristic transport time of HNO_3 from the snowpack surface to the skin layer (4 mm) is on the order of 10^0 s, which is much shorter compared to the temporal resolution of the model of 10 min (Table 1), and therefore, the HNO_3 concentration of the skin layer was assumed to be the same as above the snow."

and Sect. 4.2 (Page 12, line 390-391)

"Again, the atmospheric boundary layer is assumed to be well mixed that the nitric acid concentration at the snowpack surface would be the same as at 7-8 m"

(2) Model 2 incorporates the micro-liquid pocket. This topic is of great interest since the brine formed by impurities may not cover the entire grain surface due to limited wettability at cold temperatures. However, instantaneous air/micro-liquid pocket equilibrium is assumed. This seems to be oversimplified. For highly soluble species such as HNO_3 in liquid water (effective Henry's law constant > 10ˆ14 M atmˆ-1, Fig 1), interfacial transport or even gas diffusion (in this case, gas diffusion in the SIA) may well become the rate limiting steps. The timescale of the SIA/micropocket equilibrium needs to be examined before assuming equilibrium.

A table of characteristic times (Table 1) of different processes has been added to the manuscript. The characteristic times a) of interfacial mass transport across a liquid surface of a droplet with a 70 μm radius, b) gas-phase diffusion toward a droplet with 70 μm radius, and c) vertical mass transport to SIA at 4 mm depth are all significantly smaller than the characteristic time of surface adsorption, solid-state diffusion.

The following lines been change in Sect. 3.2, Line 314-320

"An instantaneous equilibrium is assumed because 1) the volume of the liquid solution is small (10^{-7} -10^{-6} % of the total volume of the ice grain, discussed below) 2) HNO3 is highly soluble in water; 3) the characteristic time of the interfacial mass transport across a liquid surface of a droplet with 70 μm is only ~ 10^{-7} s (Table 1); and 4) the diffusion rate is faster in liquid (At 0◦C, NO−3 diffusion of NO−3 is 9.78×10^{-10} m^2 s^{-1} in liquid, Yuan-Hui and Gregory, 1974) than in ice (At 0◦ C NO_3^- diffusion rate is 3.8×10^{-14} m^2 s^{-1} in ice). The characteristic time of liquid-phase diffusion within a 70μm diameter water droplet is ~ 10^0 s (Table 1)."

(3) From the model point of view, Model 2 does not really specify or depend on the location of liquid water, i.e. whether the liquid water is covering the whole/part of the grain surface as a thin layer, or is located in grooves at grain boundaries and tripe junctions. It appears mathematically that, in Eq(4) + Eq(17), only the liquid water content matters while the location of liquid water does not.

The reviewer is correct, in fact we don't know the location from the current data set; the liquid water is treated as micro-liquid pockets that can be found at an unspecified location in grooves at grain boundaries or triple junctions as stated in the Introduction (Line 101-102). The assumption implies the grain surface area being covered by liquid water is negligible and therefore mostly ice.

For clarification the following text has been added, in Sect. 3.2 (Page 10, line 302-303)

"Liquid water is assumed to be located in grooves at grain boundaries or triple junctions between grains and in the form of micropockets. This assumption implies the grain surface area being covered by liquid water is negligible. "

(4) The authors claim that the physical exchange models are based on "first principles" (what exactly are first principles btw) and hence without requiring any tuning parameters. This seems not true: some parameters involved in the models are still somewhat adjustable and/or lack direct observational support, such as max number of adsorption sites, threshold temperature T0, microscopic H2O density gradient, eutectic temperature, etc.

'First principles' are based on physical laws and relationship. The "tuning parameters" are referred to scaling factors that use to fit the model to observations. However, some of the physical parameter used in the current work have ill defined values which merited a study of the model sensitivity against some of the parameterisations and inputs were analyzed. The results of model sensitivity are now listed in Table 4.

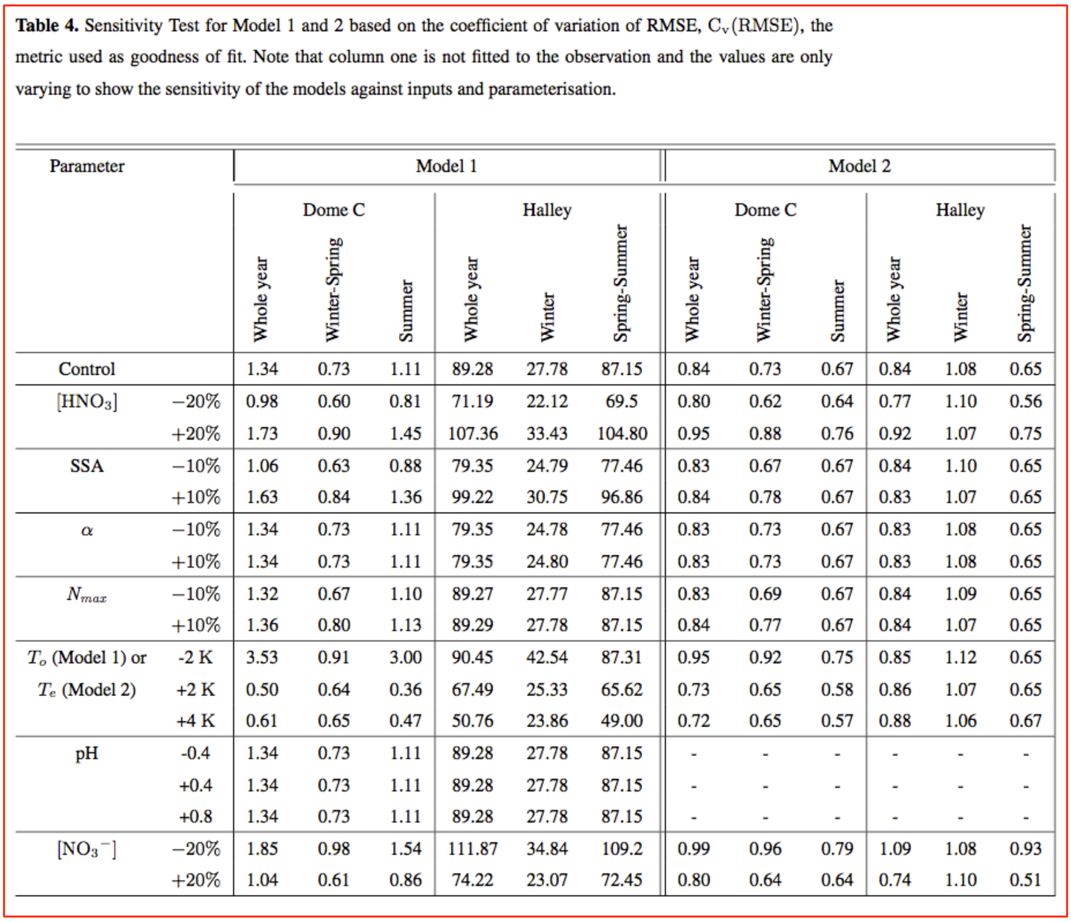

Table 4. Sensitivity Test for Model 1 and 2 based on the coefficient of variation of RMSE, C_v(RMSE), the metric used as goodness of fit. Note that column one is not fitted to the observation and the values are only varying to show the sensitivity of the models against inputs and parameterisation.

Parameter		Model 1						Model 2					
		Dome C			Halley			Dome C			Halley		
		Whole year	Winter-Spring	Summer	Whole year	Winter	Spring-Summer	Whole year	Winter-Spring	Summer	Whole year	Winter	Spring-Summer
Control		1.34	0.73	1.11	89.28	27.78	87.15	0.84	0.73	0.67	0.84	1.08	0.65
[HNO_3]	−20%	0.98	0.60	0.81	71.19	22.12	69.5	0.80	0.62	0.64	0.77	1.10	0.56
	+20%	1.73	0.90	1.45	107.36	33.43	104.80	0.95	0.88	0.76	0.92	1.07	0.75
SSA	−10%	1.06	0.63	0.88	79.35	24.79	77.46	0.83	0.67	0.67	0.84	1.10	0.65
	+10%	1.63	0.84	1.36	99.22	30.75	96.86	0.84	0.78	0.67	0.83	1.07	0.65
α	−10%	1.34	0.73	1.11	79.35	24.78	77.46	0.83	0.73	0.67	0.83	1.08	0.65
	+10%	1.34	0.73	1.11	79.35	24.80	77.46	0.83	0.73	0.67	0.83	1.08	0.65
N_{max}	−10%	1.32	0.67	1.10	89.27	27.77	87.15	0.83	0.69	0.67	0.84	1.09	0.65
	+10%	1.36	0.80	1.13	89.29	27.78	87.15	0.84	0.77	0.67	0.84	1.07	0.65
T_o (Model 1) or T_e (Model 2)	-2 K	3.53	0.91	3.00	90.45	42.54	87.31	0.95	0.92	0.75	0.85	1.12	0.65
	+2 K	0.50	0.64	0.36	67.49	25.33	65.62	0.73	0.65	0.58	0.86	1.07	0.65
	+4 K	0.61	0.65	0.47	50.76	23.86	49.00	0.72	0.65	0.57	0.88	1.06	0.67
pH	-0.4	1.34	0.73	1.11	89.28	27.78	87.15	-	-	-	-	-	-
	+0.4	1.34	0.73	1.11	89.28	27.78	87.15	-	-	-	-	-	-
	+0.8	1.34	0.73	1.11	89.28	27.78	87.15	-	-	-	-	-	-
[NO_3^-]	−20%	1.85	0.98	1.54	111.87	34.84	109.2	0.99	0.96	0.79	1.09	1.08	0.93
	+20%	1.04	0.61	0.86	74.22	23.07	72.45	0.80	0.64	0.64	0.74	1.10	0.51

(5) Comparison between models and measurements needs to be discussed in the context of their respective uncertainty ranges. What is the measurement uncertainty of skin layer nitrate concentration? What is the model uncertainty propagated from the inputs and parameters?

Results of the sensitivity tests on atmospheric nitrate concentration, accommodation coefficient, maximum number of adsorption sites, threshold temperature or eutectic temperature and skin layer snow nitrate concentration are listed in Table 4 (See the comment above).

(6) The quality of English could use some polish.

In addition, the authors claim that the photochemistry of snow nitrate can be ignored due to slow photolysis in this region. Well, "what goes up must come down" and vice versa. What processes are then responsible for the loss of snow nitrate? And what is driving the seasonal variations of snow nitrate in this region? Snow nitrate can't cannnot always accumulate. This is perhaps not the main focus of this work, but the fact that only snow nitrate sources are included in the model may be quite confusing.

See the comment above

The observed atmospheric concentration HNO_3 is used as a model constrain, which implicitly included change in atmospheric HNO_3 concentration due to air-snow exchange.

In this particular region of the snowpack the loss of nitrate by photolysis is slow compared to the physical uptake of nitrate by adsorption and co-condensation.

The following text has been added to Sect. 3, Line 187-193

"The loss or gain in the atmospheric HNO_3 due to the mass exchange between air and snow are included implicitly by constraining the models with the observed HNO_3 concentration. The aim of this paper is to focus on the exchange mechanisms between air-snow, and by limiting the working layer to the skin layer, the following assumptions can be made, 1) homogenous physical properties across the skin layer, such as snow density and SSA. 2) the HNO_3 concentration in SIA is in equilibrium with the overlying atmosphere due to a short characteristic time (Table 1)."

Specific comments:

Page 3, Line 61: the characteristic times of surface adsorption and solid-state diffusion for HNO_3... please provide more details (either literature or point to later sections).

Details are now listed in Table 1 (See above comment)

Page 3, Line 83: define skin layer. What is the thickness of this skin layer in the model and why this value is chosen? Or is it simply the layer in which the bulk ion concentrations are measured?

Information regarding to the skin layer been added to Page 2, Line 52-54

"Here in this paper, the skin layer is defined as the top 4 mm of the snowpack, which is the depth of which the surface snow nitrate samples were collected at Dome C (Sect. 4.1)."

Since the model is limited to the skin layer, it seems that there is no exchange between the skin layer and the deeper snow. However, previous studies(e.g. Traversi et al 2014) indicated that temperature gradients and wind pumping exist in the snowpack, therefore nitrate could be mobilized by physical processes reaching much deeper than the "skin layer" in this model (a few mm?).

The aim of this paper is to demonstrate the interaction between skin layer nitrate and atmospheric HNO_3 with a simple physical model without a scaling factor. Atmospheric nitrate can reach deeper than the skin layer via wind pumping and temperature gradient, however, to reproduce nitrate concentration in deeper snow requires a complicated multi-layer model. Developing a multi-layer model is an extremely large undertaking and is being performed at the time of writing. The conclusion highlighted the referee's point and further work will address this.

Within the Conclusion, Line 704-716

"Despite the simplified parameterisation of processes in Model 2, such as the impurities content in snow, liquid pockets located in different locations were treated as one and had the same chemical properties as bulk liquid, it is a promising step towards parameterising the interactions between air and snow. The models presented here are describing the exchange between air and the skin layer that the uptake processes are much quicker than the photochemical loss, and therefore, can be modelled by physical only processes. Atmospheric nitrate can reach deeper than the skin layer via wind pumping and temperature gradient, however, the nitric acid concentration in SIA is expected to be small compared to the overlying atmosphere due to the high uptake of nitrate near the surface of the snowpack. A lower HNO3 concentration in SIA implies a smaller uptake in deeper snow, and hence the photochemical loss cannot be assumed to be negligible in deeper snow. Therefore, a more complex multi-layer model including both physical and chemical processes is required to reproduce the nitrate concentration in deeper snow and being implement in regional and global atmospheric chemistry model.."

Page 5, Line 141: the solid-state diffusivity is introduced here, and hence characteristic time can be calculated. Please compare to other processes, e.g. surface accommodation and gas-phase diffusion

The characteristic times of other processes are now listed in Table 1 (See the comment above)

Page 6, Line 178: what is the size of snow grain?

The sentence is now written as (Line 194-195)

"For simplicity, the snow grain is assumed to be a radially symmetrical sphere with a radius, Reff , which is estimated from the specific surface area (SSA) with the follow equation:

(... Eq. 6) "

Eq. 14 is now Eq. 6 and moved to Sect. 3.

An extra sub-plot of the effective grain radius has been added to the Appendix, Fig A3

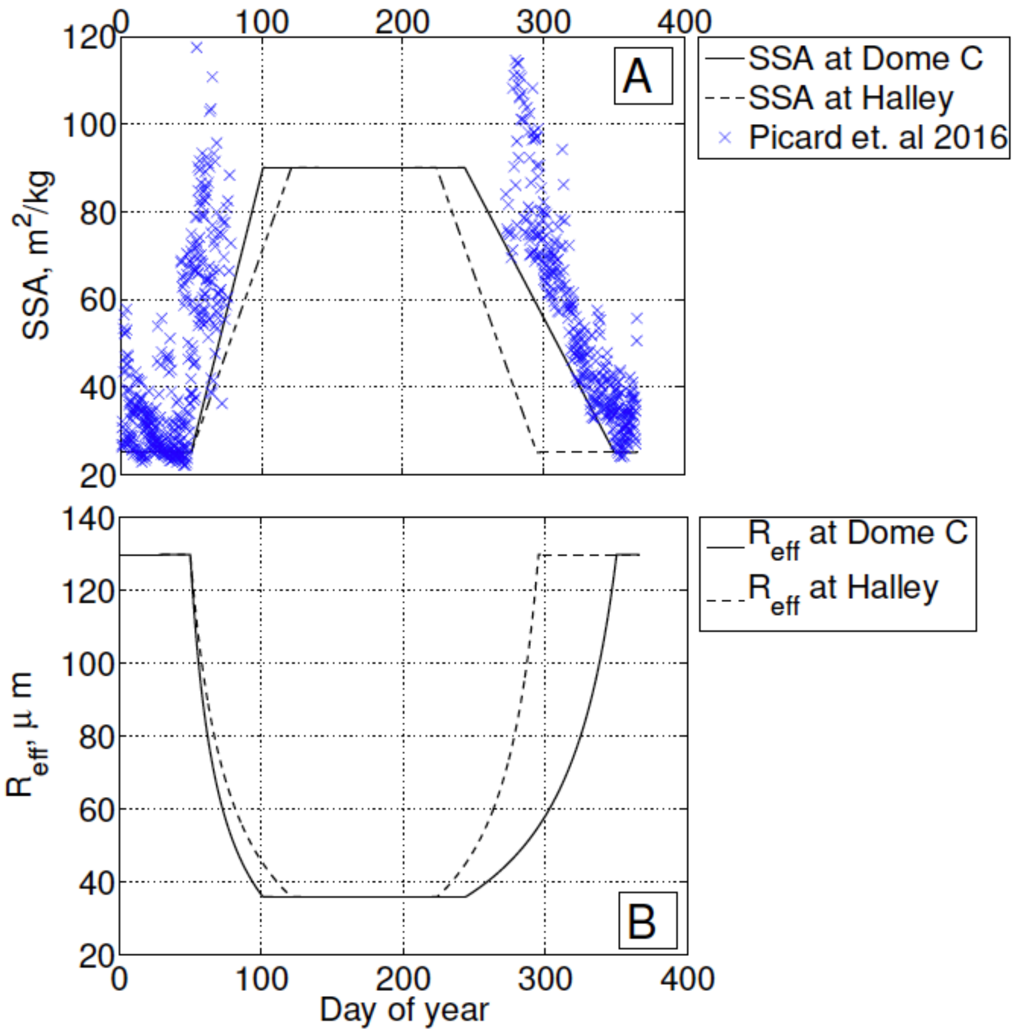

Figure A3. (A) Year-round estimates of the specific surface area (SSA) of snow at Dome C (–) and Halley (– –) were interpolated from observations at Dome C during 2012-2015 by Picard et al. (2016) (×). The SSA estimates for Halley take into account the shorter cold period compare to Dome C, which tends to have larger SSA. (B) Year-round estimates of effective grain radius (R_{eff}) at Dome C (–) and Halley (– –) derived from Eq. 6.

Page 7, Eq 7: both adsorption and co-condensation contribute to surface HNO_3. Is co-condensed HNO_3 available for desorption? Judging from Eq 6 it seems the answer is yes, yet in Eq 7 it seems co-condensed HNO_3 is not included. Also, will the cocondensed HNO_3 molecules undergo solid diffusion?

Yes, the grain surface HNO_3 concentration has contributions from the sum of adsorption, desorption and co-condensation or co-sublimation. Condensation or sublimation depends on the sign of the water vapour gradient and hence the sign of the rate of volume change (Eq. 10)

The grain surface concentration of HNO_3 is then treated as the boundary concentration for solid grain diffusion driven by concentration gradient of the grain surface and the centre of grain.

For clarification the following text has been added, in Page 7, Line 215-217 “where [HNO_3(ads)] is the concentration contributed from the sum of surface adsorption and desorption (Eq. 8), and [HNO_3(cc)] is the concentration contributed from the co-condensation or co-sublimation (Eq. 9).”

and Page 8, Line 238-240
“The temperature gradient and relative humidity gradient between the surface of the snowpack and the skin layer create a gradient in water vapour pressure, which drives condensation or sublimation of snow, depending on the sign of the gradient.”

Page 8, Line 248: what is the thickness of this DI covering the entire grain surface?
The DI is treated as the boundary of the snow grain, of which the concentration of DI is used as the boundary condition for the diffusion into the snow grain. Therefore, no thickness is assigned to the DI.
For clarification, the following lines (Page 9, line 275-277) are now included in the manuscript.
“Note that in this model the DI is treated as the boundary between the air and bulk ice. The concentration of the DI is used as the outermost boundary condition for solid-state diffusion within the grain, therefore, the DI has no thickness.”

Also, Eq 13 describes d[HNO_3(DI)]/dt, and there should be another equation for d[HNO_3(g)]/dt accordingly. Please provide this. Finally, I may be wrong but shouldn’t mass transfer (Eq 13 and d[HNO_3(g)]/dt) depend on liquid water content of some sort?
Both models presented here are constrained by the observed gas phase HNO_3 concentration with time, therefore, the loss of HNO_3(g) due to mass transfer is included implicitly.

Page 8, Eq 8: this equation describes co-condensation. How about H2O sublimation? Does HNO_3 undergo co-sublimation (or whatever the term should be) as well?
Both co-condensation or co-sublimation occur depending on the sign in Eq. 10.

Page 10, Line 294: again, for highly soluble species in liquid, interfacial transport or gas diffusion may be limiting (Schwartz, 1986). Please calculate the equilibrium timescale and discuss in the context of other mass transfer processes.
Details are now listed in Table 1.

Page 13, Line 399: define winter (and other seasons too). The Northerners would appreciate this.
Has been added to Page 11, Line 336-340. It reads
“... in summer (mid November till end of January) and down to −80°C in the winter (April to mid September). The diurnal temperature variation is ~10 K in summer, spring (mid September till mid November) and autumn (February to March).”

Page 14, Line 432: "However, Model 1... overestimated concentration by a factor of 1.5-5 in December". Which model 1? With 238 K or 242 K?

Now (Line 448-449) written as "However, Model 1 (with T0 = 238 K) did not capture the peak in early February and overestimated concentration by a factor of 1.5-5 in December."

Page 15, Line 476: "the combination of larger temperatures and a larger diurnal temperature range" this sentence is confusing.
The sentence (Line 491-192) has been corrected and now reads
"… the combination of warmer temperatures and a larger range of diurnal temperature causes …"

Page 16, Line 493: "it is possible that the snow NO3- concentration measured from Halley might be 'diluted' from deeper snow layer..." then can you extend your model to cover deeper layers, or simply increase the skin layer thickness? Also, as shown in Fig 11, Model 2 underestimated nitrate for the majority of the time (Line 458-459). If measured snow NO3- was indeed diluted, would this mean the model underestimates even more?
The models presented here would lose their physical meaning by increasing the thickness, of which is assumed to be homogenous as well as in equilibrium with the atmosphere above. A multi-layer model is required to cover deeper layers. Moreover, Model 2 underestimates the concentration of nitrate at Halley mainly in the winter period where new snowfall events were accounted for the large surface snow nitrate.

Page 16, Line 497: what do you mean by "fixed by sea salt, ammonium or terrestrial dust"?
The sentence (Line 511-512) was rewritten as " Thirdly, atmospheric nitrate can be in a more stable forms of NO_3^- , i.e. associated with Na^+,Ca^{2+} or Mg^{2+} (Beine et al., 2003)"

Page 16, Line 502: "the increase in sea salt concentration decreases the ratio of concentration of gaseous HNO_3 to total atmospheric nitrate". Please provide evidence.
A reference, Dasgupta et al., 2007, has been added.

Page 16, Line 503: "A possible explanation for the overestimation of NO3- concentration in both Model 1 and 2 in November at Dome C" this is not a complete sentence.
The sentence has been removed.

Page 17, Line 546: "In the summer, other processes are replaced..." this sentence is ill-formed. What are you trying to say?
The sentence (Line 562-564) is rewritten as "In the summer, the dominant process in Model 1 is solvation in DI (See Sect. 6.3) while in Model 2 the dominant process is partitioning in the micropockets (See Sect. 6.4), hence the contribution from co-condensation to the skin nitrate concentration is insignificant."

Page 19, Line 605: there is no purple on Fig 7.
Corrected. The sensitivity analysis is now moved to Sect. 6.5. The results from Model 1 at Halley are now in Fig. 8A. The purple line (on the right axis) is the results when T0 = 242 K and the text has been adjusted to demonstrate it.

Page 19, Line 628: Again this is only true if gas diffusion and interfacial transport are not limiting. Also, Model 1 output is quite sensitive to T0. How sensitive is Model 2 to the eutectic temperature?

A set of sensitivity tests have been run against inputs such as nitric acid concentration, SSA, accommodation coefficient (α), maximum number of adsorption site (Nmax), and either the threshold temperature in Model 1(T0) or the eutectic temperature in Model 2 (Te). The coefficient of variation of RMSE (Cv(RMSE)) is used as a metric of the goodness of fit and is listed in Table 4.

Fig 1: Please include units for the effective Henry's law constant. Also I feel this belongs in the Supplementary Information. The temperature and pH dependencies of effective Henry's law constant, although are important, do not deserve the spot of the very first figure of this particular paper.

The plot of the temperature and pH dependencies of effective Henry's law constant (Figure 1) is now moved to the Appendix

Fig 4, Fig 6-11: dates on the bottom axis are difficult to read, i.e. it is hard to identify "early Feb" or "early May", ... Please set date tick labels to the first day of each month. If not enough space, rotate 90 degrees.

Figures are now has the first day of each month on the bottom axis and day of year (DOY) on the top of the graph to make it easier to read.

Fig 5: figure legend very unclear. What exactly are the scatter points? And what are "Head 1 1213", "Head 2, 1213", ...?

The figure (now Fig. 4) had been re-plotted and legend been clarified.

Fig 7 & Fig 8: I think these two figures can be combined. Easier to tell the difference between Model 1 and Model 2. Same for Fig 10 & Fig 11.

Fig 7 and Fig 8 are now combined as Fig 6, and, Fig 10and Fig 11 are now combined as Fig 8

Table A1: temperature dependent Henry's law constant: standard temperature in 258K?

The standard temperature for the calculation of temperature-dependent Henry's law is now corrected to 298K

Referee 2
[Major comments]
1. Apparently, there is a loose interchange of what the grain-surface HNO_3 concentration (HNO_3 (surf)) represents while formulating the different processes involved/hypothesized in its determination. In Eq. (6) in Section 3.1.1, the authors simply take the sum of two terms, namely, the concentration due to surface adsorption (HNO_3(ads)) and that due to co-condensation (HNO_3(cc)). Although the unit of (HNO_3(ads)) is carefully matched to allow this summation, I am not so sure if it is really legitimate to assume that all the surface-adsorbed HNO_3 is automatically transferred into the bulk volume of the outermost solid-ice layer of the snow gain. It seems that the authors' claim for employing the first principles is partially broken here. Is it not more appropriate to assume that what happens on the surface stays on the surface and that [HNO_3(ads)] is left out from Eq. (6)? I see the same problem in Eq. (12) in Section 3.1.2 where the authors assume that all the HNO_3 dissolved in the liquid-like disordered interface (HNO_3(DI)) is automatically transferred to the outermost solid-ice layer (HNO_3(surf)). In my opinion, all these assumptions of automatic "phase" transfer (between the surface and the solid ice and between the liquid-like DI and the solid ice) should be adapted somehow to the one in compliance with the limitation of HNO_3 solubility to the solid ice (Thibert et al., 1998). The authors run an alternative model by calling it the "equilibrium approach", which I think should be adopted as a base case except that kinetic aspects should be formulated into this version of the model.

In the models, the solid-state diffusion into the grain is driven by the concentration gradient between the grain boundary and the centre of the grain and regulated by the solid-state diffusion coefficient (Thibert et al., 1998).

Abbatt, (1997), Huthwelker et al., (2004) and Cox et al., (2005) had observed a diffusion-like behaviour from flow tube study for trace gases uptake onto ice. The structure of the model presented in this paper is based on the suggestion from these references. References regarding the concurrence of surface adsorption and solid-state diffusion are now included in Sect. 2.2, Line 149- 151.

'A diffusion-like behaviour has been observed from flow tube studies for trace gas uptake onto ice (e.g. Abbatt, 1997; Huthwelker et al., 2004; Cox et al., 2005) and suggested the solid-state diffusion of nitrate molecules can occur concurrently with surface adsorption, such that …'

The reasons for adopting a kinetic approach instead of an equilibrium approach are listed in Sect. 3.1.1 and Sect. 6.1. The ice solubility parameterisation by Thibert et al., (1998) was obtained after exposing the ice with gaseous HNO_3 for a period of 1-4 weeks, however, no information and no conclusion on the time taken to reach equilibrium was presented.

2. The authors do not provide sufficient details about their model formulation of the disordered interface (DI) on the surface of the ice grain. How thick is the DI? Does the thickness of the DI change with temperature? Does it make sense to assume the fixed (constant) pH especially when the chemical composition of the DI is controlled predominantly by $HNO_3(gas) = H^+(DI) + NO_3^-(DI)$ at Dome C? These are the critical points that should be discussed in detail before rejecting the hypothesis of the HNO_3 incorporation into the DI.

The DI is treated as the boundary layer of the snow grain. The concentration of DI is used as the boundary condition for the solid-state diffusion of nitrate into the snow grain. Therefore, no thickness is assigned to the DI.
For clarification, the following lines (Page 9, line 275-277) are now included in the manuscript.
"Note that in this model the DI is treated as the boundary between the air and bulk ice. The concentration of the DI is used as the outermost boundary condition for solid- state diffusion within the grain, therefore, the DI has no arbitrary thickness."

The sensitivity of Model 1 to the value of pH in the range of pH found in natural surface snow (5-6.5, Udisti et. al, 2004) is shown in Table 4. Changing the pH within this range does not have an impact on the model performance.

3. It is not clear enough whether the kinetic limitation to the growth and decay of the snow grain HNO_3 concentrations is caused mainly by mass transfer between the gas phase and the grain surface or by solid diffusion into the entire volume of the snow gain. This question should be discussed in some detail especially when contrasting the behavior of HNO_3 between the "kinetic" and "equilibrium" approaches such as in Section 6.1. Also, the authors may want to refer to the work by Bock et al. (2016) on the matter of timescales due to various kinetic processes.

A table of the characteristic times of various physical processes are listed in Table 1. At low partial pressures of HNO_3, the characteristic time for surface adsorption to reach equilibrium is of the order of 10^3 s.

4. I am puzzled by the description of the rate of snow grain growth and shrinkage in Section 3.1.1. Eq. (9) implies that the change of the snow grain volume is calculated by the molecular diffusion of water vapor through its microscopic concentration gradient around the snow grain. But then the authors admit that this approach does not work owing to the input data limitation and instead "the macroscopic (few mm) water vapour gradient across the skin layer was used to estimate the condensation and sublimation processes". Is the same equation still used for calculating dV/dt?
For clarification now on Page 8, line 253-256 now read:
"For simplicity the macroscopic (few mm) water vapour gradient across the skin 240 layer was used to estimate the rate of volume change of snow grain due to condensation or sublimation, i.e. $(d\rho\upsilon /dx)x=r$ in Eq. 10 is replaced by $(d\rho\upsilon /dz)\ z=4mm$."

In Sections 4.1 and 4.2, the authors state that meteorological input data have been obtained at 1.6 m and 1 m above the snow surface at Dome C and Halley, respectively. Is it then assumed that the water vapor concentrations are assumed to be constant with height between a few mm and 1-1.6 m above the snow surface? Please clarify.
Information regarding the relative humidity used for calculation of water vapour gradient has been clarified in Sect 4.1, line 372-373
"Based on the assumption of a well mixed boundary layer, the RH above the snowpack surface was assumed to be the same as what measured at 1.6 m"

Also, is it possible to validate the authors' macroscopic approach of calculating the water vapor flux by field observations if any? This seems to be important as background information for discussing the role of co-condensation in Section 6.2.
Reference to an observed temperature gradient across the top 2 cm of the snowpack at Dome C has been added to support the statement in Sect 3.1.1, Line 227-231

"Field observations (Frey et al., 2013) and the results from a heat transfer model (Hutterli et al., 2003) at Dome C in summer show absolute temperature gradients of 71 K m^{-1} across the tope 2 cm and 130 K m^{-1} across the top 4 mm of the snowpack, respectively. "

By the way, I think R_{eff} in Eq. (9) should be squared to be consistent in the physical dimension between LHS and RHS of the equation. Is it simply a typographic error?
Yes, the error in Eq 9. is now fixed, thank you.

5. The authors adopt the formulation of the $\alpha 0$ (Hudson et al., 2002), N_{max} (Crowley et al., 2010) and K_{eq} (Burkholder et al., 2015) from different sources. In fact, all of these could have been adopted from Crowley et al. (2010). It seems appropriate to discuss why the authors pick their experimental values/formulae from the different sources and how much difference their choice would generate in the model behavior.
Information and reasons for the choice of parameterisation are now listed in the Appendix.

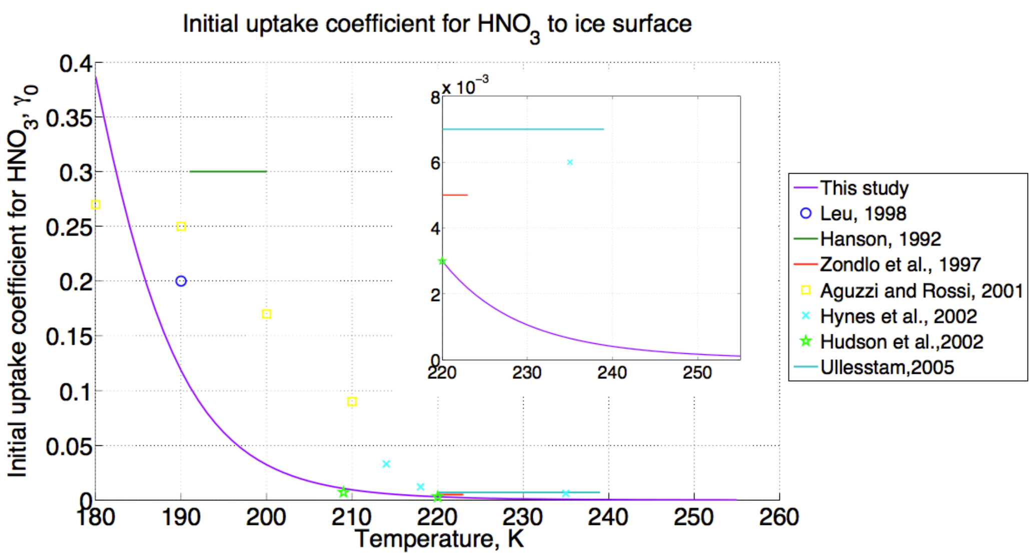

Figure A2. Initial uptake coefficient for HNO_3 as a function of temperature obtained from different studies. The parameterisation used within this study is formulated in Table A1 and is chosen to give the best representation of the dependency on temperature.

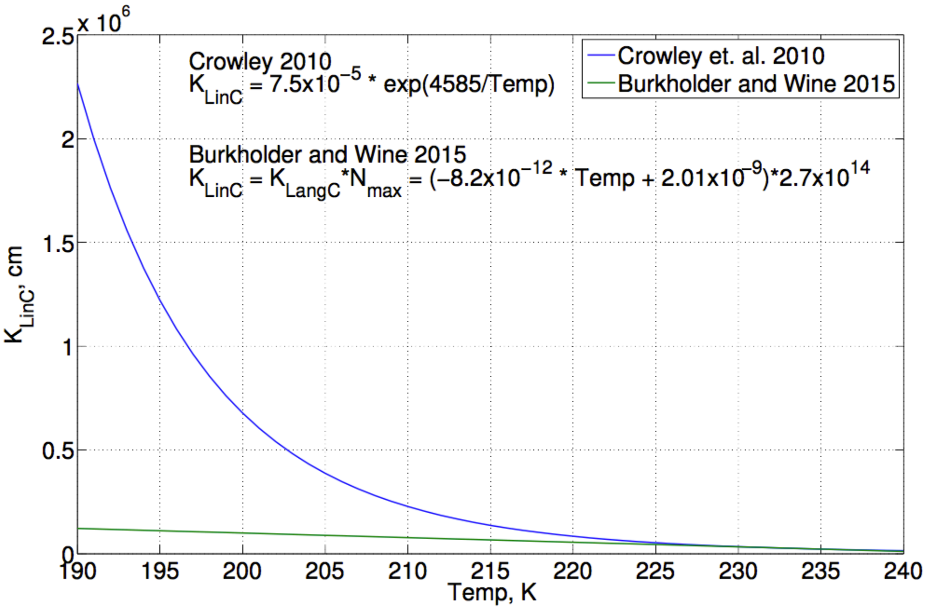

Figure A3. Langmuir adsorption equilibrium constant, $K_{\mathrm{LinC}} = K_{eq} \times N_{\mathrm{max}}$. The preferred temperature range for both parameterisation is 214-240 K and within this range the two parameterisations provide a comparable value. The Crowley et al. (2010) parameterisation deviate from the Burkholder and Wine (2015) parameterisation as temperature drop below 214 K due to the exponential temperature term. Here, the parameterisation from Burkholder and Wine (2015) was chosen based on the extreme cold temperature found in our validation sites.

6. The quality of English needs to be improved significantly. There are so many grammatical and spelling errors, only a tiny part of which I can comment below as technical suggestions. This problem is really glaring but may be largely corrected by a copyeditor once the manuscript is accepted for publication. Nonetheless, there seems to be a room for improvement that should be addressed by the authors before that stage. I strongly recommend careful and diligent proofreading by the team of the authors (especially if the editor asks another round of review).

[Minor comments]
1. I think that “T – Tf” should be reversed to “Tf – T” in Eq. (4) to let φH2O(T) be the positive values. And I think that this inherits from what I believe is a typographic error in Cho et al. (2002) cited for Eq. (4). Am I wrong? Please double check.
It is inherited from a typographic error in Cho et al (2002) and it is corrected now to “Tf - T”.

2. The variable “z” refers to the distance from the snow grain surface in Eq. (9), whereas it refers to the depth in the snowpack in Eq. (11). Please adjust the notation to avoid confusion between the two.
The variable “z” is replaced by variable “x” to avoid confusion for representing the microscopic distance.

3. On Line 92, it is stated that “thickness of the DI” is a tuning parameter in Toyota et al. (2014). In fact, they calculate the thickness of the DI on the basis of the Cho et al. formula, which is used by the present authors for calculating the volume of the micro pockets of brine. The difference from the present study is

that Toyota et al. assume the brine covers the entire surface of the snow grain just like the DI.
Yes, sorry for incorrect information. The statement has been removed.

4. On Line 255, it is stated that "Dg is the gas-phase diffusivity". It should be stated clearer that Dg is the gas-phase diffusivity of HNO_3. It would also be nice to list how D_g is calculated in Table A1.
The calculation of D_g is now listed in the footnote of Table 1.

5. Lines 615-616: It appears to me in Figure 1 that the changes in pH of the order of 1 have a similar level of impact on the effective Henry's law coefficient to the changes in temperature of the order of 10 K. I don't quite understand what the authors try to point out here.
The sentence has been removed.
The sensitivity of Model 1 to pH is now on Page 21, line 677 – 682

6. Lines 558-562, ". . ., which are 1-2 orders of magnitude higher than the averaged modelled temperature gradient (listed in Sect. 3.1.1)": It seems that this is not discussed/listed at all in Section 3.1.1. Please expand the discussion by referring to what the realistic range of the vertical temperature gradient should be.
Reference to Frey et. al (2013) is included (Page 7, line 215 and Page 18, line 589).
Frey et. al (2013) measured a temperature gradient of 71 Km^{-1} across the top 2 cm of snowpack in Dome C.

7. Lines 625-631 and Figure 11: Please be more specific and detailed about what make up the "other ions".
Fig. 11 is now in Fig. 8B and the caption has been changed to
"…other ions, where other ions refers to the sum of [Na+] and [Cl−]"

8. Table A1: Sander (2015) is a compilation of Henry's law coefficients, but here it is cited for the temperature dependence of alpha. Please double check if it is the correct reference. Also, the "enthalpy of activation" is much too vague as terminology for ΔobsH. Please expand.
ΔobsH is now referred to as the enthalpy of uptake. Reference to Thomas (2011) is used instead of Sander (2015).

9. Table A1, values of ΔsolH and ΔobsH: I think they should have been −72.3 and −44, respectively (the minus sign is missing). Please double check. 10.
Yes, has been corrected.
Table A1, footnote i: I suppose that the authors meant to formulate the temperature dependence of alpha somehow consistently with $d\ \ln[\alpha/(1-\alpha)]/d(1/T) = -\Delta_{obs}H/R$ (e.g., Jayne et al., 1991). But I cannot reconcile with the authors' formulation in this footnote. Am I wrong here? Please double check if it is formulated properly.
The listed formulation is the integrated form of the equation from Jayne et al., 1991

[Technical suggestions]
Line 216: d HNO_3 / dt -> d [HNO_3(ads)] / dt
Yes, has been corrected.

Line 217: Substituting kads -> Substituting kdes
Yes, has been corrected.

Line 321: organic -> inorganic (?)
Yes, has been corrected.

Line 407: tough -> trough (?)
The sentence has been removed.

Line 414, Eq. (19): MM_{H2O} -> M_{H2O}
Yes, is now corrected.

Line 603: . . . varying T0 by 4 K up to 242 K and pH by ±0.4 up and down between 5.2-6.4
The sentence is now removed.

Figure 1: Add the unit of temperature for the figure legends in (b): "T = 230 K", etc.
The units have been added to the figure legend.

Figure 10: Is it not possible to use the same scaling in Y-axis for all the data shown here, for example, by using logarithmic scaling?

Table A1: Accommodation coefficient at standard temperature -> Accommodation coefficient at reference temperature (220 K)
Yes, has been corrected.

Table A1, footnote ii: 258 K -> 298 K (?)
Yes, has been corrected.

Manuscript prepared for Atmos. Chem. Phys.
with version 2014/09/16 7.15 Copernicus papers of the LaTeX class copernicus.cls.
Date: 20 April 2017

Modeling the Physical Multi-Phase Interactions of HNO_3 Between Snow and Air on the Antarctic Plateau (Dome C) and coast (Halley)

Hoi Ga Chan[1,2], Markus M. Frey[1], and Martin D. King[2]

[1]British Antarctic Survey, Natural Environment Research Council, Cambridge, CB3 0ET,UK
[2]Department of Earth Sciences, Royal Holloway University of London, Egham, Surrey, TW20 0EX, UK

Correspondence to: Hoi Ga Chan
(hohan47@bas.ac.uk)

Abstract. ~~Nitrogen oxides~~ Emission of nitrogen oxide (NO_x = NO + NO_2) ~~emissions from~~ from the photolysis of nitrate (NO_3^-) ~~photolysis~~ in snow affect the oxidising capacity of the lower troposphere especially in remote regions~~of the~~ , of high latitudes with ~~low pollutionlevels. The porous structure of snowpack allows the exchange of gases with the atmosphere driven by physicochemical processes, and hence, snow can act as both source and sink of atmospheric chemical trace gases. Current~~ little pollution. Current air-snow exchange models are limited by poor ~~process understanding~~ understanding of processes and often require ~~tuning parameters, for example the recently developed air-snow exchange model by ? requires an unrealistically large growth rate of snow grains to explain the peak in surface snow at Dome C in the summer~~unphyiscal tuning parameters. Here, two ~~multi-phase physical~~ physical multi-phase models were developed from first principles ~~constrained by observed atmospheric nitrate, ,~~ to describe the ~~air-snow~~ interaction of nitrate ~~. Similar to most of the previous approaches, the first model~~ between the surface layer of the snowpack and the overlying atmosphere. The first model is similar to previous approaches and assumes that below a threshold temperature, T_o, the air-snow grain interface is pure ice and above T_o, a disordered interface (DI) emerges ~~assumed to be~~ covering the entire grain surface. The second model assumes that ~~Air-Ice~~ air-ice interactions dominate over ~~the entire temperature range below melting and that only above the eutectic temperature, liquid is present in the form of micropockets in grooves~~all temperatures below melting of ice and that any liquid is concentrated in micropockets above the eutectic temperature. The models are ~~validated~~ used to predict the nitrate in surface snow with available year-round observations of ~~nitrate in snow and~~ mixing ratios of nitric acid in air at a cold site on the ~~Antarctica~~ Antarctic Plateau (Dome C, $75^\circ 06'S, 123^\circ 33'E$, 3233 m a.s.l.) and at a relatively warm site on the ~~Antarctica~~ Antarctic coast

(Halley, $75^{\circ}35'\mathrm{S}, 26^{\circ}39'\mathrm{E}$, 35 m a.s.l). The first model agrees reasonably well with observations at Dome C ($\mathrm{C_v(RMSE)}$ = 1.34), but performs poorly at Halley ($\mathrm{C_v(RMSE)}$ = 89.28) while the second model reproduces with good agreement observations at both sites ~~without any tuning~~ ($\mathrm{C_v(RMSE)}$ = 0.84 at both sites). It is therefore suggested that in winter air-snow interactions of nitrate ~~in the winter~~ are determined by non-equilibrium surface adsorption and co-condensation on ice coupled with solid-state diffusion inside the grain, similar to **?**. In summer, however, the air-snow exchange of nitrate is mainly driven by solvation into liquid micropockets following Henry's law with contributions to total surface snow $\mathrm{NO_3^-}$ concentrations of 75% and 80% at Dome C and Halley respectively. It is also found that liquid volume of the snow grain and air-micropocket partitioning of $\mathrm{HNO_3}$ are sensitive to both the total solute concentration ~~and pH. In conclusion, the~~ of mineral ions within the snow and pH of the snow. The second model can be used to predict nitrate concentration in ~~surface snow~~ the surface snow layer over the entire range of environmental conditions typical for Antarctica and forms a basis for a future full 1D snowpack model as well as parameterisations in regional or global atmospheric chemistry models.

1 Introduction

Emissions of nitrogen oxides, $\mathrm{NO_x}$ = NO + $\mathrm{NO_2}$, from snow to the overlying air as a result of photolysis of the nitrate anion, $\mathrm{NO_3^-}$, within snow have been observed in polar (**??**) and ~~midlatitudes~~ midlatitude regions (**?**). They were found to have a significant impact on the oxidising capacity of the atmospheric boundary layer, especially in remote areas~~;~~, such as the polar regions, where anthropogenic pollution is ~~rare~~ small (**?**). The cycling of NO and $\mathrm{NO_2}$ in the troposphere alters the concentration of tropospheric ozone, $\mathrm{O_3}$, partitioning of hydroxy radicals, $\mathrm{HO_x}$, and organic peroxy radicals, $\mathrm{RO_x}$. Tropospheric ozone is a pollutant and a greenhouse gas, and changes in the concentration can ~~alter~~ impact the regional energy balance and therefore climate (**?**). Conversely, $\mathrm{HO_x}$ radicals are responsible for removal of many atmospheric pollutants ~~(?)~~(e.g. **?**), such as the greenhouse gas methane, and $\mathrm{RO_x}$ radicals play an important role in the oxidation of volatile organic compounds (VOCs). ~~There is a great need to understand more about the interaction of reactive nitrogen (= + + + + + + PAN + Organic Nitrates) between the atmosphere and snowpack, not only to predict the regional and global chemical transport and climate, but also crucial for interpreting the ice core record of . Both chemical and physical (post-)depositional processes have a strong influence on concentration preserved in snow and ice (?), and therefore~~ Moreover, the post-depositional nitrate loss from snowpacks in complicated the interpretation of polar ice core nitrate. To extract paleoclimatic information from the ice core, the interactions between the atmosphere and the snowpack need to be understood~~to enable reconstruction of past atmospheric nitrogen from ice core data~~.

The ~~physical~~ exchange of nitric acid, HNO_3, between the atmosphere or snow interstitial air (SIA) and snow ~~grain is complex. Gaseous can be taken up by different reservoirs in snow, for example it can be diffused into the ice crystal and formed solid solution or be adsorbed on the ice surface or be co-condensed to the growing ice or be dissolved to the liquid solution located in grain boundaries, grooves at triple junctions or quadruple points. Therefore, the air and snow grain form a complex multiphase interface (?)~~grains is complex, and is controlled by chemical and physical processes. The relative contribution of the chemical and physical processes has been a matter of debate (?). Isotopic studies (??) have shown photolysis of NO_3^- is the dominating loss process of NO_3^- in snow~~(??). However, the physical uptake processes of are overwhelming the photochemical loss at the skin layer snow (the top few of the snowpack). The typical nitrate photolysis rate ,~~ . Based on a typical photolysis rate coefficient of nitrate, $J_{NO_3^-}$ ~~, values measured in Antarctica in the summer are on the order of 10^{-7}, for example, ? shows the surface snow $J_{NO_3^-}$~~ $\approx 1 \times 10^{-7}\ s^{-1}$ (at the surface in Dome C at a solar zenith angle of 52°, ~~the maximum solar elevation at Dome C. Therefore, in Antarctica~~ ?), the characteristic time for ~~photochemical lost is around 10^7~~ nitrate photolysis is $\sim 10^7$ s. ~~With the general temperature range found in Antarctica, 0° – -60°, the~~ The characteristic time of ~~physical processes such as~~ nitrate photolysis is much larger compared to other physical processes near the snowpack surface, such as grain surface adsorption and solid-state diffusion ~~for are on the order of 10^2-10^3 and 10^4-10^6 respectively, much shorter than the characteristic time for the photochemical process~~(Table ??). The top few mm of snowpack, hereafter called the skin layer and the focus region of snowpack in this paper, the physical uptake of nitrate is much quicker than the chemical loss due to the availability of nitric acid at the snowpack surface. Therefore, ~~photochemical reactions of are neglected in this study.~~ it is assumed that the chemical processes are negligible and consider only the physical processes. The skin layer is defined as the top 4 mm of the snowpack, which is the depth of which the surface snow nitrate samples were collected at Dome C (Sect. ??).

~~A quantitative mechanistic understanding of the role of the physical processes is still poor. Models~~ The physical exchange of nitric acid, HNO_3, between the atmosphere or snow interstitial air (SIA) and snow grain are complex. Gaseous HNO_3 can be taken up by different reservoirs in snow, for example the molecule can 1) adsorb on the ice surface; 2) diffuse into the ice crystal and form solid solution; 3) co-condense to the growing ice or 4) dissolve into the liquid solution located in grain boundaries, grooves at triple junctions or quadruple points. Therefore, the air and snow grain form a complex multiphase interface (?).

Air-snow models have been developed to predict the ~~coupling~~ exchange of trace gases between the snowpack and the overlying atmosphere ~~. Some of the 1D~~ and the greatest challenge faced currently is the model description of the air-snow ~~and chemical models assumed an 'Air-Liquid/Disordered Interface' between snow grain and its surrounding air (e.g. ????). The~~ grain interface. One group of models assume a disordered interface, DI, ~~is~~ at the snow grain surface with liquid-like properties (e.g. ????). The DI is defined as a thin layer on the surface of the snow grain and ~~, in general,~~ is assumed to have the following characteristics; 1) DI reaction and partition rate constants are similar ~~as~~ to those in the aqueous phase, e.g. ~~using~~ Henry's Law coefficient are used to describe the partitioning between the ~~2~~ two phases; 2) DI thickness ranges from <1 to a few hundreds nm (**?**) but is often set to an arbitrary value~~in models~~, e.g. ~~both ? and ? assumed the DI is~~ 10 nm ~~thick~~(**?**) and **?**; 3) ~~The DI is where~~ These models also assume all (**?**) or a fraction (**??**) of the total solutes are located in the DI.

~~Instead of an 'Air-DI' interface, other models assuming~~ Another groups of models assume the interface between snow grain and surrounding air to be ~~'Air-Ice'~~ ice (e.g. **??**). The distribution of hydrogen peroxide, H_2O_2, and formaldehyde, HCHO, within the snowpack has been estimated using a physical ~~air-snow-firn~~ air-snow and firn transfer model which included a temperature driven 'Air-Ice' uptake and release (**??**). The air-ice exchange of H_2O_2 is defined by solid-state diffusion of H_2O_2 whereas the exchange of HCHO is described by linear adsorption isotherm ~~. The~~ of H_2O_2 on ice. A physical exchange model has been developed by **?** to describe the concentration of NO_3^- in the skin layer ~~of the snowpack~~ at Dome C, East ~~Antartica Plateaubeen estimated using a physical exchange model (?). They proposed , at Dome C,~~ Antarctic Plateau. **?** proposed the skin layer snow nitrate concentration at Dome C is determined by thermodynamic equilibrium ice solubility on the grain surface (based on a parameterisation by **?**) followed by solid-state diffusion during winter. ~~In the summer , the large~~ During summer the large increase in NO_3^- ~~concentrations in~~ concentration in the skin layer snow ~~are mainly contributed by~~ is mainly from co-condensation of ~~and~~ HNO_3 ~~,~~ and H_2O (a kinetic process~~, rather than equilibrium solubility coupled with solid-state diffusion. ? suggest there is no lost~~). The model of **?** implies no loss of NO_3^- due to ~~co-sublimilation (volatilisation) at all time during the summer, which ?~~ sublimation, a process that has been suggested to be ~~one of the important physical processes. A common aspect among all these models mentioned above with an 'Air-DI' or 'Air-Ice' interface, is they~~ important in surface snow dynamic (**?**). Both types of models require tuning parameters, for example fraction of solute in the DI (**?**), ~~thickness of the DI (?),~~ ion partitioning coefficients (**?**), or co-condensation parameter (**?**), to match the model predictions with the field observations and hence ~~limit their~~ are of limited predictive capacity.

The aim of this paper is to develop a physical exchange model from first principles to describe the exchange ~~processes~~ of nitrate between the atmosphere and the skin layer ~~snow without requiring any tuning parameters~~ of snow minimising the number of tuning parameters and is a first step towards a full snowpack model that would include deeper snow and other processes, such as wind pumping, molecular diffusion, and photochemistry. Two temperature dependent, multi-phase models, are developed to evaluate two different concepts to describe the interaction of nitrate between air and snow~~nitrate~~. Model 1 is based on the hypothesis of the existence of a DI layer ~~cover~~ covering the entire snow grain above a threshold temperature, T_o (Sect. **??**). Below T_o, the interface between snow grain and air is assumed to be 'Air-Ice', ~~which the concentration~~ and the grain surface concentration of NO_3^- is determined by non-equilibrium surface adsorption ~~, in contrast to ? equilibrium approach,~~

and co-condensation coupled ~~to~~ with solid-state diffusion into the grain. Above T_o, the interface is assumed to be 'Air-DI' of which the $\mathrm{NO_3^-}$ concentration is defined by non-equilibrium solvation ~~in~~ into the DI followed by solid-state diffusion. Model 2 is based on the hypothesis of ~~the co-existence of liquid and ice above the~~ **?**, that liquid co-exists with ice above eutectic temperature, T_e~~, and the liquid is in the form of micropockets located~~. The liquid forms micropockets and locate in grooves at grain boundaries or triple junctions due to limited wettability of ice (**?**). Therefore, at all ~~temperature~~ temperatures below melting the major interface between air and snow grain is assumed to be ~~'Air-Ice', of which the concentration is described by the same 'Air-Ice' processes mentioned above. In the presence of liquid, i.e. above~~ pure ice. Above T_e, the partitioning of $\mathrm{HNO_3}$ to the ~~micropocket~~ micropockets is described by ~~equilibrium~~ Henry's Law (Sect. **??**). ~~The~~ Both models are validated with data collected at two sites in Antarctica that have very different atmospheric composition, ~~temperature range and humidity~~temperatures and humidities; The East Antarctic Plateau at Dome C and secondly coastal Antarctica at Halley, where ~~long term~~ long-term atmospheric and meteorological observations are monitored at the Clean Air Sector Laboratory (CASLab) (**?**).

2 Current Understanding of ~~Air-Snow~~ Physical Air-Snow Processes

2.1 ~~Air-Ice Interface: Surface Adsorption~~

~~Adsorption occurs in the ice stability region of the phase diagram.~~ Below we briefly review the current understanding of physical air-snow processes, which are relevant to nitrate. A more comprehensive discussion can be found in the recent review paper (**?**).

2.1 Surface Adsorption at the Air-Ice Interface

The probability of a gas molecule being adsorbed on a clean ice surface can be described by the dimensionless surface accommodation coefficient, α (**?**). The adsorbed molecule can then be desorbed thermally ~~if the bond to the surface site is weak~~ or it can be ~~diffused~~ dissociated and diffuse into the bulk and form a solid solution ~~. The~~ (**???**). At a low partial pressure of $\mathrm{HNO_3}$, the adsorption of $\mathrm{HNO_3}$ ~~can be explained by~~ on an ice surface can be expressed as the single-site Langmuir adsorption ~~even at low partial pressures (?) and the mechanism is as follow~~(**?**) with:

$$\mathrm{HNO_{3,(g)}} + \mathrm{S} \underset{k_{\mathrm{des}}}{\overset{k_{\mathrm{ads}}}{\rightleftharpoons}} \mathrm{HNO_{3,(ads)}} \tag{R1}$$

where ~~(g) and (ads)~~ $\mathrm{HNO_{3,(g)}}$ and $\mathrm{HNO_{3,(ads)}}$ are the gas-phase and surface adsorbed ~~nitrate~~nitric acid. [S] is the ~~surface site concentration~~ concentration of surface sites, i.e. number of site available per unit volume of air ~~(?) and~~ and has a units of molecule $\mathrm{m^{-3}}$. It is defined as follows:

$$[\mathrm{S}] = (1-\theta)\, N_{max} \frac{\mathrm{A_{ice}}}{\mathrm{V_{air}}} \tag{1}$$

Here, θ is the fraction of ~~maximum~~ avilable surface sites being occupied, N_{max} is the maximum number of surface sites with a unit of molecule $\mathrm{m_{ice}^{-2}}$, $\mathrm{A_{ice}}$ is the surface area of ice per unit volume of snowpack with a unit of $\mathrm{m}^2_{\mathrm{ice}}\ \mathrm{m}^{-3}_{\mathrm{snowpack}}$, and $\mathrm{V}_{\mathrm{air}}$ is the volume of air per unit volume of snowpack with a unit of $\mathrm{m}^3_{\mathrm{air}}\ \mathrm{m}^{-3}_{\mathrm{snowpack}}$. ~~All concentration units are in .~~The adsorption coefficient, k_{ads} ,and desorption coefficient, k_{des}, in **??** ~~can be expressed~~ are defined as

$$k_{\mathrm{ads}} = \frac{\alpha\overline{v}}{4}\frac{1}{N_{max}} \tag{2}$$

$$k_{\mathrm{des}} = \frac{k_{\mathrm{ads}}}{K_{\mathrm{eq}}} \tag{3}$$

Note that k_{ads} has ~~an~~ a unit of $\mathrm{m}^3\ \mathrm{molecule}^{-1}\ \mathrm{s}^{-1}$ while the unit of k_{des} is s^{-1}~~. Here~~ , $\overline{v}$ is the average ~~gas phase~~ gas-phase molecular speed and K_{eq} is the equilibrium constant for Langmuir adsorption ~~of onto~~ on ice with a unit of $\mathrm{m}^3\ \mathrm{molecule}^{-1}$. The value of K_{eq} for $\mathrm{HNO_3}$ is inversely correlated with temperature ~~that~~ because the scavenging efficiency of ~~gas-phase~~ $\mathrm{HNO_3}$ ~~via~~ due to adsorption increases as temperature decreases. The parameterisations ~~used within this study for~~ and values for the above variables used in this study are listed in App. **??** Table **??**. A comparison of different parameterisations of α ~~, N_{max}, $\overline{v}$,~~ and K_{eq} are ~~listed~~ shown in App. **??** ~~.~~Fig. **??** and **??** respectively.

2.2 Solid-State ~~diffusion~~Diffusion

~~The nitric acid has a sufficient~~ A solid solution of $\mathrm{HNO_3}$ can be formed in ice due to its solubility and diffusivity~~in ice (~~. The solid-state diffusion in natural snow is found to be an important process for understanding the partitioning of highly soluble gases, including $\mathrm{HNO_3}$, between atmosphere and snow when interpreting the composition of environmental ice (**?**). **?** derived a solid-state diffusion coefficient, k_{diff}~~$\approx 7\times10^{-15}$ at 253 , ?) that a solid solution can be formed. ? shows~~, and a thermodynamic solubility of $\mathrm{HNO_3}$ in ice from sets of $\mathrm{HNO_3}$ concentration - diffusion profiles obtained by exposing single ice crystal to diluted $\mathrm{HNO_3}$ at different temperatures for a period of days to weeks. However, **?** did not present the the kinetics of $\mathrm{HNO_3}$ uptake on ice and a characteristic time for equilibrium between air and ice could not be established. A diffusion-like behaviour has been observed from flow-tube studies for trace gas uptake onto ice (e.g. **???**) suggesting the solid-state diffusion of nitrate molecules can occur concurrently with surface adsorption, such that

$$\mathrm{HNO}_{3,\,(\mathrm{ads})} \overset{k_{\mathrm{diff}}}{\rightleftarrows} \mathrm{HNO}_{3,\,(\mathrm{ice})} \tag{R2}$$

where ~~k_{diff} is the solid diffusion coefficient (App. ??) and (ice) is the nitrate solid state~~ $\mathrm{HNO}_{3,\,(\mathrm{ice})}$ is the nitric acid incorporated into the ice matrix~~. ? also concluded that solid-state diffusion in natural snow can be an important process for understanding the partitioning of highly soluble trace gases, such as , between atmosphere an snow and when interpreting the composition of environmental ice~~, occurs with **??**.

2.3 Coexistence of Liquid Solution with Ice

Liquid aqueous solution coexists with ice in the presence of soluble impurities, such as sea salt and acids~~,~~. The liquid exist down to the eutectic temperature ~~of ice and~~ defined by the composition and solubility of the impurities in the ice. **?** parameterised the ~~respective impurity. **?** parameterise the~~ liquid water fraction, ~~$\phi_{\mathrm{H_2O}}$, as~~ $\phi_{\mathrm{H_2O}}(T)$, as a function of total ionic concentration of impurities, $\mathrm{Ion_{tot}}$,and temperature as follows:

$$\phi_{\mathrm{H_2O}}(T) = \frac{\overline{m}_{\mathrm{H_2O}} R T_f}{1000 \Delta H_f^0} \left(\underline{\frac{T}{T - T_f}} \, \frac{T}{T_f - T} \right) \Phi_{\mathrm{bulk}}^{\mathrm{aq}} \left[\mathrm{Ion_{tot\,(bulk)}} \right] \tag{4}$$

where ~~$\phi_{\mathrm{H_2O}}$ has an unit~~ $\phi_{\mathrm{H_2O}}(T)$ has a units of $\mathrm{m^3_{liquid}\ m^{-3}_{ice}}$, $\overline{m}_{\mathrm{H_2O}}$ is the molecular weight of water, R is the ideal gas constant, T_f is the freezing temperature of pure water in K, ΔH_f^0 is the enthalpy of fusion in $\mathrm{J\ mol^{-1}}$, $\Phi_{\mathrm{bulk}}^{\mathrm{aq}}$ is the fraction of the total solute in the aqueous phase and $[\mathrm{Ion_{tot,\,bulk}}]$ is the total ionic concentration in the ~~unfrozen bulk~~melted sample. There are different hypothesises on the ~~locations~~ location of the liquid solution. ~~Some (e.g. **?**) assumed~~ Most studies assume the liquid solution forms a thin layer covering the whole grain surface (e.g. **?**) while **?** suggested the liquid is located in grooves at grain boundaries and triple junctions. ~~His arguments~~ The arguments of the latter study were 1) ~~The~~ the ionic concentration is low in natural snow that only small amount of liquid can be ~~form~~formed; and 2) ~~The wettability of~~ the wettability of liquid water on ice is imperfect~~. These arguments imply the layer thickness could~~ , preventing the liquid drop from spreading out across the solid surface. The volume of liquid is small relative to the ice grain and if spread uniformly across the ice grain the thickness would be less than a ~~monolayer solution if the liquid were covering the entire grain surface,~~ molecule which is unrealistic.

The partitioning of trace gases between air and the liquid fraction of snow can be described by Henry's law using the effective dimensionless Henry's law coefficient, $k_{\mathrm{H}}^{\mathrm{eff}}$, according to **?**

$$k_{\mathrm{H}}^{\mathrm{eff}} = k_{\mathrm{H}}^{\mathrm{cc}} \frac{\mathrm{K_a}}{[\mathrm{H^+_{(aq)}}]} \tag{5}$$

where $k_{\mathrm{H}}^{\mathrm{cc}}$ is the dimensionless temperature dependent Henry's Law coefficient (See App. **??**), $\mathrm{K_a}$ is the acid dissociation constant and $[\mathrm{H^+_{(aq)}}]$ is the concentration of hydrogen ions. Fig. **??** shows the temperature and pH dependence of $k_{\mathrm{H}}^{\mathrm{eff}}$. At a given pH, ~~the $k_{\mathrm{H}}^{\mathrm{eff}}$ at 230 is a factor greater than 200 larger than the value at 270~~ varies by a 2 orders of magnitude between -40°C and 0°C. While at a given temperature, ~~within the range of pH in~~ $k_{\mathrm{H}}^{\mathrm{eff}}$ varies within one order of magnitude (See Fig. **??**), for typical pH value of natural surface snow (5 - 6.5, **?**)~~, the values remain in the same order of magnitude~~.

3 Modelling Approach

~~Two physical exchange models, Model 1 and 2, are developed from first principles to calculate the concentration of in the skin layer of snowpack. Model constraints are~~

The model constraints are the ~~observed atmospheric~~ observed atmospheric concentration of $\mathrm{HNO_3}$~~concentration~~, air temperature, skin layer temperature, atmospheric pressure and humidity. The loss or gain in the atmospheric concentration of $\mathrm{HNO_3}$ due to the mass exchange between air and snow are included implicitly by constraining the models with the observed atmospheric concentration of $\mathrm{HNO_3}$. The aim of this paper is to focus on the exchange mechanisms of $\mathrm{HNO_3}$ between air and snow to predict the concentration of nitrate in snow, limited to the skin layer, as a first step towards a full snowpack model. The following assumptions were made, 1) homogenous physical properties across the skin layer, ~~air temperature, skin layer snow temperature, atmospheric pressure and atmospheric humidity.~~ such as snow density and specific surface area (SSA). 2) the concentration of $\mathrm{HNO_3}$ in SIA is the same as the overlying atmosphere due to a short characteristic time scale of $\sim 10^0$ s (Table **??**).

For simplicity, the snow ~~grains are~~ grain is assumed to be ~~spherical and constant in morphology~~ a radially symmetrical sphere with a radius, $\mathrm{R_{eff}}$, which is estimated from the SSA as the follows:

$$\mathrm{R_{eff}} = \frac{3}{\rho_{\mathrm{ice}}\,\mathrm{SSA}} \tag{6}$$

where ρ_{ice} is the density of ice. In addition, the grain morphology is also assumed to be constant, i.e. snow metamorphism is not taken into account.

3.1 Model 1 - Surface Adsorption/Solvation & Solid Diffusion

~~Different processes are used to define the grain surface concentration depending on the temperature. The detection of the disordered layer on the outer of a pure ice surface starts~~ In Model 1, the uptake of $\mathrm{HNO_3}$ is treated as a two-step process consisting of interfacial mass transport across the air-snow grain boundary and subsequent diffusion into the bulk. Below a threshold temperature, T_0, (Sect. **??** & Fig. **??**a) the concentration of nitrate at the snow grain boundary is defined by the combination of adsorption and co-condensation . Above T_0, the snow grain boundary concentration is defined by solvation governed by Henry's law into the disordered interface, DI, (See Sect. **??** & Fig. **??**b). A DI on pure ice has been detected between 238 and 270 K depending on the ~~measuring~~ measurement technique (**?** and references therein). ~~Here, the~~ The threshold temperature, T_o, for the work described here is set to the lower end of the range ~~of observation, 238 , such that below T_o, the grain surface is assumed to be ice and its concentration is described by the combination of non-equilibrium kinetic adsorption and co-condensation (Sect. ?? and Fig. ??a). When temperature is above T_o~~ (~~=~~238 K)~~the interfacial layer between air and snow grain is defined as 'Air-DI'. The DI concentration is specified by non-equilibrium kinetic solvation (See Sect. ?? and Fig. ??b). The concentration gradient between the surface of the grain~~ . The difference in concentration of nitrate between the grain boundary and its centre ~~leads to~~ drives the transport of $\mathrm{NO_3^-}$ within the grain, which can be characterised by the solid-state diffusion ~~and formed solid~~ of $\mathrm{NO_3^-}$ ~~solution (sect~~(Sect. **??**).

3.1.1 Ambient Temperature $\leq$ 238 K: Non-Equilibrium ~~Kinetic~~ Surface Adsorption & Co-condensation

~~At temperatures below~~

At a temperature below T_0 = 238 K the interface between air and snow grain ~~surface~~ is assumed to be pure ice. The ~~grain surface concentration~~ concentration of nitrate at the grain boundary, $[\mathrm{HNO}_{3\,(\mathrm{surf})}]$, is determined by a combination of non-equilibrium kinetic adsorption and co-condensation:

$$[\mathrm{HNO}_{3\,(\mathrm{surf})}] = [\mathrm{HNO}_{3\,(\mathrm{ads})}] + [\mathrm{HNO}_{3\,(\mathrm{cc})}] \qquad \text{if} \quad T \leq 238\mathrm{K} \tag{7}$$

where $[\mathrm{HNO}_{3\,(\mathrm{ads})}]$ is the concentration contributed ~~from~~ by the sum of surface adsorption and desorption (Eq. ??), and $[\mathrm{HNO}_{3\,(\mathrm{cc})}]$ is the concentration contributed ~~from~~ by co-condensation ~~.~~ or co-sublimation (Eq. ??).

A non-equilibrium kinetic approach is taken instead of saturation or equilibrium adsorption for ~~three~~ two main reasons: Firstly, **?** have shown that for partial pressures of HNO_3 lower than 10^{-5} Pa the ice surface is not entirely covered and therefore undersaturated. The annual average atmospheric partial pressure of HNO_3 recorded at Dome C is $\sim 10^{-6}$ Pa (**?**) and is $\sim 10^{-7}$ Pa at Halley (**?**), hence, the ice surface is unlikely to be saturated with HNO_3. Secondly, natural snowpacks are constantly undergoing sublimation and condensation of $\mathrm{H_2O}$, especially at the skin layer, due to temperature gradient over a range of timescales from a fraction of seconds to ~~diurnally and seasonally~~ days and seasons (**?**). **?** observed up to 60% of the total ice mass redistributed under a constant temperature gradient of 50 $\mathrm{K\,m^{-1}}$ over a 12 hour period. ~~In Dome C , the modelled (See Sect. ??) mean absolute temperature gradient~~ Field observations (**?**) and the results from a heat transfer model (**?**) at Dome C in summer show absolute temperature gradients of 71 $\mathrm{K\,m^{-1}}$ across the top 2 cm and 130 $\mathrm{K\,m^{-1}}$ across the top 4 mm of the snowpack~~was 130 in summer and 98 in winter and at~~ , respectively. At Halley, the ~~mean~~ modelled summer absolute temperature gradient ~~across the top 10 was around~~ in the top cm of snow is about 41 ~~and 34 in the summer and winter period respectively~~$\mathrm{K\,m^{-1}}$. Therefore, the ~~grain surface has a dynamic character of which 'fresh' grain surface would be created by 'new' water molecules before equilibrium can be reached between air and surface of~~ dynamic $\mathrm{H_2O}$ exchange and redistribution at the snow grain ~~. Lastly, as mentioned in the Introduction, at the average temperature range found in Antartica (0° – -60°) the characteristic time of surface adsorption is on the order of 10^2-10^3 , which is longer than the model time resolution (10 min).~~

surface prevent the equilibrium of adsorption from being reached and require a kinetic approach.

The net rate of adsorption can be described as ~~$\frac{d\mathrm{HNO}_3}{dt} = k_{\mathrm{ads}}[\mathrm{HNO}_{3\,(\mathrm{g})}]\,[\mathrm{S}] - k_{\mathrm{des}}[\mathrm{HNO}_{3\,(\mathrm{ads})}]$. Substituting k_{ads}~~ $\frac{d[\mathrm{HNO}_{3\,(\mathrm{ads})}]}{dt} = k_{\mathrm{ads}}[\mathrm{HNO}_{3\,(\mathrm{g})}]\,[\mathrm{S}] - k_{\mathrm{des}}[\mathrm{HNO}_{3\,(\mathrm{ads})}]$. Substituting k_{des} with Eq.

(**??**), the net adsorption rate is expressed as

$$\frac{d[\mathrm{HNO}_{3\,(\mathrm{ads})}]}{dt} = k_{\mathrm{ads}} \left([\mathrm{HNO}_{3\,(\mathrm{g})}]\,[\mathrm{S}] - \frac{[\mathrm{HNO}_{3\,(\mathrm{ads})}]}{K_{\mathrm{eq}}} \right) \tag{8}$$

The temperature gradient and relative humidity gradient between the surface of the snowpack and the skin layer create a gradient in water vapour pressure, which drives condensation or sublimation of ~~snow~~ice, depending on the sign of the gradient. ~~During the condensation process the adsorbed molecules may bury in the growing ice if its residence time on the surface is long enough compare to the frequency of water molecules hitting the grain surface (?).~~ Uptake of HNO_3 molecules to growing ice is known as co-condensation. The surface ~~concentration~~ concentration of NO_3^- contributed by co-condensation or co-sublimation, $[\mathrm{HNO}_{3\,(\mathrm{cc})}]$, is given by

$$[\mathrm{HNO}_{3(\mathrm{cc})}] = X_{\mathrm{HNO}_3} \frac{\rho_{ice}\, N_A}{\overline{m}_{\mathrm{H_2O}}} \frac{\Delta t}{\mathrm{V}_{\mathrm{grain}}} \frac{d\mathrm{V}}{dt} \tag{9}$$

where $\mathrm{X}_{\mathrm{HNO}_3}$ is the mole fraction of HNO_3 condensed along with water vapour ($\mathrm{X}_{\mathrm{HNO}_3}$ = ~~$\frac{P^{0.56}_{\mathrm{HNO}_3}}{10^{3.2}}$~~ $10^{-3.2}\, P^{0.56}_{\mathrm{HNO}_3}$, **?**), ρ_{ice} is the density of ice (in $\mathrm{kg\,m^{-3}}$), N_A is ~~the~~ Avogadro's constant ($6.022{\times}10^{23}$ molecule $\mathrm{mol^{-1}}$) and Δt is the model time step. The rate of volume change of snow grain, $\frac{dV}{dt}$, is specified by the growth law by described (**?**)

$$\frac{d\mathrm{V}}{dt} = \cancel{\frac{4\,\pi\,\mathrm{R_{eff}}}{\rho_{ice}}}\, \frac{4\,\pi\,\mathrm{R^2_{eff}}}{\rho_{ice}} D_v \left(\cancel{\frac{d\,\rho_v}{d\,z}}\, \frac{d\,\rho_v}{d\,x} \right)_{\cancel{z=r}\,x=r} \tag{10}$$

where ~~$\mathrm{R_{eff}}$ is the effective radius,~~ D_v is the diffusivity of water vapour in air and ~~$\frac{d\rho_v}{dz}$~~ $\frac{d\rho_v}{dx}$ is the local water vapour density gradient, i.e. between air away from the snow grain and the air near the grain surface. However, to the author's knowledge there are no observations reported and the calculation of water vapour density at these microscopic scales is computational costly as it would require 3-D modelling of the metamorphism of the snow grain. For simplicity, the macroscopic (few mm) water vapour gradient across the skin layer was used to estimate the ~~condensation and sublimationprocesses.~~ rate of volume change of snow grain due to condensation or sublimation, i.e. $\left(\frac{d\rho_v}{dx}\right)_{x=r}$ in Eq. **??** is replaced by $\left(\frac{d\rho_v}{dz}\right)_{z=4\mathrm{mm}}$. The water vapour density, ρ_v, ~~is defined~~ can be calculated as follows:

$$\rho_v = \frac{P_{sat}\,\mathrm{RH}}{100\,R_v\,T} \tag{11}$$

where P_{sat} is the saturated vapour pressure (Pa), RH is the relative humidity ($\%$), R_v is the gas constant ~~of water vapour~~ ($\mathrm{J\,kg^{-1}\,K^{-1}}$) and T is temperature (K). There are no ~~measurement~~ measurements of fine resolution of vertical snow profile of RH and temperature available, therefore, RH within the snowpack was assumed to be 100% and the temperature of the skin layer is estimated using a heat transfer temperature model ~~(?) of which~~ based on the heat diffusion equation (?):

$$\frac{\partial T}{\partial t} = \frac{\partial}{\partial z} k_w(z) \frac{\partial T}{\partial z} \tag{12}$$

where T is the temperature, t is time, k_w is the ~~heat conductivity~~ thermal conductivity (App. **??**) of snowpack and z is the depth.

3.1.2 Ambient Temperature > 238 K: Non-Equilibrium Solvation

At ~~temperatures above~~ temperature above T_0 = 238 K ~~,~~ the interface between air and snow grain surface is assumed to be a DI~~, with characteristics described in the Introduction. The grain surface~~. The DI is assumed to be covering the entire grain surface and the partitioning into the DI based on Henry's law. The grain boundary concentration is determined by non-equilibrium solvation ~~in the DI, which covers the entire grain surface.~~ into the DI such that

$$[\mathrm{HNO}_{3\,(\mathrm{surf})}] = [\mathrm{HNO}_{3\,(\mathrm{DI})}] \qquad \text{if} \quad T > 238\mathrm{K} \tag{13}$$

The DI is also assumed to be out of equilibrium with the surrounding air for similar reasons as discussed above ~~. The surface~~ (Sect. ??). The grain boundary concentration is then defined by the following equation:

$$\frac{d[\mathrm{HNO}_{3\,(\mathrm{DI})}]}{dt} = k_{\mathrm{mt}} \left([\mathrm{HNO}_{3\,(\mathrm{g})}] - \frac{[\mathrm{HNO}_{3\,(\mathrm{DI})}]}{k_{\mathrm{H}}^{\mathrm{eff}}} \right) \tag{14}$$

The mass-transfer coefficient, k_{mt},is defined as $k_{\mathrm{mt}} = \left(\frac{\mathrm{R_{eff}}^2}{3\,D_g} + \frac{4\,\mathrm{R_{eff}}}{3\,\bar{v}\,\alpha} \right)^{-1}$, where D_g is the gas-phase diffusivity (?).

3.1.3 ~~Solid Diffusion~~

~~In this model radially symmetrical spherical grains with a radius, $\mathrm{R_{eff}}$, are assumed and the radius is determined from snow specific surface area (SSA) measurements, as follows:~~

~~$\mathrm{R_{eff}} = \frac{3}{\rho_{\mathrm{ice}}\,\mathrm{SSA}}$~~

~~where ρ_{ice} is the density of~~ Note that in this model the DI is treated as the boundary between the air and bulk ice. The concentration ~~gradient of between the surface and the centre of the snow graincauses~~ of the DI is used as the outermost boundary condition for solid- state diffusion within the grain, therefore, the DI has no thickness.

3.1.3 Solid-State Diffusion

The concentration gradient between the grain boundary and its centre drives solid state diffusion of ~~nitric acid. The nitric acid forms a solid solution with~~ nitrate within the bulk ice. The ~~grain surface concentration~~ concentration at the grain boundary is defined by ~~either~~ surface adsorption and co-condensation ~~on ice (sect. ??) or solvation in the DI (sect. ??) as a function of temperature. The spherical solid-state diffusion equation is given by~~ at temperatures below T_0 or solvation into the DI at temperatures above T_0, discussed above. The $\mathrm{NO_3^-}$ concentration profile within the snow grain can be found by solving the following partial differential equation

$$\frac{\partial[\mathrm{NO_3^-}](r)}{\partial t} = k_{\mathrm{diff}} \left(\frac{2}{r} \frac{\partial[\mathrm{NO_3^-}](r)}{\partial r} + \frac{\partial^2[\mathrm{NO_3^-}](r)}{\partial r^2} \right) \tag{15}$$

where $[\mathrm{NO_3^-}](r)$ is the local $\mathrm{NO_3^-}$ concentration in the r^{th} concentritic layer of the ice sphere and k_{diff} is the ~~diffusion coefficient in the solid-phase~~ solid state diffusion coefficient for ice. The typical length-scale~~of the~~, <x>, a molecule diffuses in a given time, t, can be described by the root-mean square displacement, <x> = $\sqrt{6tk_{\mathrm{diff}}}$. The ~~characteristic distance~~ typical length-scale, <x~~during one model time step of $\Delta t = 10$~~ >, is 1.5 and 5.5 μm at Dome C (Sect. **??**) and Halley (Sect. **??**), respectively, during a model time step of Δt = 10 min. To optimise the performance and computational cost of the models, 85 evenly spread concentric shells (i.e. r = 1, 2, 3, ..., 85 with 85th being the outermost shell) were ~~assumed~~used to represent the snow grain, such that the ~~average~~ thickness of the concentric shell is less than the average root-mean square displacement.

The diffusion equation is solved with the ~~Crank Nicolson~~ Crank-Nicolson scheme (**?**) and the bulk ~~concentration~~ concentration of $\mathrm{NO_3^-}$ in the ice grain, $[\mathrm{NO^-_{3\,(bulk)}}]$, is the sum of the number of $\mathrm{NO_3^-}$ molecules in each layer divided by the volume of the whole grain, expressed as

$$[\mathrm{NO^-_{3\,(bulk)}}] = \frac{\sum[\mathrm{NO_3^-}](r)\,V(r)}{\sum V(r)} \tag{16}$$

where $V(r)$ is the volume of the r^{th} layer and $\sum V(r)$ is the total volume of the grain, V_{grain}, and $[\mathrm{NO_3^-}](r)$ is the concentration of nitrate in the r^{th} layer.

3.2 Model 2 - Non-Equilibrium Kinetic Adsorption & Solid Diffusion ~~+~~ and Equilibrium Air - ~~Micro-Liquid Pocket~~Liquid Micropocket

Model 2 ~~(Schematic in Fig. ??)~~ is based on the hypothesis that ~~at all temperature below~~ the major air-snow grain interface is pure ice at all temperatures below the melting, T_m~~the majority of the grain surface is ice and liquid is presented~~, and that liquid coexists with ice when the temperature is above the eutectic temperature, T_e ~~, which is in the form of micropocket and~~ (Fig. **??**). The liquid water is assumed to be located in grooves at grain boundaries ~~and triple junctions (?). The bulk concentration~~ or triple junctions between grains and in the form of micropockets. This assumption implies the grain surface area being covered by liquid water is negligible. The bulk concentration of $\mathrm{NO_3^-}$ in Model 2 is defined as ~~follow~~follows:

$$[\mathrm{NO^-_{3\,(bulk)}}] = \begin{cases} \frac{\sum[\mathrm{NO_3^-}](r)\,V(r)}{V_{\mathrm{grain}}} & \text{if} \quad T < T_e. \\ \frac{\sum[\mathrm{NO_3^-}](r)\,V(r)}{V_{\mathrm{grain}}} + \phi_{\mathrm{H_2O}}\,k_{\mathrm{H}}^{\mathrm{eff}}\,[\mathrm{HNO_{3\,(g)}}] & \text{if} \quad T_e \le T < T_m. \end{cases} \tag{17}$$

At all temperatures below T_m, $\mathrm{HNO_3}$ ~~could be adsorbedon,~~ can be adsorbed/desorbed and co-condensed~~to or~~ /co-sublimated from the surface ~~(Same description as in~~ as in Model 1 (Sect. **??**). The adsorbed and co-condensed molecules on the grain surface ~~can then be diffused~~ then diffuse into or out of the bulk ice depending on the concentration gradient of ~~between the grain surface and the grain core (Same description as in~~ nitrate as in Model 1 Sect. **??**). Above T_e, liquid co-exists with ice~~(Last term in Eq. ??, if $T_e \le T < T_m$). The volume of the micropocket is~~, and its volume can be calculated from the liquid water fraction, $\phi_{\mathrm{H_2O}}$ ~~, by~~ (Eq. **??**~~. The~~). The term '$\phi_{\mathrm{H_2O}}\,k_{\mathrm{H}}^{\mathrm{eff}}$ $[\mathrm{HNO_{3\,(g)}}]$'

in Eq. ?? is the bulk concentration of nitrate contributed from the solvation of nitric acid in the liquid micropockets. The partitioning between air and ~~the micropocket~~ liquid micropockets is described by Henry's Law, with the effective Henry's Law coefficient, $k_{\mathrm{H}}^{\mathrm{eff}}$, as the partitioning coefficient. An instantaneous equilibrium is assumed because 1) the volume of the liquid solution is small ($10^{-7} - 10^{-6}$% of the total volume of the ice grain, discussed below) ~~;~~ 2) $\mathrm{HNO_3}$ is ~~highly~~ strongly soluble in water; ~~and~~ 3) the characteristic time of the interfacial mass transport across a liquid surface of a droplet with 70 µm diameter is only $\sim 10^{-7}$ s (Table ??); and 4) the diffusion rate is faster in liquid (~~At~~ at 0°C, diffusion of $\mathrm{NO_3^-}$ is 9.78×10^{-10} $\mathrm{m^2\,s^{-1}}$ in liquid, ?) than in ice (~~At~~ at 0°C~~diffusion rate~~ , diffusion of $\mathrm{NO_3^-}$ is 3.8×10^{-14} $\mathrm{m^2\,s^{-1}}$ in ice). The ~~exact location of the micropockets are not specified in the model and it is considered as a droplet on the surface. However, the volume of the micropocket is so small the grain surface covered by the liquid is assumed to be negligible~~characteristic time of liquid-phase diffusion within a 70 µm diameter water droplet is $\sim 10^0$ s (Table ??).

Both the values of pH and $\Phi_{\mathrm{bulk}}^{\mathrm{aq}}$ (in Eq. ??) are updated at each model time step with ~~the hydrogen ion concentration and total ionic concentration from~~ values from the previous time step. At Dome C, the major anion in melted snow is $\mathrm{NO_3^-}$ (e.g. ?). ~~It~~ Therefore, it is assumed that ~~the~~ nitrate and hydrogen ions are the only ions ~~presented~~ present in the skin layer snow, i.e. $[\mathrm{Ion_{tot\,(bulk)}}] = 2\times[\mathrm{NO_3^-}]$ in Eq. ??, and the eutectic temperature of the $\mathrm{H_2O}$-$\mathrm{HNO_3}$ system of 230.64 K (?) ~~is~~ are chosen as the threshold temperature for the existence of ~~micropocket~~micropockets. In contrast, at Halley snowpack ion chemistry is dominated by NaCl (?), contributing ∼85% ~~of the total ionic~~ to the total ion concentration in the 2004-05 Halley data set, due to the proximity of sea ice and open ocean. For simplicity, the only anions ~~concentration~~ included in the calculation of $\phi_{\mathrm{H_2O}}$ at Halley are $\mathrm{NO_3^-}$ and $\mathrm{Cl^-}$, such that $[\mathrm{Ion_{tot\,(bulk)}}] = 2\times([\mathrm{Cl^-}] + [\mathrm{NO_3^-}])$ in Eq. ?? and the value of T_e used is that for a $\mathrm{H_2O}$-NaCl system of 251.95 K (?).

4 Model Validation

~~Atmospheric~~ Model calculations are constrained and validated with existing observation of atmospheric nitrate, skin layer snow $\mathrm{NO_3^-}$ concentration ~~, meteorological data and information were collected~~ and meteorological data at Dome C ~~(75°06′S, 123°33′E) from January 2009 to January 2010 and Halley(75°35′S, 26°39′E) between April 2004 and February 2005, Antarctica.~~ and Halley. Below a brief summary of the available data is given.

4.1 Observation at Dome C

Dome C is ~~chosen as~~ characterised by the following: 1) ~~All year~~ temperatures are below freezing year round, and no snow melt occurs, ~~the mean annual temperature (e.g. ?) is around~~ with an annual mean of −52°C ~~with maximum temperature~~ and a maximum of −17°C in summer (mid November till end of January) and ~~down to~~ minimum temperature of $-80^\circ\mathrm{C}$ in ~~the~~ winter (April to mid September) (e.g. **?**). The diurnal temperature variation is ~~approximately~~ $\sim$10 K in summer, spring (mid September ~~till~~ until mid November) and autumn (~~beginning of February till end of March)period~~February to March). 2) ~~Relatively simple snow nitrogen chemistry . The concentration~~ the air-snow chemistry of reactive nitrogen is relatively simple due to the remoteness of the site. In particular, concentrations of sea salt and other ~~organic~~ particles that scavenge HNO_3 ~~are low in~~ in the air are low on the East Antarctica Plateau (**?**). Hence, the main ~~source of in snow is atmospheric~~ atmospheric nitrate is gaseous HNO_3 that ~~dissolved~~ dissolves in and/or ~~adsorbed onto the grain~~ adsorbs onto snow grains (**?**). 3) ~~Low~~ Furthermore, a low snow accumulation rate of ~~snow of~~ 27 $\mathrm{kg\,m^{-2}\,yr^{-1}}$ (**?**) ~~, implies strong~~ allows post-depositional processing of nitrate before the surface snow ~~get buried by fresh~~ is buried by new snowfall (e.g. **??**).

~~The temperature, atmospheric pressure, atmospheric nitrate and~~ Observations of skin layer snow nitrate concentration~~measured~~, atmospheric nitrate concentration, temperature, and pressure during January 2009 to 2010 at Dome C ~~(published perviously by ?, Fig. 6)~~ are shown in Fig. **??**. The snow samples were collected from the ‘skin layer’ snow, the top 4 ± 2 mm of the snowpack, approximately every 3 days. The skin layer was assumed to be spatially heterogeneous with an uncertainty in thickness about 20% due to the softness of the uppermost layer and sampling by different people. The nitrate concentration in the melted sample was measured by ion chromatography (IC) (**?**).

The concentration of atmospheric nitrate, i.e. the sum of atmospheric particulate nitrate ($p{-}NO_3^-$) and the concentration of gaseous nitric acid (HNO_3), was collected on glass fibre ~~filter~~ filters by high volume air sampler (HVAS) as described in **?**. ~~The filter was positioned approximately 1 above the snow surface and was being changed on a weekly base.~~ **?** stated that the ~~particulate nitrate data~~ concentration of particulate nitrate shows good agreement with HNO_3 gas-phase concentration measured by denuder tubes at Dome C over the same time period, therefore we equate the observed atmospheric nitrate with gaseous HNO_3. ~~Maximum atmospheric of 167 was observed during summer period, while minimum concentration of 1.2 was recorded during autumn and early winter period. The snow samples were collected from the ‘skin layer ’ snow, the top~~ The filter was positioned approximately 1 m above the snow surface and changed weekly. The atmospheric boundary layer is assumed to be well mixed so that the atmospheric nitrate at the snowpack surface would be the same at 1 m. The characteristic transport time of HNO_3 from the snowpack surface to the skin layer (4 ~~± 2~~ mm~~of the snowpack, approximately every 3 days. The~~) is on the order of 10^0 s, which is much shorter than the temporal resolution of the model (10 min, Table **??**). Therefore, the concentration of HNO_3 in the skin layer was assumed to be ~~spatially heterogeneous with an uncertainty in thickness about 20% due to the softness of the uppermost layer and sampling from different people. The nitrate concentration in the melted sample was measured by ion chromatograph (IC)~~the same as above the snow. The maximum concentration of atmospheric HNO_3 of 167 $\mathrm{ng\,m^{-3}}$ was observed during the summer period, while the minimum concentration of 1.2 $\mathrm{ng\,m^{-3}}$ was recorded during the autumn and early winter period.

Continuous meteorological observation and snow science are carried out at Dome C under the ‘Routine Meteorological Observations’ of the Concordia Project by the Italian National Antarctic Research Programme, PNRA, and the French Polar Institute, IPEV (http://www.climantartide.it). ~~Here are the brief informations of the meteorological observations, details of the methodology on meteorological data collection at Dome C can be found in the URL link above. Wind, temperature and moisture were measured with10~~ Temperature and humidity were measured at 10 s resolution~~, and archived as the hourly mean. The sensor for wind speed (optoelectronic counter, WAA 15A) and direction (anemometer, WAV 15A) were mounted at 3.3 above the snow with accuracy 0.3 and 2.8 respectively. Temperature and~~ . Both the temperature and relative humidity were measured at 1.6 m above the snow surface ~~by~~ with a platinum resistance thermometer ~~,~~ (VAISALA PT100 DTS12~~, with~~) with a precision of ± 0.13 °C at $-15\,°$C, and the humidity sensor ~~was a HUMICAP by VAISALAwith~~ (HUMICAP, VAISALA) had a precision of ± 2 %. Based on the assumption of a well mixed boundary layer, the RH above the snowpack surface was assumed to be the same as that at 1.6 m. Atmospheric nitrate concentrations and meteorological data ~~have been interpolated into~~ used as model input have been linearly interpolated to 10 minute resolution~~as model input~~.

~~There are no available pH measurements of the snowpack, therefore, the pH of the DI in Model 1 and the initial pH in Model 2 is assumed to be 5.6 (?). ? shows the SSA of the near-surface snow during winter months are significantly larger than SSA in the summer months, hence, a single value of SSA is not representative and sufficient enough for a year-long model run. There are no SSA recorded during 2009-2010 for skin layer snow and the SSA is estimated base on observation at Dome C from 2012 to 2015 by ?, as shown in Fig. ?? (solid black line).~~

4.2 Observation at Halley

Halley, in coastal Antarctica, is at a similar latitude ~~to~~ as Dome C but at sea level in coastal Antarctica, as opposed to the Antarctic Plateau, with very different geographic features. Halley is ~~sitting~~ on the Brunt Ice Shelf and is close to the Weddell Sea in three directions. Hence ~~, both the temperatureand humidityare very different from Dome C and its atmospheric composition is more complex due to the larger influence by different aerosols such as sea salt and dust aerosols~~the temperature, relative humidity, and concentration of atmospheric aerosol are much larger at Halley than Dome C. The average surface temperature in summer days is around $-10\,°$C and below $-20\,°$C in the winter. ~~Being a coastal site, occasionally,~~ Occasionally, the temperature can rise above $0\,°$C (surface melt is possible) or drop to $-55\,°$C ~~.~~ (See Fig. ??). The snow accumulation rate at Halley is much larger ~~compared to~~ than at Dome C, which ~~have~~ has an average of ~~112~~ 480 $\mathrm{kg\,m^{-2}\,yr^{-1}}$ ~~(?)~~(?), limiting post-depositional processes relative to Dome C.

Meteorological and chemical data were collected at Halley under the CHABLIS (Chemistry of the Antarctic Boundary Layer and the Interface with Snow) campaign at the Clean Air Sector Laboratory (CASLab)~~. Details of the methodology of the measurements can be found in ? and ?~~, (details in **??**). Measurement of atmospheric concentration of $\mathrm{HNO_3}$ ~~concentrations~~ were carried out at weekly resolution using annular denuders (URG corporation) mounted ~~at~~ 7-8 m above the snow surface with a collection efficiency of 91% ~~during CHABLIS (?).~~ (?). The atmospheric boundary layer is assumed to be well-mixed that the nitric acid concentration at the snowpack surface would be the same as at 7-8 m. Surface snow (the top 10 to 25 mm) was collected on a daily basis and the samples were analysed using ion chromatography (IC). Bulk concentrations of the major anions and cations were measured, including $\mathrm{Cl^-}$ and $\mathrm{NO_3^-}$ (?). The concentrations were interpolated to the 10 minutes model resolution.

Other meteorological data ~~including~~ included 10 minute averages of air temperature by Aspirated PRT, RH by Humidity probe (Vaisala Corp) and wind speed and direction by Propeller vane~~, all~~. All sensors were at 1 m above ~~snow surface. The data from Halley collected during CHABLIS are shown in~~ the snow surface (Fig. **??**~~. Daily values were~~). All values were linearly interpolated to the model time step of 10 min.

4.3 Other Model Inputs

There are no available pH measurements of the snowpack, therefore, the pH of the DI in Model 1 and the initial pH in Model 2 is assumed to be 5.6 (?) at both Dome C and Halley. There are no measurement of SSA recorded during 2009-2010 for skin layer snow. The SSA and effective grain radius in this study are estimated based on observation at Dome C from 2012 to 2015 by ?, as shown in Fig. **??**, solid line. No observations of SSA are available for Halley. Therefore the ~~observation~~ observations of SSA from Dome C were adjusted taking into account ~~of~~ the shorter cold period, which ~~tend~~ tends to have a larger SSA (~~i. e. smaller grain size, Eq. **??**~~Fig. **??**, dashed line).

4.4 Statistical Analysis

Three-day running means are calculated from all model outputs to ~~match the average~~ better match the time resolution of the observations. The performance of the models ~~are~~ is assessed by the coefficient of variation of RMSE, $\mathrm{C_v(RMSE)}$, as a goodness of fit. The $\mathrm{C_v(RMSE)}$ is defined as

$$\mathrm{C_v(RMSE)} = \frac{\sqrt{\sum_{t=1}^{n}(obs(t) - model(t))^2\,/\,n}}{\overline{obs}} \tag{18}$$

where $obs(t)$ and $model(t)$ are the observed value and modelled value at time t respectively, n is the number of ~~observation points~~observations, and $\overline{obs}$ is the observation mean.

5 Results

~~Below we describe the results from Model 1 and 2 at Dome C and Halley. Model fits for observations are assessed by C_v(RMSE) and summarised in Table **??** and **??**.~~

5.1 Dome C

The ~~modelled results from~~ predicted concentration of nitrate in skin layer snow for Model 1 ~~- 'Surface Adsorption/Solvation & Solid Diffusion' are shown in Fig. **??** and results from~~ and Model 2 in Dome C (Fig. **??** and Table **??**) are discussed by season - ~~'Surface Adsorption & Solid Diffusion + micropocket' is presented in Fig~~Winter to Spring (April - Mid November) and Summer (Mid November - January). ~~**??**. Both models are temperature dependent, therefore, the results will be presented by season .~~

5.1.1 Winter to Spring

The average temperature ($\pm 1\sigma$) at Dome C between late autumn to late spring in 2009 is 213.7 ($\pm$7.9) K (Fig. **??**a), which is ~~lower than~~ below the threshold temperature, T_0, for detection of DI layer (set at 238 K) ~~within~~ for Model 1 and ~~lower than eutectic temperature~~below the eutectic temperature, T_e, for a H_2O-HNO_3 mixture (230 K) ~~within~~ for Model 2. Therefore, ~~during~~ in winter, the ~~dominant controlling mechanisms are the combination of~~ skin layer concentration of nitrate described well by non-equilibrium kinetic surface adsorption and co-condensation coupled to ~~solid state~~ solid-state diffusion within the snow grain ~~for~~ in both models. The ~~combination of these two processes~~ models combine both processes and agreed very well with the observations ~~, such as~~ of nitrate (Fig. **??**a) with a C_v(RMSE) = 0.73. Both models captured the small peak from mid April to early May and another peak from mid to end of August ~~, followed by a tough and~~ then a steady increase from middle September ~~to~~ till the end of October, ~~apart from one~~ except for the peak in late February~~(Fig. ??).~~ .

~~As mentioned in Introduction, **?** suggested during the winter months the skin layer snow nitrate concentration is driven by thermodynamic equilibrium ice solubility in ice followed by solid-state diffusioninstead (Configuration 2 - BC1 within **?**, and is referring as~~ Below we compare our 'Kinetic approach' (a 'non-equilibrium surface adsorption followed by solid diffusion' configuration) with the 'Equilibrium ~~' approachhereon~~approach' suggested by **?**, Configuration 2 - BC1 in estimating skin layer $[NO_3^-]$ in the winter period (Fig. **??**a). The grain surface concentration, $[HNO_{3\,(surf)}]$, for the 'Equilibrium' approach is determined by parameterisation from **?**:

$$[\mathrm{HNO}_{3\,(\mathrm{surf})}] = 2.37 \times 10^{-12} \exp\left(\frac{3532.2}{T}\right) P_{\mathrm{HNO}_3}^{1/2.3} \frac{\rho_{ice} N_A}{M M_{\mathrm{H2O}}} \frac{\rho_{ice} N_A}{M_{\mathrm{H_2O}}} \tag{19}$$

where T is the snow temperature (K), P_{HNO_3} is the partial pressure of HNO_3 (Pa) ~~. To compare the two different approaches for estimating skin layer in the winter period, the 'Equilibrium Approach' was run along with an 'non-equilibrium kinetic surface adsorption followed by solid diffusion' configuration (referring as the 'Kinetic' approach hereon)~~and M_{H_2O} is the molar mass of H_2O. Note that the co-condensation was excluded in these model runs for a direct comparison between the two different approaches. Both the ‘Equilibrium’ and ‘Kinetic’ ~~Approach resulted~~ approaches resulted in a very similar trend and variation until mid Sept~~(Fig. ??, Left).~~ . Despite the ‘Kinetic’ approach yielding a larger C_v(RMSE) compared to the ‘Equilibrium’ approach ~~,~~ (C_v(RMSE) = 0.65 & 0.52, respectively, Table. ??), the ‘Kinetic’ approach ~~appears to capture the temporal patten~~ captures the temporal pattern from mid September till early November, yet, the ‘Equilibrium’ approach does not.

5.1.2 Summer

The average temperature (±1σ) ~~in late spring , summer and~~ from late spring to early autumn is 240.0 (±5.0) K ~~and so the main controlling process is the~~ (Fig. ??a) and the dominant process determining the snow nitrate concentration are solvation in DI coupled to solid state diffusion in Model 1 and partitioning ~~in the micropocket~~ of nitrate to the micropockets in Model 2.

~~In~~ Model 1 ~~the solvation of in DI followed by solid-state diffusion captured~~ captures some trends observed in early spring and during the summer period~~(Fig. ??)~~, including the decrease in concentration of nitrate from the beginning of February, the rise between mid and late November, and the sharp increase in mid December ~~.~~ (Fig. ??a). It also reproduced the steep decrease in concentration at the beginning of ~~2010.~~ 2010 (Fig. ??a) . However, Model 1 (with T_0 = 238 K) did not capture the peak in early February and overestimated ~~concentration~~ the concentration of nitrate by a factor of 1.5-5 in December ~~.~~ (Fig. ??a).

The results from Model 2 ~~was reasonably well agreed~~ agreed reasonably well with the observation in these few months with C_v(RMSE) of ~~0.6703. The decrease in concentration at beginning of February was captured with the additional~~ 0.67. With the contribution from the partitioning of HNO_3 in ~~micropocket so as other trends such as the rise and dip in November and from mid December till January next year~~ the micropockets, the features in early February and the peaks between November and mid December were captured (Fig. ~~??~~??b). The ~~modelled bulk concentrations in the summer were also the same order of magnitude yet either over or underestimated~~ model underestimates the the nitrate concentration from mid December until January 2010 by a factor of ~~3, that of observations~~3. During the summer period, the partitioning into the micropockets contributed ~75% of the total NO_3^- concentration.

5.2 Halley

~~The modelled results from~~ Model results for Model 1 ~~– ‘Surface Adsorption/Solvation & Solid Diffusion’ are shown in Fig. ?? and results from~~ and Model 2 ~~– ‘Surface Adsorption & Solid Diffusion + micropocket’ are presented in Fig. ??.As in Sect. ??, results will be~~ in Halley (Fig. ?? and Table ??).are presented by the season ~~. Halley is located at sea level and is influenced by atmospheric advection of moist air so that spring and early autumn are significantly warmer than winter compared to Dome C. The C_v(RMSE) values for different modelled results are shown in~~

~~Table ??.~~ - Late Autumn to Winter (April - Mid September) and Spring to Early Autumn (Mid September - February).

5.2.1 Late Autumn to Winter

The mean temperature ($\pm 1\sigma$) during this period at Halley is 244.72($\pm$7.7) K ~~, which is higher than the threshold temperature for detection of DI layer majority of the time but lower than~~ (Fig. **??**a). During this period, the temperature was mostly above the threshold temperature (T_0 = 238 K) used in Model 1 but below the eutectic temperature for a H_2O-NaCl mixture (251 K) ~~.~~ used in at Halley in Model 2. Therefore, the main ~~controlling process is solvation in DI in~~ process controlling the concentration of NO_3^- in Model 1 is solvation into the DI whereas in Model 2 the main controlling processes are the combination of non-equilibrium adsorption and co-condensation coupled with solid-state diffusion. Performance of Model 1 was poor (C_v(RMSE) = 27.78), ~~it has overestimated the concentration by an order~~ overestimating the concentration of NO_3^- by two orders of magnitude (Fig. ~~**??**~~**??**a). However, ~~few~~ some of the trends were reproduced during this cold period such as the two small peaks in mid April and early May, and the rise in mid September ~~.~~ (Fig. **??**a).

The modelled results from Model 2 ~~were~~ (C_v(RMSE) = 1.08) were a much closer match to the ~~observation~~ observations compared to Model ~~1 (C_v(RMSE) = 1.08). It has~~ 1. It captured the first peak in mid April ~~, the steady rise in July~~ and the small peak in beginning of September. However, it did not reproduce the ~~sharp~~ peak in mid August and underestimated the NO_3^- concentration for the majority of the time.

Similar to the Dome C site, the ‘Equilibrium’ approach after **?** was run alongside the ‘Kinetic’ approach from late autumn until winter, again, no co-condensation processes were included in these 2 runs for a direct comparison. The modelled results from both approaches are very similar in value and temporal variations (Fig. **??**~~, Right). Again, both~~ b). Both the ‘Kinetic’ and ‘Equilibrium’ approach failed to reproduce the ~~sharp~~ peak in mid August.

5.2.2 Spring ~~- Summer -~~ to Early Autumn

Similar to the winter months, Model 1 overestimated the bulk NO_3^- concentration at Halley by an order of magnitude and failed to capture any of the variability (Fig. ~~**??**~~**??**a). Model 2, however, reproduced some features during the warmer months, such as the peak in late September followed by a steady rise in October, the spikes in mid December, beginning of and mid January and also the peak and trough in late January (Fig. ~~**??**~~**??**b). The ~~modelled~~ partitioning to the micropockets contributed ~80% of the total NO_3^- concentration during this period. The model results are within the same order of magnitude ~~and obtained a~~ compared to the observations (C_v(RMSE) ~~of 0.6510~~= 0.65).

6 Discussion

~~The model~~ The results from both Model 1 and 2 show that the bulk $\mathrm{NO_3^-}$ concentration in surface snow can be reasonably well described by ~~physical~~ non-equilibrium adsorption and co-condensation coupled with solid-state diffusion during autumn to spring at Dome C and in winter at Halley, i.e. when it is cold and the solar irradiance is small. In the summer months, the combination of ~~larger~~ warmer temperatures and a larger ~~diurnal temperature range~~ range of diurnal temperature causes the 'Air-Ice' only processes to no longer provide an accurate prediction. ~~For the majority of this period, the~~ The concentration of $\mathrm{NO_3^-}$ ~~concentration in surface snow is governed by solvation~~ in the surface snow, during the warmer months, is mainly determined by solvation into DI in Model 1 or partitioning ~~in micropocket in~~ into micropockets in Model 2.

Overall, the results from Model 1 ~~matches reasonably well~~ match reasonably well with the year-round observations at Dome C ($\mathrm{C_v}(\mathrm{RMSE})$ = 1.34)~~, yet, it overestimates those at Halleyby an~~ . However, for Halley, Model 1 overestimated the concentration by two order of magnitude ($\mathrm{C_v}(\mathrm{RMSE})$ = 89.28). On the other hand, results from Model 2 agree well for both study sites all year-round ($\mathrm{C_v}(\mathrm{RMSE})$ = 0.84 for both Dome C and Halley). ~~Generally, the~~ The mismatch between the models and observations can be separated into 2 categories - data limitations and model configurations, and will be discussed below.

~~Firstly, the~~ The temporal resolution of ~~atmospheric nitrate concentration data~~ the concentration of atmospheric nitrate at both study sites ~~were~~ was roughly 5 to 10 days, therefore, any substantial changes in the atmospheric input within a short time scale might be missed and consequently the relative changes in ~~nitrate snow concentration~~ concentration of nitrate in snow might not be ~~detected~~observed. Secondly, the vertical snow pit profile of $\mathrm{NO_3^-}$ ~~in Antarctica tends~~ at Dome C (and sites with a low accumulation rate) tended to have a maximum concentration ~~in the surface snow~~ of $\mathrm{NO_3^-}$ at the surface of the snowpack (**?**), especially during the summer period, and the concentration of ~~snow~~ $\mathrm{NO_3^-}$ decreases sharply with ~~depth. It is this thin layer of surface snow that had most post-depositional influence by the atmospheric nitrate. The Dome C snow samples~~ the depth inf the snowpack. The skin layer is the most responsive layer of snow to the changes in the concentration of $\mathrm{HNO_3}$ in the atmosphere above. The snow samples from Dome C were collected carefully from the top 4±2 mm while the snow samples from Halley were collected from the ~~near-surface snow (top 0 to~~ top 25 mm~~)~~. It is possible that the snow $\mathrm{NO_3^-}$ ~~concentration measured from Halley might~~ concentrations measured at Halley may be 'diluted' from deeper snow~~layer and does not fully represent the interaction between the thin layer on the surfaceof the snowpack and the overlying atmosphere. Hence, the model might appears to be 'overestimating' the due to this dilution~~, with a smaller nitrate concentration than the surface, layer leading to a positive model bias. Thirdly, atmospheric nitrate can be ~~in the labile form of nitric acid () or fixed by sea salt~~ find in a more stable forms of $\mathrm{NO_3^-}$, i.e. associated with $\mathrm{Na^+}$, ~~ammonium or terrestrial dust, therefore, the assumption of~~ $\mathrm{Ca^{2+}}$ or $\mathrm{Mg^{2+}}$ (**?**). An increase in sea salt aerosol concentration can shift gaseous $\mathrm{HNO_3}$ ~~concentration to~~

~~be equal to the total measured atmospheric nitratemight cause mismatch between the modelled and observation. Atmospheric~~ to particle-phase (i.e. $NaNO_3$, ?), hence, decreases the ratio of gaseous HNO_3 to the total atmospheric nitrate. At Dome C, the atmospheric sea salt aerosol ~~concentrations have~~ concentration has a strong seasonal variability~~at Dome C~~. The maximum ~~sea-salt~~ sea salt aerosol concentration tends to be in ~~late winter/early spring and can be up to~~ the late winter or early spring which can be a factor of 4 ~~times~~ larger than the annual mean (?). ~~The increase in sea salt concentration decreases the ratio of concentration of gaseous to total atmospheric nitrate. A possible explanation for the overestimation of concentration in both Model 1 and 2 in November~~ Therefore, using the total measured atmospheric nitrate as gaseous HNO_3 for constraining the models might cause the mismatch between the modelled results and observations at Dome C~~.~~, especially around Novemeber.

~~Last but not least, information on precipitation, such as occurrence of new snowfall and the nitrate concentration of fresh snow, were incomplete for both datasets~~Lastly, no detailed information on timing and amount of snowfall events for the time periods in question at both study sites. Single snowfall events can increase the nitrate concentration in surface snow by up to a factor of 4 ~~higher than the surrounding~~ above the background (?). The contribution of snow nitrate from fresh precipitation ~~might not be as influential at the low accumulation site, like~~ maybe less important at low accumulation sites, such as Dome C - 27 $\mathrm{kg\,m^{-2}\,yr^{-1}}$ (?), ~~compare to site with high~~ compared to sites with large snow accumulation like Halley $\sim$~~112~~ 480 $\mathrm{kg\,m^{-2}\,yr^{-1}}$ (?). ? reports that the large ~~bulk concentration~~ concentration of NO_3^- recorded from mid ~~till~~ until end of August ~~is corresponded~~ was due to new snowfall, which ~~explained why it is not captured by both models~~ explains why both models failed to reproduce the peak. In the following sections, ~~the specific processes included within the two models presented in this paper~~ various processes included in Model 1 and 2 will be discussed.

6.1 ‘Kinetic’ Approach vs ‘Equilibrium’ Approach

The ‘Kinetic’ approach defines the ~~ice surface concentration~~ snow grain boundary concentration of NO_3^- by non-equilibrium, kinetic surface adsorption while the ‘Equilibrium’ approach after **?** defines the ~~ice surface concentration~~ concentration of the outermost layer of the snow grain (outermost layer thickness = 0.5-1.5 µm in this study) by thermodynamic equilibrium ice solubility. Both approaches ~~are used to~~ describe the interaction between air and ice, therefore, only results from the winter period are compared. For both sites, the ‘Kinetic’ and ’Equilibrium’ approach resulted in very similar trends except the peak in late October at Dome C (Fig. **??**), of which the ‘Kinetic’ approach managed to ~~capture~~ reproduce but not the ‘Equilibrium’ approach. ~~The late October peak~~

The peak of snow nitrate in late October at Dome C ~~is corresponded to the~~ corresponds to an increase in atmospheric ~~nitrate~~ HNO_3 (Fig. **??**~~). In ?, the late October peak was achieved after adding in an adjustable co-condensation parameter.~~

b). The grain surface concentration of the 'Equilibrium' approach is ~~defined as Eq. **??** and is~~ a function of the partial pressure of HNO_3 with an exponent of 1/2.3 ~~while the grain surface~~ (Eq. **??**), while the concentration of the grain boundary defined by the 'Kinetic Approach' is ~~defined as Eq. **??** and is~~ linearly related to the ~~atmospheric nitrate concentration, therefore, the 'Equilibrium~~concentration of atmospheric nitrate (Eq. **??**). Therefore, the 'Kinetic' approach is ~~less~~ more responsive to changes in the atmospheric nitrate concentration ~~compares~~ compared to the '~~Kinetic~~Equilibrium' approach. ~~There are other advantages of applying a 'Kinetic' approach~~ Other advantages of the former approach are, 1) ~~as it suits the dynamic character~~ dynamic characteristics of the grain surface due to ~~constantly changing temperature gradient.~~ changing temperature gradients are taken into consideration; 2) ~~as it suits sites with a high accumulation rate~~ applicability even for sites with high accumulation rates where the skin layer is buried by subsequent snowfall before reaching equilibrium.

At Halley, ~~the~~ in winter, the concentrations of NO_3^- ~~concentration is~~ are underestimated by both approaches ~~.~~ (Fig. **??** and Table **??**). There are 2 possible explanations. First, the SSA values used maybe underestimated and ~~leads~~ lead to an underestimation on adsorption or dissolution in the outermost layer of the snow grain, further field observations are required to ~~confirm it~~verify this. Secondly, ~~it might indicate~~ due to higher temperatures at Halley compared to Dome C, other processes might be involved in ~~defining~~ controlling the snow surface concentration of NO_3^-, such as ~~precipitation or micropocket (~~snowfall (not included in the models) or partitioning into liquid micropockets in Model 2 (discussed in Sect. **??**).

6.2 Co-Condensation - 'Air-Ice' Interaction

The process of co-condensation/sublimation is considered as part of the 'Air-Ice' interaction in both Models 1 and 2. It is driven by the difference in water vapour density across the skin layer snow and the overlying atmosphere. The water vapour density gradient depends exponentially on the temperature gradient. At Dome C ~~temperatures are extremely low~~ the temperature is extremely low and relatively dry, especially in winter, and therefore it is not surprising that only 2% of the grain surface concentration ~~is contributed by~~ of NO_3^- is from co-condensation during winter and spring (Fig. **??**~~, Left in light blue~~a, difference between the light and dark blue line). In contrast, at Halley, where winter is warmer and it is relatively humid, $\sim$21% of the grain surface concentration is contributed by co-condensation during winter (Fig. **??**~~, Left in dark blue~~ b, difference between the light and dark blue line). As shown in Table **??**, the C_v(RMSE) decreased slightly ~~during~~ in winter after including co-condensation as part of the 'Air-Ice' interaction. In the summer, ~~other processes are replaced (e.g. by 'Air-DI' processes~~ the dominant process in Model 1 ~~,~~ is solvation in the DI (See Sect. **??**) ~~or being overwhelmed (e.g. by partitioning in micropocket in~~ while in Model 2 ~~,~~ the dominant process is partitioning in the micropockets (See Sect. **??**)~~the~~ , hence the contribution from co-condensation ~~process to the overall concentration~~ to the skin nitrate concentration is insignificant.

There are a few possible sources of uncertainties in the calculation of co-condensation/sublimation processes. For example, the macro-scale gradients of water vapour pressure (across few mm) were used instead of micro-scale gradients (across few $\mu\mathrm{m}$) and there were no precise measurements of skin layer snow density. Uncertainty in the density would lead to uncertainty in the modelled skin layer snow temperature. Despite the potential errors in the calculation of co-condensation, the large $\mathrm{NO_3^-}$ ~~concentration~~ concentrations in the skin layer in the summer ~~is unlikely due to the~~ are unlikely to be driven by co-condensation~~process as an unrealistically high~~ . An unrealistically large average rate of volume change, $\frac{dV}{dt}$, of 130 and 118 $\mu\mathrm{m}^{-3}\,\mathrm{s}^{-1}$, equivalent to an average grain volume increases of 170% and 135% ~~everyday~~per day, would be required for Dome C and Halley respectively if the large concentration of $\mathrm{NO_3^-}$ in summer was contributed by co-condensation. Assuming the RH of skin layer snow to be 100% and RH of the overlying atmosphere is the same as measured at 1 m above snowpack, a macro-temperature gradient as high as 2.7×10^3 $\mathrm{K\,m^{-1}}$ would be require across the top 4 mm of the snowpack to match the large concentration of bulk $\mathrm{NO_3^-}$ in the summer at Dome C and in an average temperature gradient of 500 $\mathrm{K\,m^{-1}}$ would be ~~require~~ required across the top 10 mm of the snowpack in Halley, which are 1- 2 orders of magnitude higher than ~~the averaged~~ observations (?) and the modelled temperature gradient (listed in Sect. ??).

6.3 Disordered Interface - Model 1 (Temperature $>$ 238 K)

In Model 1, the interfacial layer between air and snow grain is described as 'Air-DI' when the ambient ~~temperature is warmer than~~ temperatures are above the threshold temperature, T_0 = 238 K. ~~At~~ Therefore, at Dome C, the 'Air-DI' regime ~~is only applicable~~ applies only during summer months due to the ~~extreme cold temperatures~~ extremely cold temperatures in winter, whereas, ~~yet,~~ at Halley ~~for the majority~~ most of the time the interface is considered as '~~Air-ID'. It is clear that having~~ Air-DI'. The model simulations suggest that an 'Air-ID' interface above 238 K ~~resulted in large all year round overestimation of bulk concentration at Halley and the overestimation of~~ (the lower end of the ~~concentration peak~~ DI detection limit of pure ice (?)) leads to an overestimation of nitrate concentration in early December at Dome C ~~. The temperature threshold of 238 was chosen as it is the lowest detection temperature for 'liquid-liker' properties in pure ice (?). However, the onset temperature of the~~ and all year round at Halley.

The onset temperature for observation of DI on pure ice varies with different experimental setups, ~~such as~~ probing techniques and how the samples were prepared ~~, the detecting temperature is ranging from 198 to 268 (as discussed by ?). Simulation by ? found the DI begins~~ (?). ? also found a small fraction of water molecules beginning to leave the outermost crystalline layer of the ice and becoming mobile at 100 K below the melting point ~~, of the~~ of that particular mixture of H_2O and impurities ~~, of which a small fraction of water molecules leaving the outermost crystalline layer and becoming mobile . Increasing the temperature up to~~ and the number of mobile molecules increases with increasing temperature. When the temperature is larger than 10 K below the melting point, ~~the~~

~~number of mobile or molecules increase on the outermost crystalline layerand above that temperature the disorder might extend to an additional ice layer. The appearance and thickness~~ molecules might even begin to leave the deeper crystalline layer. The existence of DI not only depends on temperature, but also the speciation and quantity of impurities present within the snow grain (**?**). Different impurities have different impacts on the hydrogen bonding network at the ice surface and hence have a different impact on the characteristics, such as thickness, of the DI (**?**). ~~Some studies suggest that in the presence of impurities, a thick ion-containing disorder region would coexist with a region of pure ice with thin DI layer instead of a homogenous uniform DI across the whole grain surface (?). In order to identify the sensitivity of Model 1 to the~~ Therefore, the chosen threshold temperature, ~~T_o, details and results of the sensitivity test is presented in the following section.~~ T_0, might be substantially different from what would be found in natural snow or it might not be representative enough to be used as the threshold all year-round (See Sect. **??** for the sensitivity analysis regarding to T_0).

~~Other major assumptions made in Model 1 is the partition coefficient, the effective Henry's coefficient and the~~ Moreover, the partitioning coefficient and mass transport coefficient ~~, k_{mt}, in the DI . The values were~~ of the DI were assumed to be the same as those in the ~~liquid aqueous phaseand~~ aqueous phase. These assumptions might not be realistic and could lead to overestimation of solvation of HNO_3 in the DI. However, the real values for partition and mass transport coefficients are difficult to measure with the current measurement techniques and need to be re-examined in the future. ~~The sensitivity of Model 1 to the value of pH in the DI, hence the effective Henry's coefficient, is presented in the following section.~~

There are 2 possible explanations for why Model 1 provided a reasonable estimation ~~for~~ of skin layer snow NO_3^- concentration at Dome C, but not ~~Halley. First~~at Halley. Firstly, the chemical composition of surface snow ~~in~~ at Dome C is ~~relative~~ relatively simple, dominated by nitrate anion, which would induce insignificant changes to the hydrogen bonding network at the DI surface ~~(?). Compared to surface snow at Halley and that its properties would be more similar~~ compared to a more complicated snow composition (**?**) suggesting the surface properties of snow at Dome C are likely to be comparable to pure ice. Secondly, the temperature at Halley occasionally rises above 0 °C potentially causing melting and significant changes in snow grain morphology ~~.~~ at the surface especially.

6.3.1 ~~Sensitivity Study~~

~~The work presented highlighted that the Model 1 is sensitive to the threshold temperature, T_o, but not the pH of the DI layer. In order to investigate the model sensitivity to T_o, Model 1 was evaluated by varying T_o with ΔT = 2 up till 242 and pH range 5.2-6.4 with ΔpH = ±0.4. Having a slightly larger threshold temperature smoothed out some of the sharp peaks in the modelled results in the summer period at Dome C (Fig. **??**, in Purple). At Halley, despite the improvement in C_v(RMSE)~~

~~when a higher temperature threshold was used, the modelled is still an order of magnitude larger than the observation (Fig. ??, in Purple).~~

~~The exponential dependency of the effective Henry's law on the inverse of temperature is responsible for the sensitivity of the threshold temperature for Model 1. The solvation of increases as temperature decreases (Fig. ??). Having a lower threshold temperature implies including some larger surface nitrate concentration in the DI which leads to greater concentration gradient across the grain and hence larger bulk concentration.~~

~~Varying the pH value of the DI layer between the range of 5.2-6.4 does not have significant changes (all resulted the same C_v(RMSE), not shown) to the estimated bulk concentration. The effective Henry's law coefficient found within this range of pH are in the same order of magnitude (Fig. ??).~~

6.4 Micro-Liquid Pocket - Model 2 (Temperature > Eutectic Temperature)

Model 2, ~~with the liquid micropocket and~~ which includes non-equilibrium surface adsorption and co-condensation coupled with solid diffusion within the grain ~~, managed to replicate the bulk concentration of~~ and partitioning in liquid micropockets, successfully reproduces the concentration of NO_3^- of the surface snow without any tuning parameters for both Dome C and Halley ~~even in the summer months. In the summer, the partitioning to the micropocket contributed ∼75% and ∼80% of the total concentration at Dome C and Halley respectively.~~ all year round. This is a crucial outcome as it ~~indicated~~ indicates that Model 2 can be used for predicting the air-snow exchange of nitrate ~~for~~ at the surface for a wide range of meteorological ~~conditions and locations, which have impacts on the chemical composition of snow~~and depositional conditions that typical for the entire Antarctica.

The ~~over or underestimation of concentration by Model 2 can be explained by the simplification of nitrate only impurity at Dome C or nitrate and salt as impurity at Halley. The~~ liquid water fraction is a function of the total ionic concentration (~~See~~ Eq. **??**). Hence, neglecting the existence of other ions ~~might~~ may lead to underestimation of the micropocket volume. The additional liquid would increase the dissolution capacity ~~for~~ of HNO_3 and hence increase the estimated NO_3^- concentration. As shown in Fig. ~~??~~??b, the estimated bulk NO_3^- concentration followed a similar trend as the ~~measured ionic concentration, which was simplified (See Sect. ??).~~

'other ions concentration' (the observed Cl^- concentration). Despite NO_3^- being the major anion in the surface snow in Dome C, other anions, such as Cl^- and SO_4^{2-}, were also detected from the same samples (?). ? also measured SO_4^{2-} along with Cl^- and NO_3^- from the surface snow samples from Halley. The mismatch between modelled and observed nitrate concentration in the summer can be explained by assuming nitrate to be the only impurity at Dome C, or nitrate and sea salt as the only impurities at Halley. Nevertheless, the underestimation of the NO_3^- concentration due to underestimating the liquid-water content ~~might be balanced out~~ may be compensated or even overwhelmed if ~~the~~ atmospheric deposition of other ~~acidic solutes increase,~~ acids such as HCl or

H_2SO_4 ~~, on the surface snow, which lower~~ increases, which lowers the pH and ~~reduce~~ reduces the solubility of HNO_3 in the micropocket.

Note that the micropockets only ~~existed at temperature higher than~~ exist above the eutectic temperature~~, for~~. For simplification, the eutectic temperature was ~~assumed to be the eutectic temperature of the system of~~ based on a system containing H_2O and the most abundant solute within surface snow. However, in reality, the presence of other impurities might have an impact on ~~that~~ the eutectic temperature.

6.5 Sensitivity Analysis

In order to assess the robustness of the findings presented here they were analysed as a function of model sensitivities to constraints, parameterisations and measurement uncertainties. Parameters were varied one at a time by the given range while keeping all others constraints and parameterisation the same (Table. **??**, Col. 1,). The coefficient of variation, C_v(RMSE), was calculated from each sensitivity test (Table. **??**) and compared with the C_v(RMSE) of the 'Control', which uses the observed values and parameterisation listed in Sect. **??** and Table. **??**.

Both Model 1 and ~~would require confirmation with future experimental data.~~ 2 are sensitive to the concentration of HNO_3 in the air and the concentration of NO_3^- in snow. Reducing concentration of HNO_3 in the atmosphere by 20% or increasing the concentration of NO_3^- in snow by 20% improves the performance of both models. This supports the suggestion that the atmospheric nitrate observed at Dome C only represents the upper limit of nitric acid and it is likely to lead to an overestimation of the concentration of nitrate in snow (Sect. **??**) while at Halley, the skin layer snow might well be 'diluted' by snow sample from the deeper layer (Sect. **??**).

Both models are sensitive to the value of SSA as a smaller SSA implies a smaller surface area per unit volumn of snow, and hence, less surface sites available for adsorption per unit volumn of snow. It has a more notable impact in Model 1 and in the winter, when the grain boundary processes play an important role for the overall snow nitrate concentration due to the cold temperature. A similar explanation applies the value of the maximum number of adsorption site, N_{max}. However, varying the accommodation coefficient, α by ± 10% does not have a significant impact on the performance of the models (Table **??**).

Model 1 is very sensitivity to the threshold temperature, T_0. At Dome C, the best match (lowest C_v(RMSE)) between modelled and observation is with a threshold temperature 2 K larger than the control T_0 = 238 K. However, increasing T_0 to 242 K worsens the model performance further (Fig. **??**A, Green line & Table **??**). In general, the grain boundary concentration of nitrate defined by solvation into the DI is much larger than when it is defined by the combination of surface adsorption and co-condensation on ice. A larger temperature is required to assume the interface is 'Air-DI' when a large value of T_0 is used. At Dome C, a larger value of T_0 may have reduced the overestimation in late November due to a larger fraction of time falling below the threshold but compromised the good fit from mid December onward and yield a higher C_v(RMSE). At Halley, despite the improvement in C_v(RMSE) when a higher temperature threshold was used, the modelled [NO_3^-] is still an order of magnitude larger than the observation (Fig. **??**b).

Model 1 is not sensitive to the pH of the DI layer. Even though the effective Henry's law coefficient increases by an order of magnitude when pH increases from 5 to 6.5 (Fig. **??**), the C_v(RMSE) remains the same. This behaviour can be explained by the combination of the kinetic approach and slow diffusion rate of nitrate in ice that the rate of change in the grain boundary concentration remains small even the boundary concentration increases.

Model 2 is sensitive to the eutectic temperature, T_e, but not as much as for T_0 in Model 1. Increasing T_e in Model 2, only improves the performance at Dome C but not Halley. Higher T_e implies that a larger temperature is required for the co-existence of liquid micropockets. For Dome C, increasing T_e by 2-4 K reduces the overestimation in November without compromising the results from mid December onwards, as the average temperature during that period was higher than $T_e = 234$K.

7 Conclusions

Two surface physical models were developed from first principles to estimate the bulk ~~concentration~~ concentration of NO_3^- in the skin layer of snow using observed atmospheric nitrate concentration, temperature and humidity as inputs. Model 1 ~~,~~ is based on the assumption of a homogeneous ~~DI~~ disordered interface (DI) as the interface between air and snow grain above 238 K and Model 2 ~~,~~ is based on the hypothesis of ~~majority of~~ the majority of the snow crystal surfaces being ice~~and liquid is located~~ , and above the eutectic temperature a liquid exists in grooves at grain boundaries and triple junction~~above the eutectic temperature~~.

The modelled skin layer ~~concentration~~ concentration of NO_3^- from Model 1 ~~are reasonably well agreed with observations from the cold~~ agreed reasonably well with observations at Dome C but overestimated observations by an order of magnitude at the relatively warmer Halley site. The uncertainties in Model 1 are the temperature threshold, T_o, that ~~define the~~ defines the onset of 'Air-DI' interface and the partition coefficient of DI. The poor performance of Model 1 at the warmer site supports the argument in previous studies (**??**) that the disordered interface cannot be parameterised as a thin, homogenous water-like layer ~~coving~~ covering the entire grain surface ~~and its interactions with the solutes are not the same as in aqueous phase~~or that its air-DI partitioning is the same as air-liquid partitioning.

Model 2 reproduced the skin layer ~~concentration~~ concentration of NO_3^- with good agreement at both Dome C and Halley without any tuning parameters. ~~This indicated~~ Thus the major interface between skin layer snow grain and surrounding air can well be described as 'Air-Ice' with a liquid formed by impurities ~~presented as micropocket~~ present as micropockets as suggested by **?**. ~~The~~

In the winter the interaction of nitrate between the air and skin layer snow can be described as a combination of non-equilibrium kinetic ice surface adsorption and co-condensation coupled with solid diffusion within ~~grain in the winter. During~~ the grain. In summer, the equilibrium solvation ~~in liquid micropocket dominate~~ into liquid micropockets dominates the exchange of nitrate between air and skin layer snow.

Additional modelling studies, e.g. including uptake of other chemical species or aerosols, backed up by field observations from other locations with various meteorological conditions as well as laboratory studies on the eutectic point of a multi-ions - H_2O system, uptake coefficient at a higher temperature, are needed to confirm the representativeness and improve the performance of Model 2.

Despite the simplified parameterisation of processes in Model 2, such as the impurities content in snow ~~, liquid pockets located in different locations were treated as one and had the same chemical properties as bulk liquid~~ and the behaviour of the liquid micropockets, it is ~~still sufficient enough to be implemented in regional and global atmospheric chemistry models and possibly improve the accuracy of the boundary layer chemistry and oxidation capacity. As mentioned in the Sect. **??** both models developed here are purely physical~~ a excellent step towards parameterising the interactions between air and snow. The models presented here are describing the exchange between air and the skin layer of snowpack as the uptake processes ~~overwhelm the photochemical processes in~~ are much quicker than the photochemical loss, and therefore, can be modelled by ‘physical-only’ processes.

Atmospheric nitrate can reach deeper than the skin layer ~~snow~~via wind pumping and temperature gradient, however, ~~this assumption is not be applicable to the entire snowpack(???). Other processes, such as chemical and photochemical processes needs to be included within the model to be implemented into a 1-D Air-Snow model to estimate the vertical profile of concentration~~ the nitric acid concentration in snow interstitial air (SIA) is expected to be small compared to the overlying atmosphere due to the high uptake of nitrate near the surface of the snowpack. A smaller concentration of HNO_3 in SIA implies a smaller uptake in deeper snow, and hence the photochemical loss cannot be assumed to be negligible in deeper snow. Therefore, a more complex multi-layer model including both physical and chemical processes is required to reproduce the nitrate concentration in deeper snow and being implement in regional and global atmospheric chemistry model.

Acknowledgements. HGC is funded by the Natural Environment Research Council through Doctoral Studentship NE/L501633/1. We are thankful to our colleagues (Anna Jones, Neil Brough and Xin Yang) for helpful discussion.

8 Notation

~~Notation of constants and parameters~~

Symbol	Description	units
α	Accommodation coefficient	dimensionless
$\mathrm{A_{ice}}$	Surface area of ice per unit volume of snowpack	$\mathrm{m^2\,m^{-3}_{snowpack}}$
$\mathrm{C_v\,(RMSE)}$	Coefficient of variation	N/A
DI	Disordered Interface	N/A
D_v	Water vapour diffusivity	$\mathrm{m^2\,s^{-1}}$
D'_s	Gas-phase diffusivity in snow	$\mathrm{m^2\,s^{-1}}$
$[\mathrm{HNO_{3\,(ads)}}]$	Nitric acid concentration contributed by surface adsorption	$\mathrm{molecule\,m^{-3}}$
$[\mathrm{HNO_{3\,(cc)}}]$	Nitric acid concentration contributed by co-condensation	$\mathrm{molecule\,m^{-3}}$
$[\mathrm{HNO_{3\,(DI)}}]$	Nitric acid concentration in the DI	$\mathrm{molecule\,m^{-3}}$
$[\mathrm{HNO_{3\,(ice)}}]$	Nitric acid concentration in solid ice	$\mathrm{molecule\,m^{-3}}$
$[\mathrm{HNO_{3\,(surf)}}]$	Nitric acid concentration on surface of grain	$\mathrm{molecule\,m^{-3}}$
k_{ads}	Adsorption coefficient on ice	$\mathrm{m^3\,molecule^{-1}\,s^{-1}}$
k_{des}	Desorption coefficient on ice	$\mathrm{s^{-1}}$
$k_{\mathrm{H^{cc}}}$	Henry's Law coefficient	dimensionless
$k_{\mathrm{H}}^{\mathrm{eff}}$	Effective Henry's Law coefficient	dimensionless
k_{diff}	Diffusion coefficient in ice	$\mathrm{m^2\,s^{-1}}$
k_w	Thermal conductivity of snowpack	$\mathrm{Wm^{-1}K^{-1}}$
$\mathrm{K_a}$	Acid dissociation constant	$\mathrm{molecule\,m^{-3}}$
$\mathrm{K_{eq}}$	Equilibrium constant for Langmuir adsorption	$\mathrm{m^3\,molecule^{-1}}$
N_{max}	Maximum number of adsorption sites	$\mathrm{molecule\,m^{-2}}$
$[\mathrm{NO^-_{3\,(bulk)}}]$	Bulk nitrate concentration	$\mathrm{molecule\,m^{-3}}$
$\phi_{\mathrm{H_2O}}$	Liquid water fraction	dimensionless
$\Phi^{\mathrm{aq}}_{\mathrm{bulk}}$	Fraction of the total amount of solute in aqueous phase	dimensionless
R_{eff}	Effective radius of snow grain derived from SSA data	m
ρ_{ice}	Density of ice	$\mathrm{kg\,m^{-3}}$
ρ_v	Water vapour density	$\mathrm{kg\,m^{-3}}$
[S]	Number of available surface sites per unit volume of air	$\mathrm{molecule\,m^{-3}_{air}}$
SSA	Specific surface area	$\mathrm{m^2\,kg^{-1}}$
T_e	Eutectic temperature	K
T_f	Reference temperature	K
T_o	Threshold temperature in Model 1	K
$\overline{v}$	Mean molecular speed	$\mathrm{m\,s^{-1}}$
V_{air}	Volume of air per unit volume of snowpack	$\mathrm{m^3_{air}\,m^{-3}_{snowpack}}$
V_{grain}	Volume of a snow grain	$\mathrm{m^3}$

Table 1. Characteristic times associated with gas-phase diffusion, mass transport and uptake of gas into ice grain

Process	Expression	Order of magnitude, s
Interfacial mass transport to a liquid surface[i]	$\frac{3\overline{v}\alpha_{aq}}{4R_{\mathrm{eff}}}$	10^{-7}
Gas-phase diffusion to the surface of a spherical droplet[ii]	$\frac{3\,D'_s}{R_{\mathrm{eff}}^2}$	10^{-4}
Molecular diffusion between snowpack and the atmosphere[iii]	$\frac{z^2}{D'_s}$	10^{0}
Liquid-phase diffusion within a water droplet[iv]	$\frac{4\,R_{\mathrm{eff}}^2}{\pi^2 k_{\mathrm{diff(aq)}}}$	10^{0}
Surface adsorption on ice[v]	$\frac{1}{k_{\mathrm{des}}}$	10^{3}
Solid-state diffusion within a snow grain[vi]	$\frac{4\,R_{\mathrm{eff}}^2}{\pi^2 k_{\mathrm{diff}}}$	10^{6}
Photolysis at a snowpack surface[vii]	$\frac{1}{J}$	$> 10^{7}$

[i] ?, with an effective radius, $R_{\mathrm{eff}} = 70$ μm, and accommodation coefficient on liquid water, $\alpha_{aq} = 7.5 \times 10^{-5} \exp(2100/\mathrm{Temp})$ (?). [ii] ?, with an effective molecular diffusivity, $D'_s = D_a/\tau_g$, where the tortuosity, $\tau_g = 2$ and molecular diffusivity in free air at 296 K, $D_a(296\mathrm{K}) = 87$ Torr cm^2 s^{-1} (?). [iii] ?, with a snow layer thickness, $z = 4$ mm. [iv] ?, with a diffusion coefficient in liquid water, $k_{\mathrm{diff(aq)}} = 1 \times 10^{-9}$ m^2 s^{-1} (?) . [v] ?, with an equilibrium constant for Langmuir adsorption, $K_{eq} = 2 \times 10^{-16}$ m^3 molecule^{-1} and adsorption coefficient, $k_{\mathrm{ads}} = 1.7 \times 10^{-19}$ m^3 molecule^{-1} s^{-1}. [vi] ?, with a diffusion coefficient in ice, $k_{\mathrm{diff}} = 6 \times 10^{-16}$ m^2 s^{-1} (?). [vii] ?, with a surface NO_3^- photolysis rate, $J, = 10^7$ s^{-1} (?).

Table 2. Summary of model performance at Dome C based on the coefficient of variation of RMSE, C_v(RMSE)

Model description	Short name	Whole year DOY 30 - 385	Winter-Spring DOY 90 - 318	Summer DOY 319 - 385
Surface Adsorption & Solid Diffusion	Kinetic Approach	-	0.65	-
Ice Solubility & Solid Diffusion	Equilibrium Approach	-	0.52	-
Surface Adsorption-Co Condensation/DI Solvation & Solid Diffusion				
No threshold (no Solvation)	Model 1-none	1.07	0.65	0.88
Threshold ≤ 238 K	Model 1-238K	1.34	0.73	1.11
~~Threshold ≤ 240 K Model 1-240K 0.50 0.64 0.36 Threshold ≤ 242 K Model 1-242K0.61 0.65 0.46~~ Surface Adsorption-Co Condensation & Solid Diffusion + micropocket	Model 2	0.84	0.73	0.67

Table 3. Summary of model performance at Halley based on the coefficient of variation of RMSE, $\mathrm{C_v(RMSE)}$

Model description	Short name	Whole year DOY 87 - 406	Winter DOY 90 - 257	Spring -Early Autumn DOY 258 - 406
Surface Adsorption & Solid Diffusion	Kinetic Approach	-	1.13	-
Ice Solubility & Solid Diffusion	Equilibrium Approach	-	1.12	-
Surface Adsorption-Co Condensation/DI Solvation & Solid Diffusion				
No threshold (no Solvation)	Model 1-none	1.06	1.06	0.95
Threshold $\leq$ 238 K	Model 1-238K	89.28	27.78	87.15
~~Threshold $\leq$ 242 K~~	~~Model 1-242K~~	~~50.76~~	~~23.86~~	~~49.00~~
Surface Adsorption-Co Condensation & Solid Diffusion + micropocket	Model 2	0.84	1.08	0.65

Table 4. Sensitivity test for Model 1 and 2 based on the coefficient of variation of RMSE, C_V(RMSE), the metric was used to measure a goodness of fit. Note that column one is not fitted to the observation and the values are only varying to show the sensitivity of the models against inputs and parameterisation.

Parameter		Model 1						Model 2					
		Dome C			Halley			Dome C			Halley		
		Whole year	Winter-Spring	Summer	Whole year	Winter	Spring-Summer	Whole year	Winter-Spring	Summer	Whole year	Winter	Spring-Summer
Control		1.34	0.73	1.11	89.28	27.78	87.15	0.84	0.73	0.67	0.84	1.08	0.6
$[HNO_3]$	-20%	0.98	0.60	0.81	71.19	22.12	69.5	0.80	0.62	0.64	0.77	1.10	0.5
	$+20\%$	1.73	0.90	1.45	107.36	33.43	104.80	0.95	0.88	0.76	0.92	1.07	0.7
SSA	-10%	1.06	0.63	0.88	79.35	24.79	77.46	0.83	0.67	0.67	0.84	1.10	0.6
	$+10\%$	1.63	0.84	1.36	99.22	30.75	96.86	0.84	0.78	0.67	0.83	1.07	0.6
α	-10%	1.34	0.73	1.11	79.35	24.78	77.46	0.83	0.73	0.67	0.83	1.08	0.6
	$+10\%$	1.34	0.73	1.11	79.35	24.80	77.46	0.83	0.73	0.67	0.83	1.08	0.6
N_{max}	-10%	1.32	0.67	1.10	89.27	27.77	87.15	0.83	0.69	0.67	0.84	1.09	0.6
	$+10\%$	1.36	0.80	1.13	89.29	27.78	87.15	0.84	0.77	0.67	0.84	1.07	0.6
T_o (Model 1) or T_e (Model 2)	-2 K	3.53	0.91	3.00	90.45	42.54	87.31	0.95	0.92	0.75	0.85	1.12	0.6
	+2 K	0.50	0.64	0.36	67.49	25.33	65.62	0.73	0.65	0.58	0.86	1.07	0.6
	+4 K	0.61	0.65	0.47	50.76	23.86	49.00	0.72	0.65	0.57	0.88	1.06	0.6
pH	-0.4	1.34	0.73	1.11	89.28	27.78	87.15	-	-	-	-	-	-
	+0.4	1.34	0.73	1.11	89.28	27.78	87.15	-	-	-	-	-	-
	+0.8	1.34	0.73	1.11	89.28	27.78	87.15	-	-	-	-	-	-
$[NO_3{}^-]$	-20%	1.85	0.98	1.54	111.87	34.84	109.2	0.99	0.96	0.79	1.09	1.08	0.9
	$+20\%$	1.04	0.61	0.86	74.22	23.07	72.45	0.80	0.64	0.64	0.74	1.10	0.5

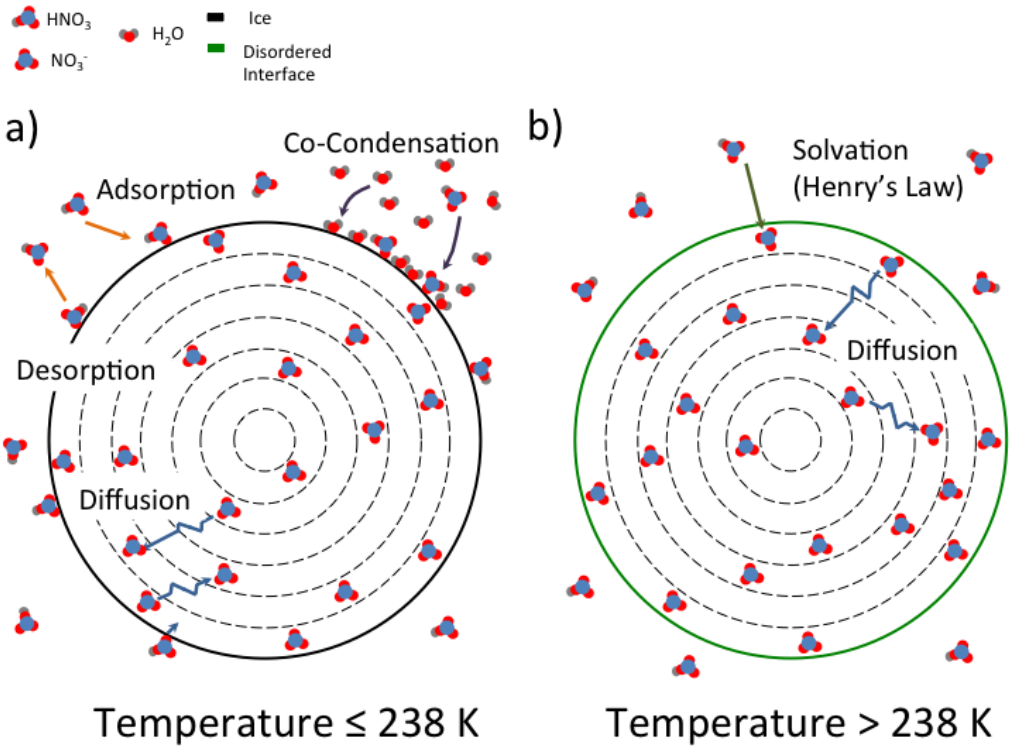

Figure 1. Schematic of Model 1. a) At temperatures below 238 K the concentration of NO_3^- at the surface of the snow grain is determined by Air-Ice processes, i.e. non-equilibrium adsorption and co-condensation. b) At temperatures above 238 K the concentration of NO_3^- at the surface of the snow grain is determined by Air-DI processes, i.e. non-equilibrium solvation.

~~The dependence of the effective Henry's Law coefficient, $k_{\mathrm{H}^{\mathrm{eff}}}$, of on temperature (a.) and pH (b.)~~

~~Year-round estimates of SSA fro Dome C (—) and Halley (—·) are based on observations at Dome C from 2012 to 2015 by ?. The SSA estimates for Halley take into account the shorter cold period compare to Dome C, which tends to have larger SSA.~~

~~Model 2 output of Dome C skin layer snow concentration. The major interface between air and snow is assumed to be ice ('Air-Ice') at all temperatures below melting and the concentration in ice is determined by a combination of non-equilibrium adsorption and co-condensation coupled with solid-state diffusion. Above eutectic temperature, T_e (230), liquid co-existed with ice in the form of micropocket. The partition between air and micropocket is determined by Henry's law. Pink: 'Air-Ice' plus micropocket; Light Blue: 'Air-Ice'; Orange squares: observation.~~

~~Model 2 output of Halley skin layer snow concentration. The major interface between air and snow is assumed to be ice ('Air-Ice') at all temperature below melting and the concentration in ice is determined by a combination of non-equilibrium adsorption and co-condensation coupled~~

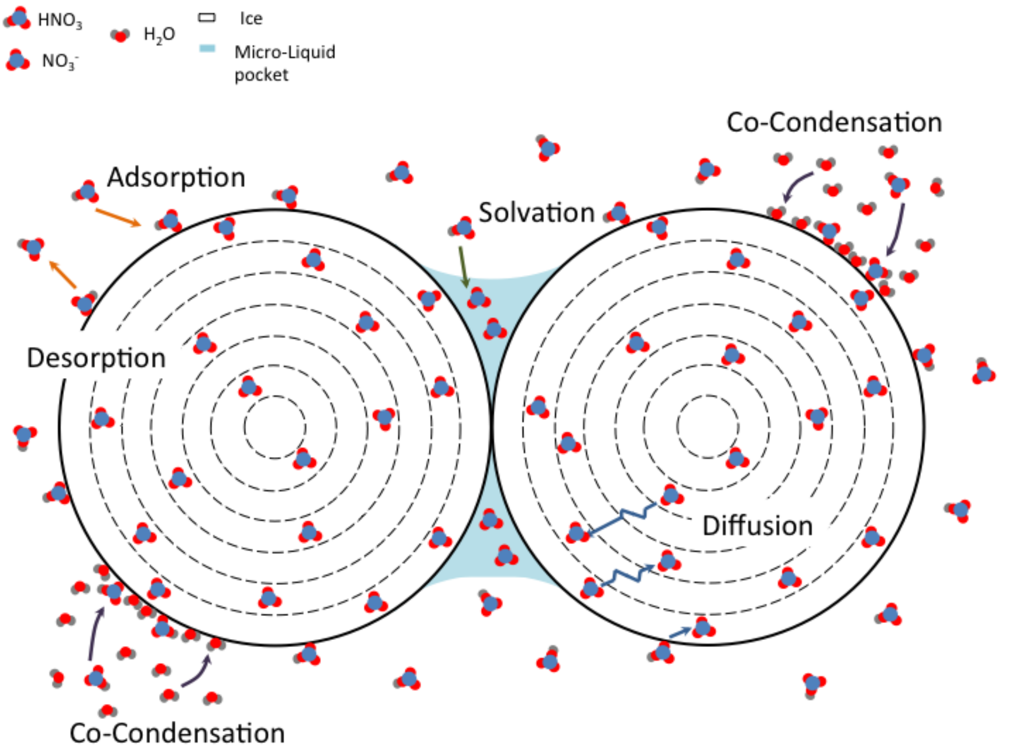

Figure 2. Schematic of Model 2. At all temperatures below melting, the concentration of NO_3^- at the surface of the snow grain is determined by Air-Ice processes, i.e. non-equilibrium adsorption and co-condensation. At temperatures above the eutectic temperature, liquid is assumed to co-exist with ice and the liquid fraction is in the form of micropockets that are located at grain boundaries and triple junctions (**?**).

~~with solid-state diffusion. Above eutectic temperature, T_e (252), liquid co-exists with ice in the form of micropocket. The partition between air and micropocket is determined by Henry's law. Pink: 'Air-Ice' plus micropocket interaction ; Light Blue: 'Air-Ice' only interaction; Orange squares: observation. Grey (Right axis) - measured bulk concentration of other ions, e.g. + .~~

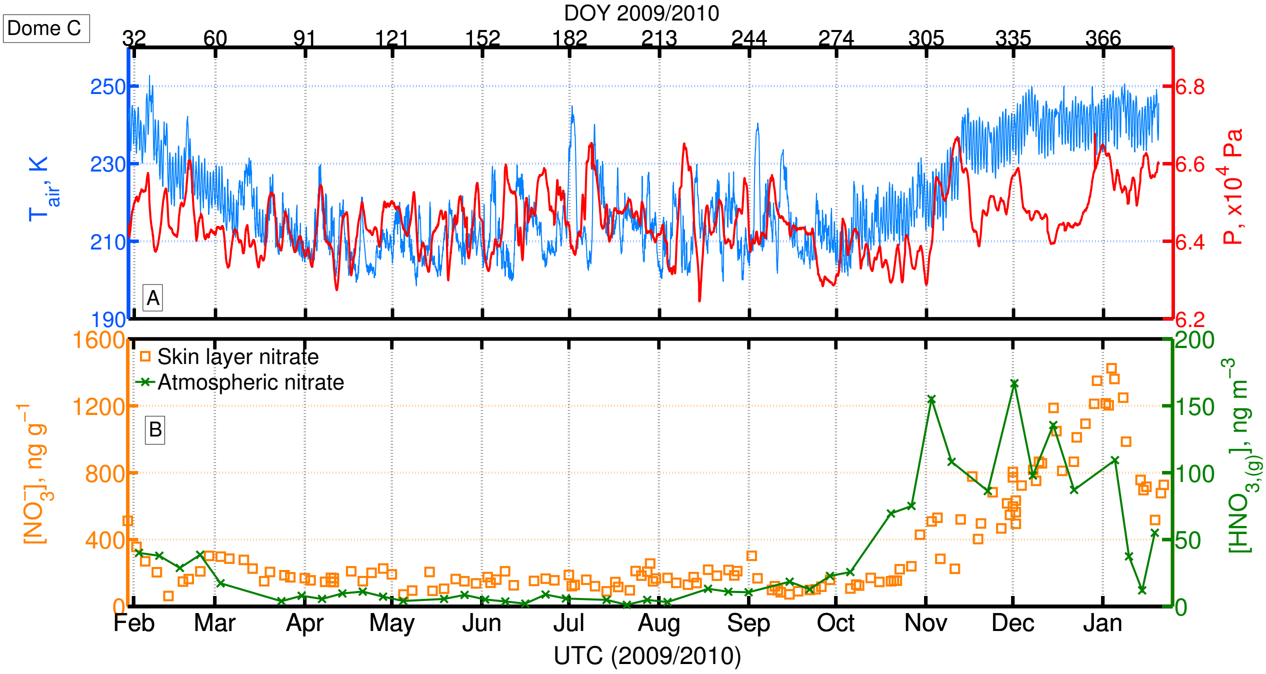

Figure 3. Atmospheric and snow observations from Dome C ~~(?)~~(published previously by **?**, Fig. 6). ~~Top:~~ (**A**) Air temperature (blue, left axis) and atmospheric pressure (red, right axis). ~~Bottom:~~ (**B**) skin layer snow (i.e. top 4 ± 2 mm) nitrate concentrations (orange square, left axis) and atmospheric nitrate concentrations, sum of the atmospheric particulate nitrate and HNO_3 (green, right axis).

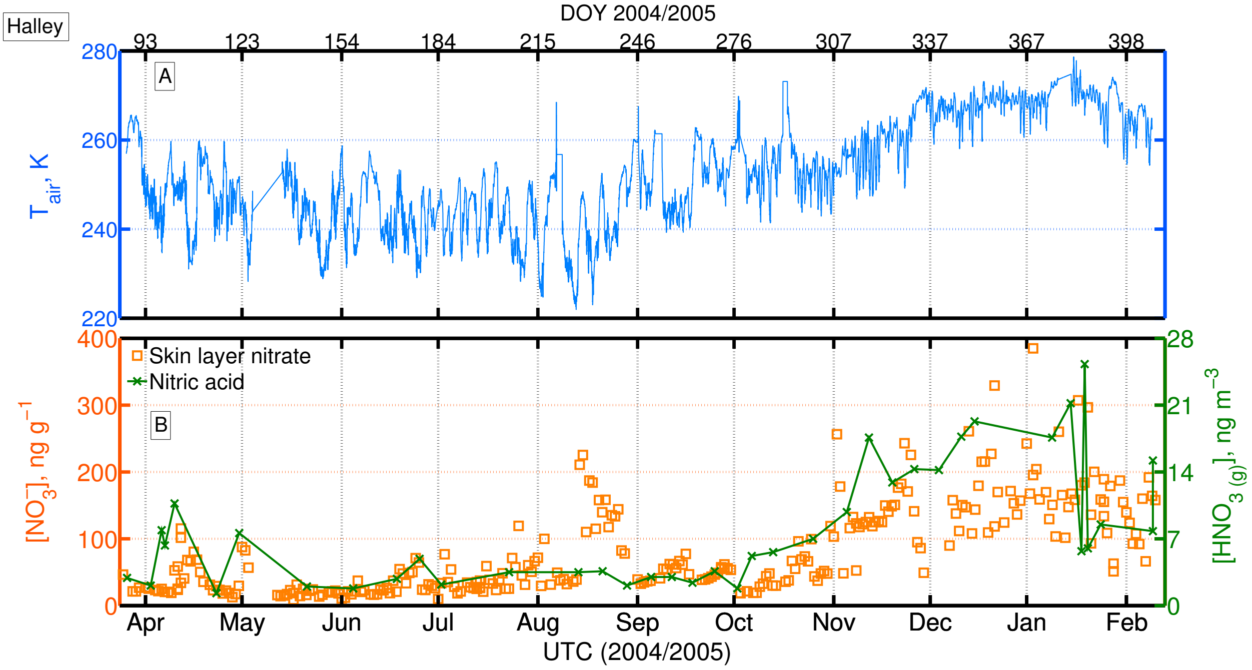

Figure 4. Atmospheric and snow observations at Halley between 27th March 2004 and 9th February 2005 (**?**). ~~Top:~~ **(A)** Air temperature. ~~Bottom:~~ **(B)** surface snow, the top $10 \pm 15\ \mathrm{mm}$, nitrate concentrations (orange square, left axis) and gas-phase nitric acid concentrations (green, right axis).

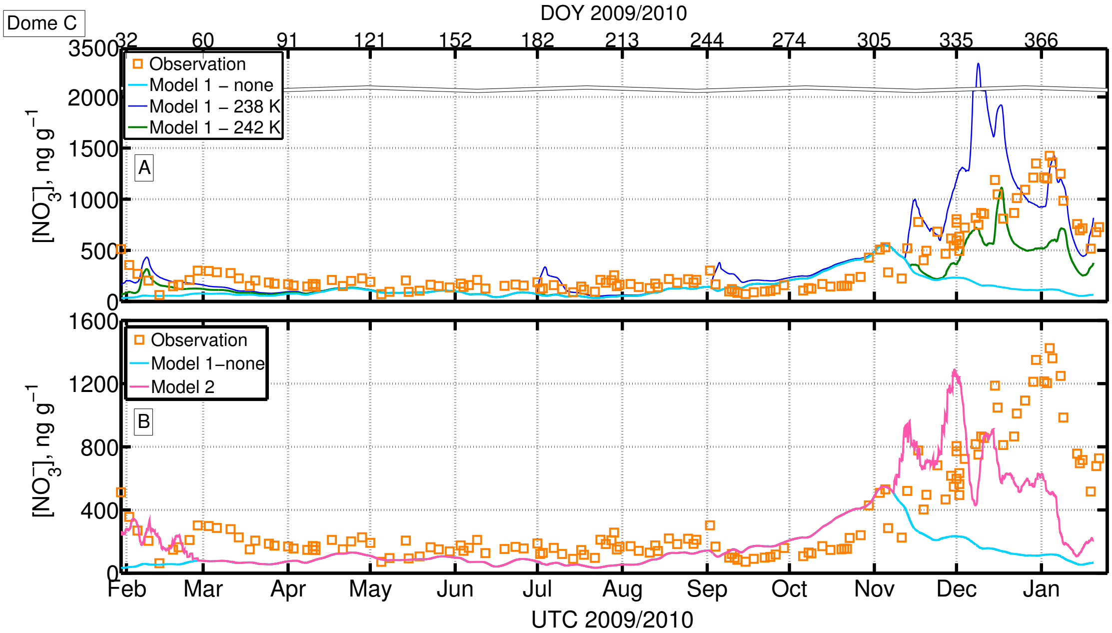

Figure 5. (**A**) Model 1 output of Dome C skin layer snow concentration of NO_3^-. At temperatures less than the threshold temperature, T_o, the interface between air and snow grain is assumed to be ice ('Air-Ice') and the NO_3^- concentration is determined by a combination of non-equilibrium adsorption on ice and co-condensation coupled with solid-state diffusion. Above T_o, the interface between air and snow grain is assumed to be DI ('Air-DI'), i.e. the NO_3^- concentration is determined by combination of non-equilibrium solvation in DI coupled with solid-state diffusion. Note that the y-axis is broken between 2000-3500 ng g. Orange squares: observation. Dark blue: 'Mode 1 - 238 K', Model 1 with T_o set as 238 K; Green: 'Mode 1 - 242 K', Model 1 with T_o set as 242 K; Light blue: '~~Air-Ice~~Mode 1 - none', Model 1 with T_o set above the melting temperature, i.e. air-ice only interaction; (**B**) Model 2 output of Dome C skin layer snow NO_3^- concentration. The major interface between air and snow is assumed to be ice ('Air-Ice') at all temperatures below melting and the NO_3^- concentration in ice is determined by a combination of non-equilibrium adsorption and co-condensation coupled with solid-state diffusion. Above eutectic temperature, T_e (230 K), liquid co-existed with ice in the form of micropocket. The partition between air and micropocket is determined by Henry's law. Orange squares: observation; Light blue: 'Mode 1 - none', Model 1 with T_o set ~~as~~ above the melting temperature, i.e. air-ice only interaction; ~~Orange squares~~Pink: ~~observation~~'Model 2' - air-ice interaction plus micro-liquidpockets.

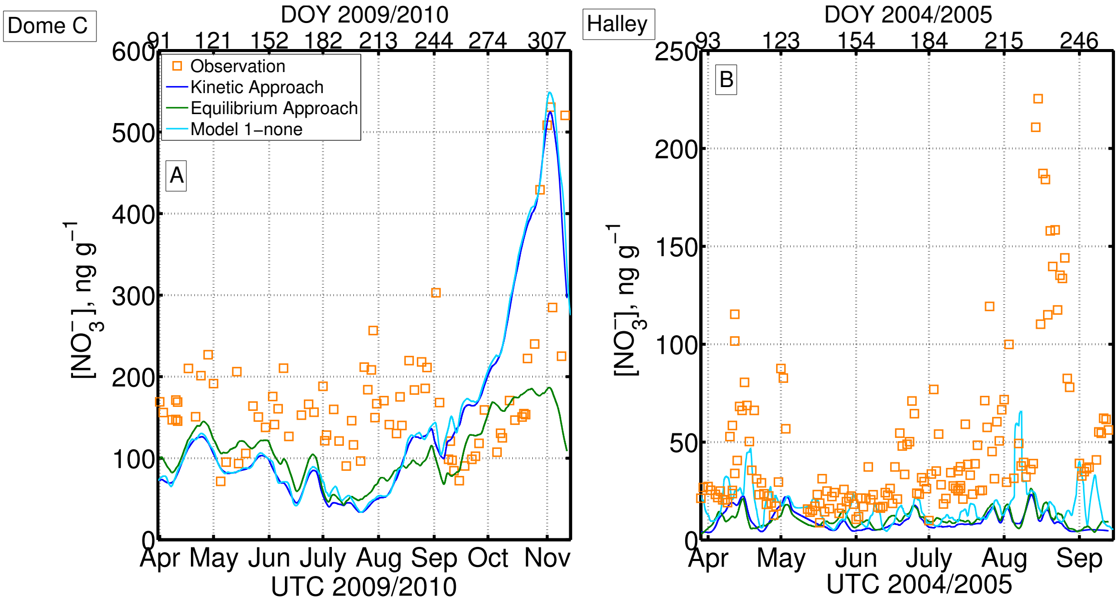

Figure 6. Comparison of the ~~nitrate Air-Ice interaction between the~~ '~~Equilibrium~~Kinetic' approach (~~similar to ?~~this work, in ~~green~~dark blue) ~~,~~ with the '~~Kinetic~~Equilibrium' approach (~~this work~~similar to **?**, in ~~dark blue~~green), and the contribution from the co-condensation process (~~this work:~~ Results from Model 1- none, in light blue) in winter. The 'Kinetic' approach describes the air-snow interaction of nitrate as non-equilibrium kinetic surface adsorption coupled with solid diffusion inside the grain whereas the 'Equilibrium' approach describes the interaction as equilibrium solubility coupled with solid diffusion inside the grain. The 'Model 1-none' describes the interaction as co-condensation plus non-equilibrium kinetic surface adsorption coupled with solid diffusion within the grain. (**A**) Results at Dome C. (**B**) Results at Halley.

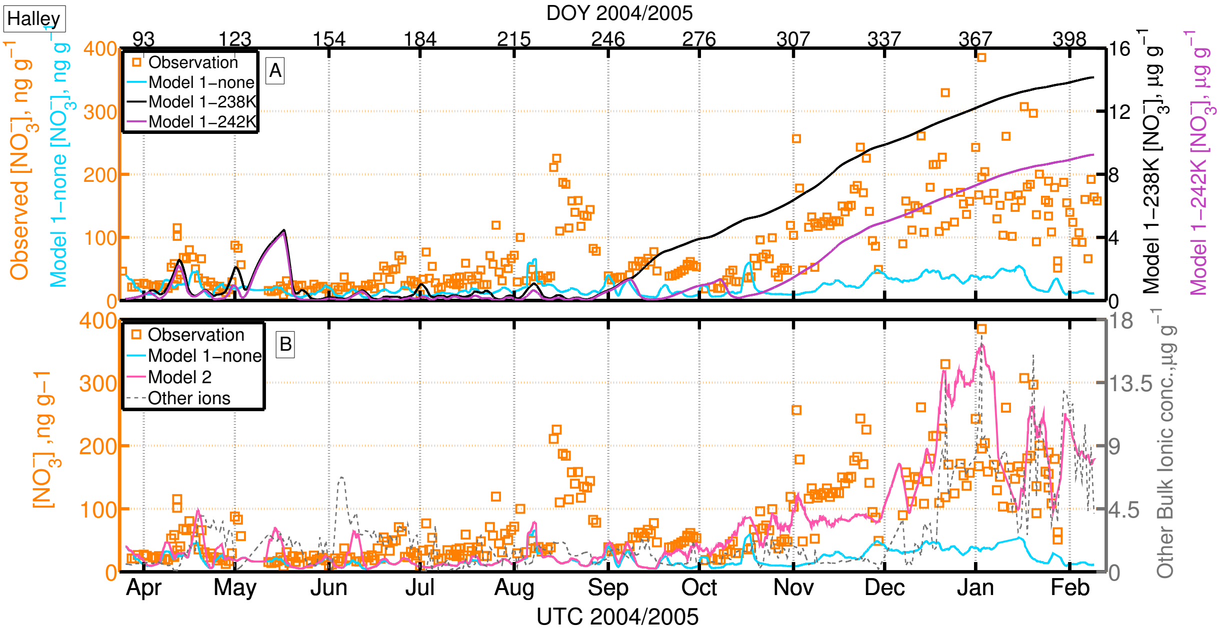

Figure 7. (A) Model 1 output of ~~Halley~~ skin layer snow concentration of NO_3^- at Halley. At temperatures ~~less than~~ below the threshold temperature, T_o, the interface between air and snow grain is assumed to be ice ('Air-Ice') and the NO_3^- concentration is determined by a combination of non-equilibrium adsorption on ice and co-condensation coupled with solid-state diffusion. At temperature above T_o, the interface between air and snow grain is assumed to be DI ('Air-Ice'), ~~that~~ where the NO_3^- concentration is determined by a combination of non-equilibrium solvation in DI coupled with solid-state diffusion. Orange square (Left axis) - observation; Light blue (Left axis) : 'Mode 1 - none', Model 1 with T_o set above the melting temperature, i.e. air-ice only interaction; Black (Right axis): 'Model 1-238 K' - Model 1 with T_o set ~~as~~ to 238 K; Purple (Right axis): 'Model 1-242 K' - Model 1 with T_o set ~~as~~ to 242 K~~; Light blue~~. (~~Left axis~~**B**) ~~:~~ Model 2 output of Halley skin layer snow NO_3^- concentration. The major interface between air and snow is assumed to be ice ('Air-Ice') at all temperature below melting and the NO_3^- concentration in ice is determined by a combination of non-equilibrium adsorption and co-condensation coupled with solid-state diffusion. Above eutectic temperature, ~~i~~T_e (252 K), liquid co-existes with ice in the form of micropocket. ~~e~~The partition between air and micropocket is determined by Henry's law. Orange squares: observation; Light Blue: 'Mode 1 - none', Model 1 with T_o set ~~as~~ above the melting temperature, i.e. air-ice only interaction; ~~Orange square~~ Pink: 'Model 2' - air-ice interaction plus micro-liquidpockets; Grey (~~Left~~ Right axis) - ~~observation~~measured bulk concentration of other ions, where other ions refers to the sum of $[Na^+]$ and $[Cl^-]$.

Appendix A: ~~Air-Ice interface~~Parameterisation

Table A1. Parameterisation for HNO_3

Symbol	Parameter	Value/Parameterisation	units	Reference
α_0	Accommodation coefficient at reference temperature	3×10^{-3} [i]	Dimensionless	**?**
k_{diff}	Diffusion coefficient of nitrate in ice	$1.37 \times 10^{-2610/T}$	$\mathrm{cm^2\,s^{-1}}$	**?**
k_w	Thermal conductivity of snowpack	$k_w = k_{ice}\left(\frac{\rho}{\rho_{ice}}\right)^{2-0.5\frac{\rho}{\rho_{ice}}}$	$\mathrm{Wm^{-1}K^{-1}}$	**?** therein
k_{ice}	Thermal conductivity of ice	$k_{ice} = 9.828\exp(-0.0057T)$	$\mathrm{Wm^{-1}K^{-1}}$	**?** therein
$\Delta_{\mathrm{sol}}H$	Enthalpy of solution at standard temperature	-72.3	$\mathrm{kJ\,mol^{-1}}$	**?**
$\Delta_{\mathrm{obs}}H$	Enthalpy of uptake	-44	$\mathrm{kJ\,mol^{-1}}$	**?**
k_{H}^0	Henry constant at 298 K	1.7×10^5 [ii]	$\mathrm{M\,atm^{-1}}$	**?**
N_{max}	Maximum adsorption site	2.7×10^{18}	$\mathrm{molecules\,m^{-2}}$	**?**
$\overline{v}$	Mean molecular speed	$\sqrt{\frac{8RT}{M_m \pi}}$ [iii]	$\mathrm{m\,s^{-1}}$	**?**
$X^0_{\mathrm{HNO_3}}$	Molar fraction of HNO_3 in ice	$X^0_{\mathrm{HNO_3}} = 2.37 \times 10^{-12}\exp(\frac{3532.2}{T})P^{1/2.3}_{\mathrm{HNO_3}}$	$\mathrm{mol\,mol^{-1}}$	**?**
K_{eq}	Langmuir adsorption equilibrium constant	$-8.2 \times 10^{-18}\mathrm{T} + 2.01 \times 10^{-15}$	$\mathrm{m^3 molecule^{-1}}$	**?**
D_v	Water vapour diffusivity	$D_v = 2.11 \times 10^{-5}(\frac{T}{T_o})^{1.94}\frac{P_o}{P}$	$\mathrm{m^2\,s^{-1}}$	**?**

[i] Temperature dependent accommodation coefficient, $\alpha = \frac{\exp\{\ln(\frac{\alpha_0}{1-\alpha_0})[-\frac{\Delta_{\mathrm{obs}}H}{R}(\frac{1}{T}-\frac{1}{T_f})]\}}{1-\exp\{\ln(\frac{\alpha_0}{1-\alpha_0})[-\frac{\Delta_{\mathrm{obs}}H}{R}(\frac{1}{T}-\frac{1}{T_f})]\}}$, where R is the molar gas constant, T is the temperature, $\mathrm{T_f}$ is the reference temperature (220 K)

[ii] Temperature dependent dimensionless Henry's Law coefficient, $k_{\mathrm{H}}^{\mathrm{cc}} = k_{\mathrm{H}}^0 \times RT \times \exp\left(\frac{-\Delta_{\mathrm{sol}}H}{R}\left(\frac{1}{T} - \frac{1}{T^{\ominus}}\right)\right)$, where $T^{\ominus}$ is the standard temperature (298 K).

[iii] M_m is the molar mass of the gas.

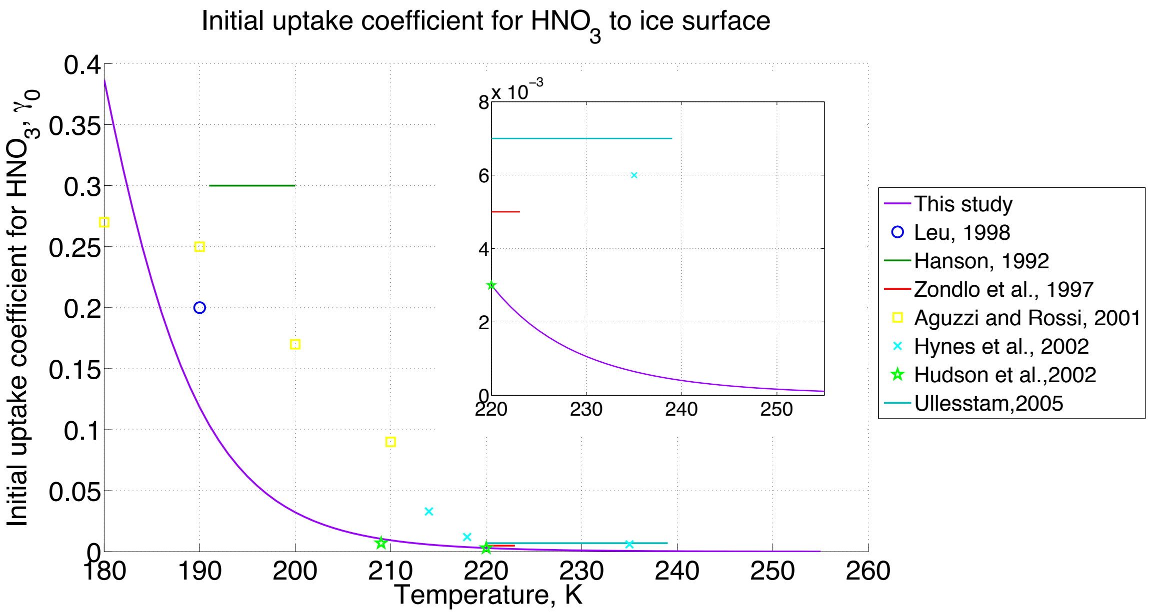

Figure A1. Initial uptake coefficient for $\mathrm{HNO_3}$ as a function of temperature obtained from different studies. The parameterisation used within this study is formulated in Table **??** and is chosen to give the best representation of the dependency on temperature.

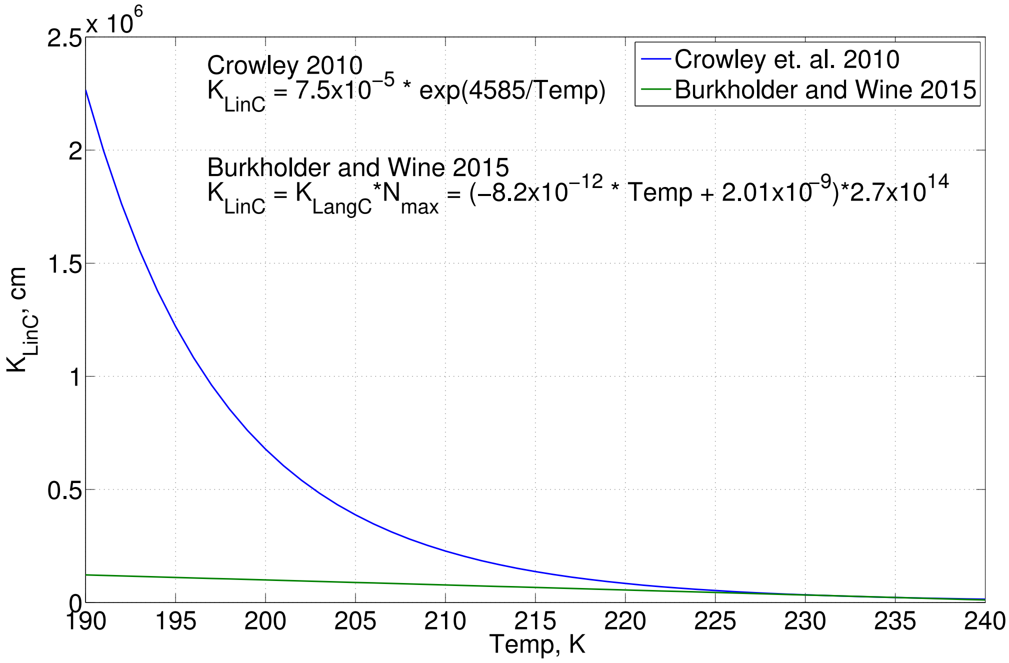

Figure A2. Langmuir adsorption equilibrium constant, $K_{\mathrm{LinC}} = K_{eq} \times N_{\mathrm{max}}$. The preferred temperature range for both parameterisation is 214-240 K and within this range the two parameterisations provide a comparable value. The **?** parameterisation deviate from the **?** parameterisation as temperature drop below 214 K due to the exponential temperature term. Here, the parameterisation from **?** was chosen based on the extreme cold temperature found in our validation sites.

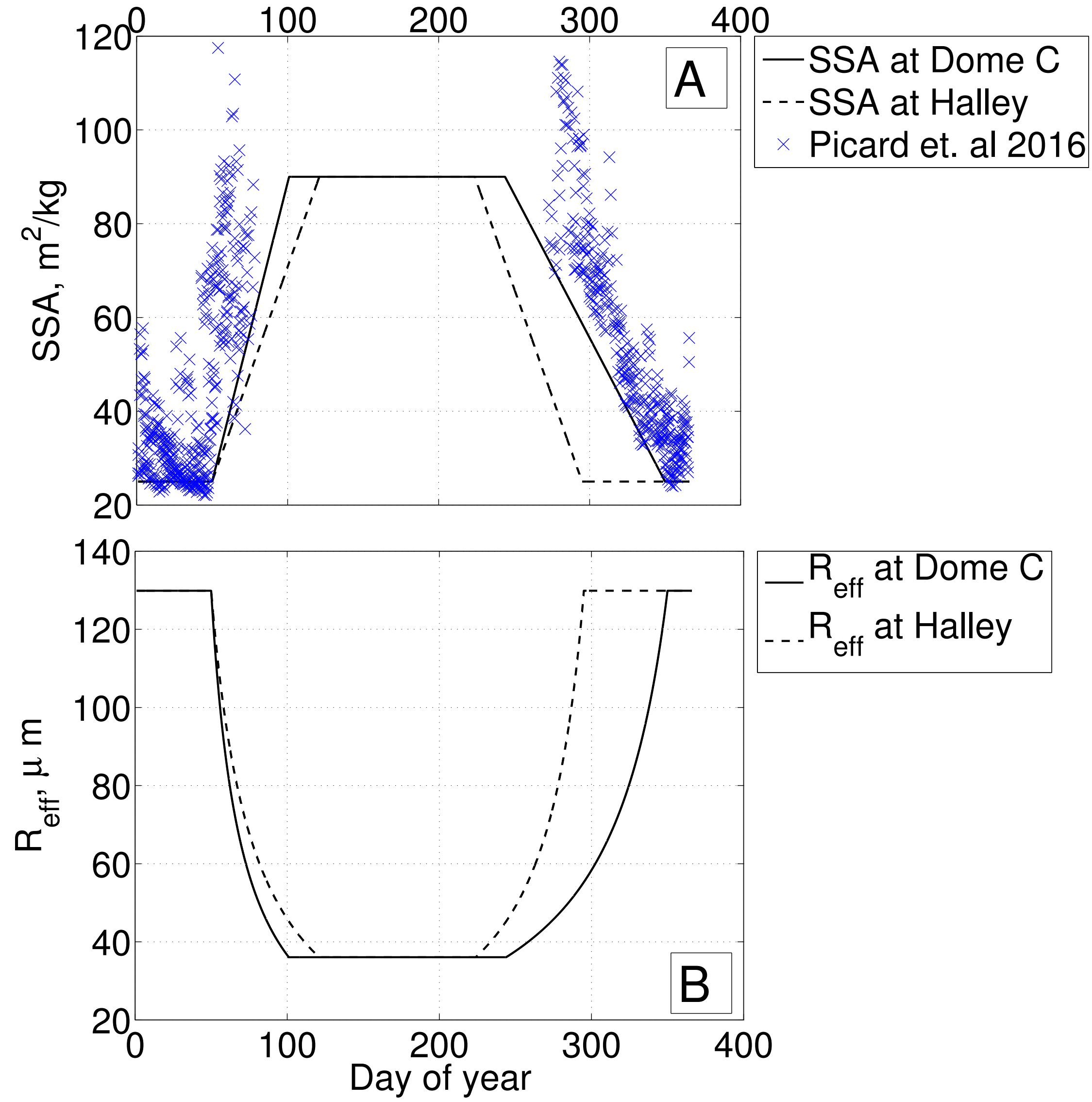

Figure A3. (**A**) Year-round estimates of the specific surface area (SSA) of snow at Dome C (–) and Halley (– –) were interpolated from observations at Dome C during 2012-2015 by **?** (×). The SSA estimates for Halley take into account the shorter cold period compare to Dome C, which tends to have larger SSA. (**B**) Year-round estimates of effective grain radius (R_{eff}) at Dome C (–) and Halley (– –) derived from Eq. **??**.

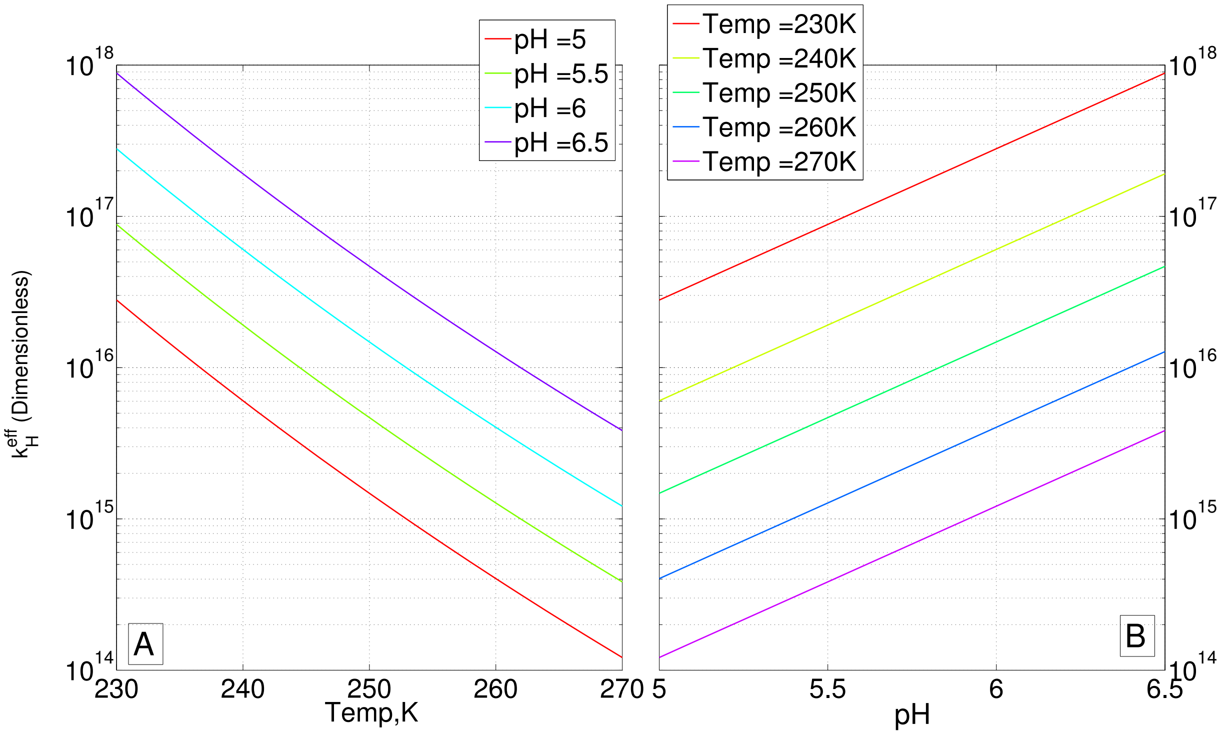

Figure A4. The dependence of the effective Henry's Law coefficient, $k_{H^{eff}}$, of HNO_3 on (A) temperature and (B) pH

References

Abbatt, Jonathan P. D.: Interaction of HNO3 with water?ice surfaces at temperatures of the free troposphere, Geophysical Research Letters, 24, 1479–1482, doi:10.1029/97GL01403, http://dx.doi.org/10.1029/97GL01403, 1997.

Akinfiev, N. N., Mironenko, M. V., and Grant, S. A.: Thermodynamic Properties of NaCl Solutions at Subzero Temperatures, Journal of Solution Chemistry, 30, 1065–1080, doi:10.1023/A:1014445917207, http://dx.doi.org/10.1023/A:1014445917207, 2001.

Ammann, M., Cox, R. A., Crowley, J. N., Jenkin, M. E., Mellouki, A., Rossi, M. J., Troe, J., and Wallington, T. J.: Evaluated kinetic and photochemical data for atmospheric chemistry: Volume VI ? heterogeneous reactions with liquid substrates, Atmospheric Chemistry and Physics, 13, 8045–8228, doi:10.5194/acp-13-8045-2013, http://www.atmos-chem-phys.net/13/8045/2013/, 2013.

Argentini, S., Pietroni, I., Mastrantonio, G., Viola, A. P., Dargaud, G., and Petenko, I.: Observations of near surface wind speed, temperature and radiative budget at Dome C, Antarctic Plateau during 2005, Antarctic Science, 26, 104–112, doi:10.1017/S0954102013000382, 2014.

Arthern, R. J., Winebrenner, D. P., and Vaughan, D. G.: Antarctic snow accumulation mapped using polarization of 4.3-cm wavelength microwave emission, Journal of Geophysical Research: Atmospheres, 111, n/a–n/a, doi:10.1029/2004JD005667, http://dx.doi.org/10.1029/2004JD005667, d06107, 2006.

Bartels-Rausch, T., Jacobi, H.-W., Kahan, T. F., Thomas, J. L., Thomson, E. S., Abbatt, J. P. D., Ammann, M., Blackford, J. R., Bluhm, H., Boxe, C., Domine, F., Frey, M. M., Gladich, I., Guzmán, M. I., Heger, D., Huthwelker, T., Klán, P., Kuhs, W. F., Kuo, M. H., Maus, S., Moussa, S. G., McNeill, V. F., Newberg, J. T., Pettersson, J. B. C., Roeselová, M., and Sodeau, J. R.: A review of air ice chemical and physical interactions (AICI): liquids, quasi-liquids, and solids in snow, Atmospheric Chemistry and Physics, 14, 1587–1633, doi:10.5194/acp-14-1587-2014, http://www.atmos-chem-phys.net/14/1587/2014/, 2014.

Beine, H. J., Honrath, R. E., DominÈ, F., Simpson, W. R., and Fuentes, J. D.: NOx during background and ozone depletion periods at Alert: Fluxes above the snow surface, Journal of Geophysical Research: Atmospheres, 107, ACH 7–1–ACH 7–12, doi:10.1029/2002JD002082, http://dx.doi.org/10.1029/2002JD002082, 4584, 2002.

Beine, H. J., DominÈ, F., Ianniello, A., Nardino, M., Allegrini, I., Teinilä, K., and Hillamo, R.: Fluxes of nitrates between snow surfaces and the atmosphere in the European high Arctic, Atmospheric Chemistry and Physics, 3, 335–346, doi:10.5194/acp-3-335-2003, http://www.atmos-chem-phys.net/3/335/2003/, 2003.

Beyer, K. D., , and Hansen, A. R.: Phase Diagram of the Nitric Acid/Water System: Implications for Polar Stratospheric Clouds, The Journal of Physical Chemistry A, 106, 10 275–10 284, doi:10.1021/jp025535o, http://dx.doi.org/10.1021/jp025535o, 2002.

Bock, J., Savarino, J., and Picard, G.: Air–snow exchange of nitrate: a modelling approach to investigate physicochemical processes in surface snow at Dome C, Antarctica, Atmospheric Chemistry and Physics, 16, 12 531–12 550, doi:10.5194/acp-16-12531-2016, http://www.atmos-chem-phys.net/16/12531/2016/, 2016.

Boxe, C. S. and Saiz-Lopez, A.: Multiphase modeling of nitrate photochemistry in the quasi-liquid layer (QLL): implications for NO$_x$ release from the Arctic and coastal Antarctic snowpack, Atmospheric Chemistry and Physics, 8, 4855–4864, doi:10.5194/acp-8-4855-2008, http://www.atmos-chem-phys.net/8/4855/2008/, 2008.

Brimblecombe, P. and Clegg, S. L.: The solubility and behaviour of acid gases in the marine aerosol, Journal of Atmospheric Chemistry, 7, 1–18, doi:10.1007/BF00048251, http://dx.doi.org/10.1007/BF00048251, 1988.

Burkholder,J. B. , Sander, S. P. , Abbatt, J. P., Barker, J. R., Huie, R. E., Kolb, C. E., Kurylo, M. J., Orkin, V. L., Wilmouth, D. M., Wine, P. H. : Chemical Kinetics and Photochemical Data for Use in Atmospheric Studies, Evaluation No. 18, JPL Publication 15-10, Jet Propulsion Laboratory, Pasadena, 2015.

Cho, H., Shepson, P. B., Barrie, L. A., Cowin, J. P., Zaveri, R.: NMR Investigation of the QuasiBrine Layer in Ice/Brine Mixtures, The Journal of Physical Chemistry B, 106, 11 226–11 232, doi:10.1021/jp020449, http://dx.doi.org/10.1021/jp020449+, 2002.

Conde, M. M., Vega, C., and Patrykiejew, A.: The thickness of a liquid layer on the free surface of ice as obtained from computer simulation, The Journal of Chemical Physics, 129, 014702, doi:http://dx.doi.org/10.1063/1.2940195, http://scitation.aip.org/content/aip/journal/jcp/129/1/10.1063/1.2940195, 2008.

Cox, R. A., Fernandez, M. A., Symington, A., Ullerstam, M., and Abbatt, J. P. D.: A kinetic model for uptake of HNO3 and HCl on ice in a coated wall flow system, Phys. Chem. Chem. Phys., 7, 3434–3442, doi:10.1039/B506683B, http://dx.doi.org/10.1039/B506683B, 2005.

Crowley, J. N., Ammann, M., Cox, R. A., Hynes, R. G., Jenkin, M. E., Mellouki, A., Rossi, M. J., Troe, J., and Wallington, T. J.: Evaluated kinetic and photochemical data for atmospheric chemistry: Volume V heterogeneous reactions on solid substrates, Atmospheric Chemistry and Physics, 10, 9059–9223, doi:10.5194/acp-10-9059-2010, http://www.atmos-chem-phys.net/10/9059/2010/, 2010.

Dasgupta, P. K., Campbell, S. W., Al-Horr, R. S., Ullah, S. R., Li, J., Amalfitano, C., and Poor, N. D.: Conversion of sea salt aerosol to NaNO3 and the production of HCl: Analysis of temporal behavior of aerosol chloride/nitrate and gaseous HCl/HNO3 concentrations with {AIM}, Atmospheric Environment, 41, 4242 – 4257, doi:http://dx.doi.org/10.1016/j.atmosenv.2006.09.054, http://www.sciencedirect.com/science/article/pii/S1352231006012921, (BRACE)Bay Region Atmospheric Chemistry Experiment, 2007.

Domine, F., Bock, J., Voisin, D., and Donaldson, D. J.: Can We Model Snow Photochemistry? Problems with the Current Approaches, The Journal of Physical Chemistry A, 117, 4733–4749, doi:10.1021/jp3123314, http://dx.doi.org/10.1021/jp3123314, pMID: 23597185, 2013.

Erbland, J., Vicars, W. C., Savarino, J.,Morin, S., Frey, M. M., Frosini, D., Vince, E., Martins, J. M. F.: Air snow transfer of nitrate on the East Antarctic Plateau Part 1: Isotopic evidence for a photolytically driven dynamic equilibrium in summer , Atmospheric Chemistry and Physics, 13, 6403–6419, doi:10.5194/acp-13-6403-2013, http://www.atmos-chem-phys.net/13/6403/2013/, 2013.

Finlayson-Pitts, B. J. and Jr., J. N. P.: {CHAPTER} 5 - Kinetics and Atmospheric Chemistry, in: Chemistry of the Upper and Lower Atmosphere, edited by Finlayson-Pitts, B. J. and Pitts, J. N., pp. 130 – 178, Academic Press, San Diego, doi:http://dx.doi.org/10.1016/B978-012257060-5/50007-1, http://www.sciencedirect.com/science/article/pii/B9780122570605500071, 2000.

Fowler, D., Amann, M., Anderson, F., Ashmore, M., Cox, P., Depledge, M., Derwent, D., Grennfelt, P., Hewitt, N., Hov, O., Jenkin, M., Kelly, F., Liss, P. S., Pilling, M., Pyle, J., Slingo, J. and Stevenson, D.: Ground-level ozone in the 21st century: future trends, impacts and policy implications, vol. 15/08 of *Science Policy*, The Royal Society, London, http://nora.nerc.ac.uk/8577/, prof. David Fowler was Chair of the Working Group, 2008.

France, J. L., King, M. D., Frey, M. M., Erbland, J., Picard, G., Preunkert, S., MacArthur, A., and Savarino, J.: Snow optical properties at Dome C (Concordia), Antarctica; implications for snow emissions and snow chemistry of reactive nitrogen, Atmospheric Chemistry and Physics, 11, 9787–9801, doi:10.5194/acp-11-9787-2011, http://www.atmos-chem-phys.net/11/9787/2011/, 2011.

Frey, M. M., Savarino, J., Morin, S., Erbland, J., and Martins, J. M. F.: Photolysis imprint in the nitrate stable isotope signal in snow and atmosphere of East Antarctica and implications for reactive nitrogen cycling, Atmospheric Chemistry and Physics, 9, 8681–8696, doi:10.5194/acp-9-8681-2009, http://www.atmos-chem-phys.net/9/8681/2009/, 2009.

Frey, M. M., Brough, N., France, J. L., Anderson, P. S., Traulle, O., King, M. D., Jones, A. E., Wolff, E. W., and Savarino, J.: The diurnal variability of atmospheric nitrogen oxides (NO and NO_2) above the Antarctic Plateau driven by atmospheric stability and snow emissions, Atmospheric Chemistry and Physics, 13, 3045–3062, doi:10.5194/acp-13-3045-2013, http://www.atmos-chem-phys.net/13/3045/2013/, 2013.

Flanner, M. G. and Zender, C. S.: Linking snowpack microphysics and albedo evolution, Journal of Geophysical Research: Atmospheres, 111, n/a–n/a, doi:10.1029/2005JD006834, http://dx.doi.org/10.1029/2005JD006834, d12208, 2006.

Gligorovski, S., Strekowski, R., Barbati, S., and Vione, D.: Environmental Implications of Hydroxyl Radicals (OH), Chemical Reviews, 115, 13 051–13 092, doi:10.1021/cr500310b, http://dx.doi.org/10.1021/cr500310b, pMID: 26630000, 2015.

Grannas, A. M., Jones, A. E., Dibb, J., Ammann, M., Anastasio, C., Beine, H. J., Bergin, M., Bottenheim, J., Boxe, C. S., Carver, G., Chen, G., Crawford, J. H., Dominé, F., Frey, M. M., Guzmán, M. I., Heard, D. E., Helmig, D., Hoffmann, M. R., Honrath, R. E., Huey, L. G., Hutterli, M., Jacobi, H. W., Klán, P., Lefer, B., McConnell, J., Plane, J., Sander, R., Savarino, J., Shepson, P. B., Simpson, W. R., Sodeau, J. R., von Glasow, R., Weller, R., Wolff, E. W., and Zhu, T.: An overview of snow photochemistry: evidence, mechanisms and impacts, Atmospheric Chemistry and Physics, 7, 4329–4373, doi:10.5194/acp-7-4329-2007, http://www.atmos-chem-phys.net/7/4329/2007/, 2007.

Honrath, R. E., Peterson, M. C., Dziobak, M. P., Dibb, J. E., Arsenault, M. A., and Green, S. A.: Release of NOx from sunlight-irradiated midlatitude snow, Geophysical Research Letters, 27, 2237–2240, doi:10.1029/1999GL011286, http://dx.doi.org/10.1029/1999GL011286, 2000.

Hudson, P. K., Zondlo, M. A., , and Tolbert*, M. A.: The Interaction of Methanol, Acetone, and Acetaldehyde with Ice and Nitric Acid-Doped Ice: Implications for Cirrus Clouds, The Journal of Physical Chemistry A, 106, 2882–2888, doi:10.1021/jp012718m, http://dx.doi.org/10.1021/jp012718m, 2002.

Huthwelker, T. , Malmström, M. E., Helleis, F. , Moortgat, G. K. and Peter, T.: , Kinetics of HCl Uptake on Ice at 190 and 203 K: Implications for the Microphysics of the Uptake Process, The Journal of Physical Chemistry A, 30, 6302–6318, doi:10.1021/jp0309623, http://dx.doi.org/10.1021/jp0309623, 2004.

Hutterli, M. A. and Röthlisberger, R.: Atmosphere-to-snow-to-firn transfer studies of HCHO at Summit, Greenland, GEOPHYSICAL RESEARCH LETTERS, 26, 1691–1694, 1999.

Hutterli, M. A., McConnell, J. R., Bales, R. C., and Stewart, R. W.: Sensitivity of hydrogen peroxide (H2O2) and formaldehyde (HCHO) preservation in snow to changing environmental conditions: Implications for ice core records, Journal of Geophysical Research: Atmospheres, 108, ACH 6–1–ACH 6–9, doi:10.1029/2002JD002528, http://dx.doi.org/10.1029/2002JD002528, 4023, 2003.

Jones, A. E., Weller, R., Anderson, P. S., Jacobi, H.-W., Wolff, E. W., Schrems, O., and Miller, H.: Measurements of NOx emissions from the Antarctic snowpack, Geophysical Research Letters, 28, 1499–1502, doi:10.1029/2000GL011956, http://dx.doi.org/10.1029/2000GL011956, 2001.

Jones, A. E., Wolff, E. W., Salmon, R. A., Bauguitte, S. J.-B., Roscoe, H. K., Anderson, P. S., Ames, D., Clemitshaw, K. C., Fleming, Z. L., Bloss, W. J., Heard, D. E., Lee, J. D., Read, K. A., Hamer, P., Shallcross, D. E., Jackson, A. V., Walker, S. L., Lewis, A. C., Mills, G. P., Plane, J. M. C., Saiz-Lopez, A., Sturges, W. T., and Worton, D. R.: Chemistry of the Antarctic Boundary Layer and the Interface with Snow: an overview of the CHABLIS campaign, Atmospheric Chemistry and Physics, 8, 3789–3803, doi:10.5194/acp-8-3789-2008, http://www.atmos-chem-phys.net/8/3789/2008/, 2008.

Jones, A. E., Wolff, E. W., Ames, D., Bauguitte, S. J.-B., Clemitshaw, K. C., Fleming, Z., Mills, G. P., Saiz-Lopez, A., Salmon, R. A., Sturges, W. T., and Worton, D. R.: The multi-seasonal NO_y budget in coastal Antarctica and its link with surface snow and ice core nitrate: results from the CHABLIS campaign, Atmospheric Chemistry and Physics, 11, 9271–9285, doi:10.5194/acp-11-9271-2011, http://www.atmos-chem-phys.net/11/9271/2011/, 2011.

Kuo, M. H., Moussa, S. G., and McNeill, V. F.: Modeling interfacial liquid layers on environmental ices, Atmospheric Chemistry and Physics, 11, 9971–9982, doi:10.5194/acp-11-9971-2011, http://www.atmos-chem-phys.net/11/9971/2011/, 2011.

Legrand, M., Yang, X., Preunkert, S., and Theys, N.: Year-round records of sea salt, gaseous, and particulate inorganic bromine in the atmospheric boundary layer at coastal (Dumont d'Urville) and central (Concordia) East Antarctic sites, Journal of Geophysical Research: Atmospheres, 121, 997–1023, doi:10.1002/2015JD024066, http://dx.doi.org/10.1002/2015JD024066, 2015JD024066, 2016.

McConnell, J. R., Bales, R. C., Stewart, R. W., Thompson, A. M., Albert, M. R., and Ramos, R.: Physically based modeling of atmosphere-to-snow-to-firn transfer of H2O2 at South Pole, Journal of Geophysical Research: Atmospheres, 103, 10 561–10 570, doi:10.1029/98JD00460, http://dx.doi.org/10.1029/98JD00460, 1998.

McNeill, V. F., Grannas, A. M., Abbatt, J. P. D., Ammann, M., Ariya, P., Bartels-Rausch, T., Domine, F., Donaldson, D. J., Guzman, M. I., Heger, D., Kahan, T. F., Klán, P., Masclin, S., Toubin, C., and Voisin, D.: Organics in environmental ices: sources, chemistry, and impacts, Atmospheric Chemistry and Physics, 12, 9653–9678, doi:10.5194/acp-12-9653-2012, http://www.atmos-chem-phys.net/12/9653/2012/, 2012.

Morin, S., Savarino, J., Frey, M. M., Yan, N., Bekki, S., Bottenheim, J. W., and Martins, J. M. F.: Tracing the Origin and Fate of NOx in the Arctic Atmosphere Using Stable Isotopes in Nitrate, Science, 322, 730–732, doi:10.1126/science.1161910, http://science.sciencemag.org/content/322/5902/730, 2008.

Murray, K. A., Kramer, L. J., Doskey, P. V., Ganzeveld, L., Seok, B., Dam, B. V., and Helmig, D.: Dynamics of ozone and nitrogen oxides at Summit, Greenland. II. Simulating snowpack chemistry during a spring high ozone event with a 1-D process-scale model, Atmospheric Environment, 117, 110 – 123, doi:http://dx.doi.org/10.1016/j.atmosenv.2015.07.004, http://www.sciencedirect.com/science/article/pii/S135223101530203X, 2015.

Picard, G., Libois, Q., Arnaud, L., Vérin, G., and Dumont, M.: Time-series of snow spectral albedo and superficial snow specific surface area at Dome C in Antarctica, 2012-2015, doi:10.1594/PANGAEA.860945, https://doi.pangaea.de/10.1594/PANGAEA.860945, supplement to: Picard, G et al. (2016): Development and calibration of an automatic spectral albedometer to estimate near-surface snow SSA time series. The Cryosphere, 10(3), 1297-1316, doi:10.5194/tc-10-1297-2016, 2016.

Pinzer, B. R., Schneebeli, M., and Kaempfer, T. U.: Vapor flux and recrystallization during dry snow metamorphism under a steady temperature gradient as observed by time-lapse micro-tomography, The Cryosphere, 6, 1141–1155, doi:10.5194/tc-6-1141-2012, http://www.the-cryosphere.net/6/1141/2012/, 2012.

Press, .W. H, Teukolsky, S. A., Vetterling, W. T., F.lannery, B. P.: Numerical Recipe in Fortran 90, Cambridge Univeristy Press, 2 edn., 1996.

Pruppacher, H. R. and Klett, James D., .: Microphysics of clouds and precipitation, Dordrecht ; Boston : Kluwer Academic Publishers, 2nd rev. and enl. ed edn., "With an introduction to cloud chemistry and cloud electricity.", 1997.

Röthlisberger, R., Hutterli, M. A., Sommer, S., Wolff, E. W., and Mulvaney, R.: Factors controlling nitrate in ice cores: Evidence from the Dome C deep ice core, Journal of Geophysical Research: Atmospheres, 105, 20 565–20 572, doi:10.1029/2000JD900264, http://dx.doi.org/10.1029/2000JD900264, 2000.

Sander, R.: Modeling Atmospheric Chemistry: Interactions between Gas-Phase Species and Liquid Cloud/Aerosol Particles, Surveys in Geophysics, 20, 1–31, doi:10.1023/A:1006501706704, http://dx.doi.org/10.1023/A:1006501706704, 1999.

Sander, R.: Compilation of Henry's law constants (version 4.0) for water as solvent, Atmospheric Chemistry and Physics, 15, 4399–4981, doi:10.5194/acp-15-4399-2015, http://www.atmos-chem-phys.net/15/4399/2015/, 2015.

Sazaki, G, and Zepeda S, Nakatsubo S, Yokomine. M. Furukawa. Y.: Quasi-liquid layers on ice crystal surfaces are made up of two different phases, Proc Natl Acad Sci U S A., 4, 1052–1055, doi:10.1073/pnas.1116685109, 2012.

Tang, M. J., Cox, R. A., and Kalberer, M.: Compilation and evaluation of gas phase diffusion coefficients of reactive trace gases in the atmosphere: volume 1. Inorganic compounds, Atmospheric Chemistry and Physics, 14, 9233–9247, doi:10.5194/acp-14-9233-2014, http://www.atmos-chem-phys.net/14/9233/2014/, 2014.

Thibert, E., , and Dominé, F.: Thermodynamics and Kinetics of the Solid Solution of HNO3 in Ice, The Journal of Physical Chemistry B, 102, 4432–4439, doi:10.1021/jp980569a, http://dx.doi.org/10.1021/jp980569a, 1998.

Thomas, J. L., Stutz, J., Lefer, B., Huey, L. G., Toyota, K., Dibb, J. E., and von Glasow, R.: Modeling chemistry in and above snow at Summit, Greenland? Part 1: Model description and results, Atmospheric Chemistry and Physics, 11, 4899–4914, doi:10.5194/acp-11-4899-2011, http://www.atmos-chem-phys.net/11/4899/2011/, 2011.

Toyota, K., McConnell, J. C., Staebler, R. M., and Dastoor, A. P.: Air-snowpack exchange of bromine, ozone and mercury in the springtime Arctic simulated by the 1-D model PHANTAS - Part 1 In-snow bromine activation and its impact on ozone, Atmospheric Chemistry and Physics, 14, 4101–4133, doi:10.5194/acp-14-4101-2014, http://www.atmos-chem-phys.net/14/4101/2014/, 2014.

Traversi, R., Udisti, R., Frosini, D., Becagli, S., Ciardini, V., Funke, B., Lanconelli, C., Petkov, B., Scarchilli, C., Severi, M., and Vitale, V.: Insights on nitrate sources at Dome C (East Antarctic Plateau) from multi-year aerosol and snow records, Tellus B, 66, http://www.tellusb.net/index.php/tellusb/article/view/22550, 2014.

Waddington, E. D., Cunningham, J., and Harder, S. L.: The Effects Of Snow Ventilation on Chemical Concentrations, pp. 403–451, Springer Berlin Heidelberg, Berlin, Heidelberg, doi:10.1007/978-3-642-61171-1_18, http://dx.doi.org/10.1007/978-3-642-61171-1_18, 1996.

Wolff, E. W., Jones, A. E., Bauguitte, S. J.-B., and Salmon, R. A.: The interpretation of spikes and trends in concentration of nitrate in polar ice cores, based on evidence from snow and atmospheric measurements, Atmospheric Chemistry and Physics, 8, 5627–5634, doi:10.5194/acp-8-5627-2008, http://www.atmos-chem-phys.net/8/5627/2008/, 2008.

Udisti, R., Becagli, S., Benassai, S., Castellano, E., Fattori, I., Innocenti, M., Migliori, A., and Traversi, R.: Atmospheresnow interaction by a comparison between aerosol and uppermost snow-layers composition at Dome C, East Antarctica, Annals of Glaciology, 39, 53–61, doi:doi:10.3189/172756404781814474, http://www.ingentaconnect.com/content/igsoc/agl/2004/00000039/00000001/art00010, 2004.

Ullerstam, M. and Abbatt, J. P. D.: Burial of gas-phase HNO3 by growing ice surfaces under tropospheric conditions, Phys. Chem. Chem. Phys., 7, 3596–3600, doi:10.1039/B507797D, http://dx.doi.org/10.1039/B507797D, 2005a.

Ullerstam, M., Thornberry, T., and Abbatt, J. P. D.: Uptake of gas-phase nitric acid to ice at low partial pressures: evidence for unsaturated surface coverage, Faraday Discuss., 130, 211–226, doi:10.1039/B417418F, http://dx.doi.org/10.1039/B417418F, 2005b.

~~Wolff, E. W., Jones, A. E., Bauguitte, S. J.-B., and Salmon, R. A.: The interpretation of spikes and trends in concentration of nitrate in polar ice cores, based on evidence from snow and atmospheric measurements, Atmospheric Chemistry and Physics, 8, 5627–5634, , , 2008.~~

Yuan-Hui, L. and Gregory, S.: Diffusion of ions in sea water and in deep-sea sediments, Geochimica et Cosmochimica Acta, 38, 703 – 714, doi:http://dx.doi.org/10.1016/0016-7037(74)90145-8, http://www.sciencedirect.com/science/article/pii/0016703774901458, 1974.